SHEAR STRENGTHENING OF TIMBER STRINGERS USING GFRP SHEETS

BY

SHAUN W. HAY

A Thesis
Submitted to the Faculty of Graduate Studies
In Partial Fulfillment of the Requirements
For the Degree of

MASTER OF SCIENCE

Department of Civil Engineering
Faculty of Engineering
University of Manitoba
Winnipeg, Manitoba
Canada

© October 2004

THE UNIVERSITY OF MANITOBA

FACULTY OF GRADUATE STUDIES

*****

COPYRIGHT PERMISSION PAGE

Shear Strengthening of Timber Stringers Using GFRP Sheets

BY

Shaun W. Hay

A Thesis/Practicum submitted to the Faculty of Graduate Studies of The University of Manitoba in partial fulfillment of the requirements of the degree of

MASTER OF SCIENCE

SHAUN W. HAY ©2004

Permission has been granted to the Library of The University of Manitoba to lend or sell copies of this thesis/practicum, to the National Library of Canada to microfilm this thesis and to lend or sell copies of the film, and to University Microfilm Inc. to publish an abstract of this thesis/practicum.

The author reserves other publication rights, and neither this thesis/practicum nor extensive extracts from it may be printed or otherwise reproduced without the author's written permission.

ABSTRACT

A large number of sawn timber stringer bridges in Manitoba are in need of shear strengthening because of horizontal splits, or checks, at the ends of the stringers. This thesis describes the experimental investigation of two schemes of shear strengthening of creosote-treated timber beams with unidirectional sheets of glass fibre reinforced polymer (GFRP). In one scheme, vertical sheets are applied at the ends of the beams, and in the other, the sheets were oriented at a 45° angle. A number of stringers, mostly with checks at their ends, were removed from a 40-year old bridge. Ten of these stringers were tested at each of their ends to determine the distribution of shear strengths in un-strengthened samples. Five stringers strengthened with vertical GFRP sheets and twenty one with diagonal sheets, were also tested for their shear strength at each end.

It was found that the vertical GFRP sheets improved the average ultimate load over control beams by 16% and the 5^{th} percentile shear stress by 10%. The diagonal sheets improved the average ultimate load over control specimens by 34% and the 5^{th} percentile shear stress by 31%. The ability of the vertical sheets to improve flexural stiffness was marginal with a 3.5% increase from the pre-strengthening modulus of elasticity test to the final strengthened test. The deformability of beams with vertical sheets was enhanced, however the sheets tended to peel off in the vicinity of the splits. The diagonal GFRP sheets, on the other hand, significantly improved both the flexural stiffness and deformability of the beams, and did not peel off. The flexural stiffness increased by 47% from the pre-strengthening apparent modulus of elasticity test to the final test. The reason for this significant increase in flexural stiffness for a shear strengthening method is because the

sheets tie the top and bottom of the split beam together, which effectively increases the moment of inertia and thus the stiffness.

The strains within the GFRP sheets varied considerably; however when the split end of the beam was loaded the sheets on that end experienced on average 5,000 μstrain, and the sheets on the solid end experience less than a 1000 μstrain. When loaded near the solid end, the split end experienced on average 3,500 μstrain, while the solid end experienced 2,500 μstrain. It is noted that since the rupture strain of the GFRP sheets is 20,000 μstrain, the strength of the sheets were not utilized fully.

The control specimens failed in different modes, such as in flexure, shear, dap splitting, and bearing at the support and/or under load point. The vertical sheet specimens frequently failed in flexure, while the diagonal sheet specimens either failed by dap splitting or bearing.

A reliability analysis was completed for the purpose of determining whether this strengthening method is able to increase the strength of timber bridges to support modern truck loads. Using a span of 3.4 m, a stringer spacing of 0.4 m and a CL-625 truck, the β value for control, vertical and diagonal sheet specimens was 1.9, 2.2 and 2.7 respectively. The desired value is 3.5. The reliability index shows that the proposed strengthening method improves the reliability index of timber bridges by 42%, however a greater improvement is needed and thus further research is recommended.

ACKNOWLEDGEMENTS

The author would like to express his sincere appreciation to Dr. Dagmar Svecova and Dr. Baidar Bakht. Their encouragement, enthusiasm and generosity throughout this work have made it an enriching experience. The author is thankful for the opportunity to work and learn from both of these professors.

Support for this research was provided by the Manitoba Department of Transportation and Government Services, Vector Construction and ISIS Canada Network of Centres of Excellence on Intelligent Sensing for Innovative Structures are gratefully acknowledged. The Faculty of Architecture is also acknowledged for making their CAST lab available for the experimental testing.

The author would also like to express his gratitude to Dr. Robin Hutchinson for guiding me towards graduate studies, and Ms. Ruth Eden of the Bridges and Structures Branch of Manitoba Department of Transportation and Government Services for her continued assistance and support throughout this research program. The assistance of the technicians and EIT's at the University of Manitoba's structural laboratory, Mr. Scott Sparrow, Mr. Grant Whiteside, Mr. Moray McVey, Mr. Chad Klowak and Mr. Dino Philopulos, is gratefully acknowledged. Summer students that assisted the author Ms. Irini Akhnoukh, Mr. Carlos Mota and Mr. Kenton Thiessen are also gratefully acknowledged.

Finally, the author wishes to express his thanks to his parents, and sister and brother-in-law for their unconditional encouragement, patience and support. The support of fellow students, Mr. Kevin Amy, Mr. Shahryar Davoudi, Ms. Sara Gomez and Mr. Hugues Vogel, throughout this project is also gratefully acknowledged.

TABLE OF CONTENTS

LIST OF FIGURES

LIST OF TABLES

LIST OF SYMBOLS

a	=	distance from support to load point;
b	=	beam width;
b	=	distance from support to load point (Fig. 4.13);
E	=	modulus of elasticity;
EI	=	flexural stiffness;
F_{GFRP}	=	force in the sheets parallel to the grain;
F_{vl}	=	longitudinal shear force;
h	=	beam depth;
h_{frp}	=	depth of GFRP sheets
I	=	moment of inertia;
J	=	horizontal shearing stress (τ);
L	=	span;
l_v	=	longitudinal shear length;
M	=	bending moment;
n	=	number of layers of sheets per stringer;
n	=	E_{FRP}/E_{wood}
P	=	load;
Q	=	first moment of area above horizontal plane at stringer depth of interest;
R	=	shear modification factor for reinforced beams;
R	=	reaction at nearer support (V);
t	=	thickness of GFRP sheet;
u	=	mean shift on either side of the neutral plane;

V	=	shear force due to loading;
w	=	width of GFRP sheet;
y	=	distance from neutral axis to extreme fibre;
β	=	safety index;
δ	=	deflection;
ε	=	strain recorded in sheets during test;
θ	=	angle of GFRP sheet with the horizontal plane;
μ_R	=	mean of resistances;
μ_S	=	mean of load effects;
ρ_{frp}	=	reinforcement ratio;
σ	=	flexural stress;
σ	=	stress in GFRP sheets;
σ_R	=	standard deviation of resistances;
σ_S	=	standard deviation of load effects;
τ	=	shear stress;
τ_{max}	=	maximum shear stress in a section.

LIST OF ABBREVIATIONS

ASTM	American Society of Testing and Materials
CFRP	Carbon Fibre Reinforced Polymers
CHBDC	Canadian Highway Bridge Design Code
FRP	Fibre Reinforced Polymers
GFRP	Glass Fibre Reinforced Polymers
NLGA	National Lumber Grades Authority

GLOSSARY

Beams – A structural member supporting a load applied transversely to it. Beams used in bridge include stringers, girders, and joists.

Beams and Stringers – Beams and stringers are rectangular wood pieces whose larger dimension is at least 51 mm greater then its smaller dimension and the smaller dimension is at least 114 mm.

Characteristic Strength – The permissible material stress tabulated in appropriate design specifications. The characteristic strengths must be adjusted by all applicable modification factors to arrive at the stress used for design.

Check – A lengthwise separation of the wood that usually extends across the rings of annual growth and usually the result of seasoning.

Clear – Free or practically free of all defects and strength reducing characteristics.

Creosote – A wood preservative which is a distillate derived from coal tar produced by the carbonization of coal.

Dap – A notch cut into the end of a flexural member (See Figure 3.3).

Dry – The condition of having a relatively low moisture content, i.e. not more than 19% for sawn lumber.

Edge – The narrow face of rectangular-shaped pieces of lumber.

Glued Laminated Timber (Glulam) – An engineered, stress-rated product that consists of specially selected and prepared laminations secured together with an adhesive.

Grade – The designation of the material quality of a manufactured piece of wood.

Grain – The direction, size, arrangement, appearance and quality of wood fibres in a piece of wood or timber.

Knot – That portion of a branch or limb that has been surrounded by subsequent growth of the stem.

Laminate – A product made by bonding together two or more layers (laminations) of material or materials.

Lumber – A product derived from a log at a sawmill, or a saw and planing mill in which it has not been further manufactured other than by cross-cutting, ripping, resawing or planing.

Modulus of Rupture (MOR) – The maximum stress at the extreme fibre in bending, calculated from the maximum bending moment on the basis of an assumed stress distribution.

Moisture Content – The amount of water contained in the wood expressed as a percentage of the mass of the oven dry wood.

Preservative – Any substance that is effective in preventing development and action of wood-decaying fungi, borers of various kinds, and harmful insects.

Sawn Lumber – The product of a sawmill not further manufactured other than by sawing, resawing, passing lengthwise through a standard planing mill, and cross-cutting to length.

Shake – A lengthwise separation of the wood which occurs between or through the rings of annual growth.

Split – A separation of the wood through the piece to the opposite surface or to an adjoining surface due to the tearing apart of the wood cells.

Stringer – A structural member supporting a load applied transversely to it. (i.e. a flexural member)

Timber – Useful construction material produced from the logs of trees or lumber that is nominally 125 mm or more in the least dimension.

Visual Stress Graded Lumber – A grade of structural lumber determined by estimating the strength-reducing characteristics by visual examination of the surfaces.

Wood – Defect free wood.

CHAPTER 1 INTRODUCTION

1.1 OVERVIEW

A large number of timber bridges in the province of Manitoba are in need of rehabilitation and strengthening, mainly because of age, damage, and possibly due to increased truck loads since these bridges were designed and built. Since replacement of all timber bridges is prohibitively expensive, there is an urgent need for developing cost-effective means of rehabilitating and strengthening these structures. In response to this need, an experimental research program has been undertaken at the University of Manitoba to develop methods of rehabilitating and strengthening timber bridges. This thesis details the research undertaken in the area of shear strengthening using glass fibre reinforced polymer (GFRP) sheets.

1.2 PROBLEM DEFINITION

The Department of Transportation and Government Services in the province of Manitoba has more than 700 timber bridges that are at least 20 years old (New timber bridges are no longer built by the Department of Transportation and Government Services). Due to weathering damage and increased loads, timber bridges are no longer able to perform as expected. Table 1.1 shows the comparison between live load shear induced by design trucks and, the analytical shear resistance of select structural stringers in sizes typically in use and the stringer size used in this experimental project. Most timber stringers have a dap cut into the ends which is frequently where failure begins as can be seen in Figure 1.1. To increase shear capacity of timber beams it is therefore necessary to prevent failure at daps. The sawn

timber stringers also develop horizontal splits at approximately mid-depth of the stringer, compromising its shear strength. When these splits develop, the compressive and tensile forces in the stringer are no longer able to react against each other, through shear, preventing it from acting as a single member. It can be seen that the split must be close to restore a stringer to its full strength.

Table 1.1 Comparison of shear loads to resistances

Bridge Span	Stringer Size	Stringer Spacing	Shear Due To Design Truck		Shear Resistance (Grade: S.S.)	Increase Needed In Shear Capacity	
			CL-625	CL-700		CL-625	CL-700
m	mm	mm	kN	kN	kN	%	%
10.0	200 x 600	600	103.5	116.0	62.9	65	85
6.4	150 x 500	600	88.0	99.0	46.6	89	113
3.4	100 x 400	600	80.2	98.9	30.5	163	224
3.4	100 x 400	400	53.5	65.9	30.5	76	116

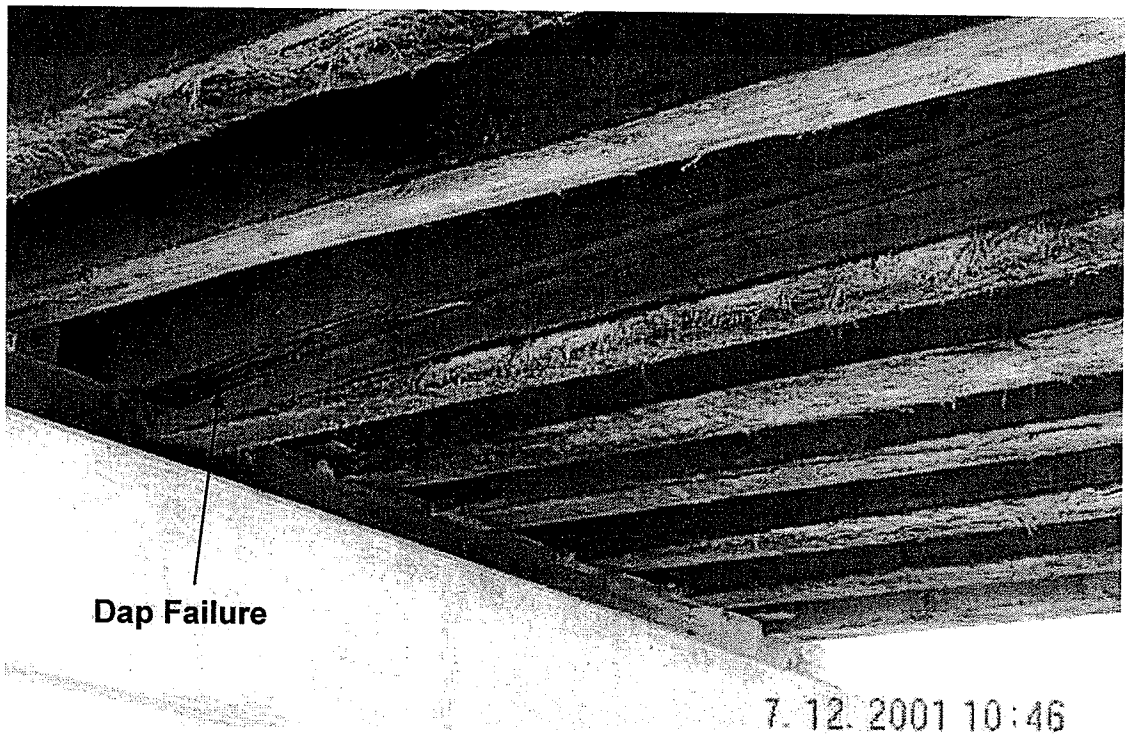

Figure 1.1 Shear split that propagated from dap

1.3 OBJECTIVES

The objectives of this research are:

1. To develop a cost effective method of rehabilitating timber bridges for shear deficiency,
2. To develop a method of rehabilitation that is environmentally friendly,
3. To develop a durable method of rehabilitation, and
4. To determine the most effective GFRP sheet orientation and arrangement.

1.4 SCOPE

This research project investigates the feasibility of using glass fibre reinforced polymer (GFRP) sheets to prevent shear failures and only deals with static testing of creosote pressure treated Douglas fir stringers recycled from a dismantled timber bridge. Fatigue, dynamic response, bond between creosote treated wood and GFRP, and durability were not part of this investigation and require further research.

CHAPTER 2 LITERATURE REVIEW

2.1 Structural Behaviour of Timber

According to Madsen (1992), timber is a "useful construction material produced from logs of trees" while wood is clear "defect-free wood". Madsen (1992) further states that timber acts in a different manner than clear defect free wood and this is the fundamental difference. Timber subjected to bending fails by tension perpendicular to the grain because of defects such as knots in the wood. Clear wood on the other hand fails by wrinkles in the compression zone when used as a bending member. Thus the practice of using small clear defect free samples of wood as the basis to derive timber properties is flawed, since the two materials are essentially different despite coming from the same source. The second fundamental difference between timber and wood is that wood has consistent properties along its length while timber, being filled with many defects, has variable strength. This of course leads to size effects where the larger member has greater probability that a strength reducing defect will occur. Thus the strength of timber is determined probabilistically and not deterministically.

2.2 Shear Strength of Timber

Two very important aspects of shear strength need to be dealt with, the first is what are the shear stresses in a beam due to the applied loads and beam geometry, and the second is what level of shear stress is needed to produce failure. Many research projects have been conducted to address these issues. The following is a review of some of these that are of interest to this research.

An interesting study involving checked timber beams was conducted by Newlin et al. (1934). The study found that checked beams acted as two essentially independent beams with the result that neutral plane shear stress was relieved. However, the shear stresses in either of the two beams would be higher, although not as high as when the beam was a solid unit. It also found that this two-beam action was more pronounced when the load was closer to the support and that the point of loading that caused shear failure was actually some significant distance from the support, which previously was thought to occur just beside the support. From this research a new way of calculating longitudinal shear was developed, shown in Equation 2.1, where the beam is considered to be comprised of two beams and resulted in a more accurate representation of the shear stresses in the beam which were lower and allowed for a reduction in member size in comparison to previous methods.

$$R = \frac{2Jbh}{3} + \frac{Eubh^2}{6a^2} \qquad \text{(Equation 2.1)}$$

In Equation 2.1, R = reaction at nearer support (V), J = horizontal shearing stress (τ), b = width of beam, h = depth of beam, E = modulus of elasticity, u = mean shift on either side of the neutral plane and a = distance between load point and nearer support. The first part of Equation 2.1 is the shear stress in the neutral plane calculated in the usual way and is referred to as the single beam portion, while the second part is the two beam portion and is not associated with shearing the neutral plane.

A later study to address the shear strength of Douglas-fir was completed by Foschi and Barrett (1976), who used the Weibull's theory of brittle fracture to derive a model for ultimate stresses at a given survival probability and under different loading conditions. This model was capable of rationalizing the size effects for shear and also the differences between the ASTM shear block test and beam tests. Their model, using beam volume, depth and

location of load as the size parameter in deriving the allowable stresses, was verified by comparing the results with those from experiments on Griplam nailed connections and shear tests on torque tubes. From this study the characteristic values used in timber shear design were derived as shown in Table 2.1. Foschi and Barrett (1977) used the above derivation of the shear strength in which they suggested a design method for various beam configurations and loadings. They provided the required parameters and proposed a method for extending it to other species. They also noted that their method was only applicable to unsplit beams.

Table 2.1 Specified shear strengths for various species and grades

Species	Grade	Structural Joists and Planks	Light Framing Grades	Beam and Stringer Grades	Grade	Post and Timber Grades
		MPa	MPa	MPa		MPa
D Fir-L	All Grades	1.1	1.9	0.9	SS	1.2
					No. 1	0.9
					No. 2	0.9
Hem-Fir	All Grades	0.9	1.5	0.7	SS	1.0
					No. 1	0.7
					No. 2	0.7
S-P-F	All Grades	1	1.7	0.7	SS	0.9
					No. 1	0.7
					No. 2	0.7
Northern	All Grades	0.9	1.5	0.6	SS	0.8
					No. 1	0.6
					No. 2	0.6

Another study into the shear strength of timber was completed by Rammer et al. (1996). This research project included 280 tests on solid sawn Douglas-fir timbers using two setups and 5 different beam sizes. They recommended that 5-point bending test be used to determine beam shear because they were able to consistently fail the beams in shear. They verified that shear strength varies with beam size and were able to model it with an equation similar to that which was developed for glue laminated beams and which is based on the ASTM shear block strength. It was concluded that shear area, which is defined as the

product of the length under high shear, both positive and negative, and beam width, is the preferred parameter over beam volume or depth to model shear variations due to size. And finally they found little correlation between shear strength and modulus of rupture for matched beams.

A study similar to Rammer et al. (1996) was done by Lam et al. (1997). This study used the same five-point setup and was conducted on Canadian softwood structural lumber for span to depth ratios of 6:1 and 5:1. The researchers used the ASTM shear block test results, finite element analysis and Weibull weakest link theory to predict the shear failure loads with good agreement. They also found that the Weibull shape parameter is species-dependent potentially making the characteristic shear strength values conservative.

An experimental and analytical research project involving glued-laminated Douglas-fir beams was completed by Huggins et al. (1966) who investigated the effects of delamination on strength. One hundred and seventy five glued laminated beams were tested with various delaminations intentionally introduced into the beams. An approximate analytical method was developed to evaluate the stresses in the beams and was found to predict them within tolerable limits. They also found that (a) interior delaminations did not significantly affect stiffness, (b) end delaminations cause greater strength loss than equivalent interior delaminations at the mid-spans, and (c) delaminations make beams susceptible to shear failures. They concluded that the shear strengths of beams are substantially less than those obtained by the shear block tests and are affected by the shear span to beam depth ratio. They speculated that vertical compression near the load points and supports helped to resist the horizontal shearing forces. Another study involving glued-laminated timbers by Keenan and Selby (1973) applied compressive stresses perpendicular to grain and found that shear

strength was not significantly affected. They also concluded that there was a general relationship between shear strength and sheared area and also looked at using shear span to depth as a strength parameter, but failed to find this as a useful parameter and considered it as just another way of expressing the size effect. A final interesting conclusion of this study was that the "two-beam" shear behaviour is not applicable to Douglas-fir and may actually be unsafe.

For timbers, all properties are based on the small clear green specimens. For all wood products the shear values are still based on the ASTM shear block tests using small clear green specimens. In developing the structural strengths for timber, there are two important documents: The first is ASTM D143-94 (ASTM 1994) which details how small clear green specimens are used to determine strength values; the second one is ASTM D245-99 (ASTM 1999) which converts the values found using ASTM D143-94 into allowable stresses for the various structural grades. These documents are the basis for the characteristic values used in Canadian wood design. ASTM D245-99 makes allowances for the different strength reducing defects found in timber. Most notable is the allowance for a split which is 50% of the 5^{th} percentile value found from ASTM D143-94 shear block tester. Ethington et al. (1979) produced a report that follows the development of shear stresses for timber. This report examines the research that was involved in the development of the shear factors used in ASTM D245. One of its most interesting findings is that the Two-Beam Theory developed by Newlin et al. (1934) was inaccurate although it provided useful insights into split beam behaviour. This report also felt the research by Foschi and Barrett (1976) held promise and should be pursued.

2.3 Environmental Impact of Pressure Treated Timbers

Untreated timber does not have an economically viable lifespan in outdoor applications. Treating the timber thus has become essential. However, the treatment affects the environment adversely. A study conducted by Brooks (2000) for the United States Department of Agriculture has addressed the use of the three most common preservatives for timber bridges in the USA. The three common preservatives in use are chromated copper arsenate type C (CCA), pentachlorophenol (penta) and Creosote. The timber bridges in Manitoba that are being studied are treated with creosote. In studying creosote-treated bridges this project examines two bridges: one newly constructed and the other being 8 years old. Both bridges crossed slow moving biologically active waterways that would represent worst case scenarios. The purpose of the report was to determine the concentrations of the preservatives that are lost and assess the environmental response to these preservatives. The compounds that are derived from creosote are poly-cyclic aromatic hydrocarbons (PAHs) and are of concern because many of them are toxic to marine animals. The study found that there were no PAHs in the water column itself but it did find them in the sediment under the bridges and immediately downstream. The total PAH concentration did not exceed standard value but individual compounds of PAHs did marginally exceed accepted standards. However, this is not a large concern since the invertebrate communities found in these waterways were robust and not susceptible to PAHs levels found. More sensitive organisms that would be affected adversely are typically found in faster moving waterways and rely on dilution to bring the PAHs down to tolerable levels. There are no adverse affects found in the study's invertebrate community and also in laboratory bioassays. Concerns were raised about shavings from construction falling into the waterways as well as creosote dripping

from the bridges on hot days. These problems can be solved by using good construction practices. It was finally concluded that preservative treated timber bridges present very little environmental risk.

2.4 Steel Reinforcement of Timber

The first attempts to reinforce timber used steel as the reinforcing material. An early project was completed by Peterson (1965) who bonded pre-stressed steel plates to the bottom of glued-laminated beams. Improvements in stiffness and strength with reductions in variability were found when compared to match control specimens. The problem with pre-stressing is that transferring the stresses in the steel is quite difficult and in this project a new way of achieving transfer was developed. The analysis that was completed showed that the beams acted as expected and this method seemed feasible for application to solid sawn lumber. Steel rods placed in grooves between laminates of glued-laminated beams were used as reinforcement by Lantos (1970). A successful analysis was developed for bond stresses, bending stresses and deflections. The project demonstrated that the technique was able to develop the full composite action of the two materials. It was found that with as little as 1% reinforcement ratio, 40-60% increase in stiffness and strength could be achieved with reductions in variability. It was recommended that this method be used for upgrading lower grade beams to the sample stiffness and strength of higher grade beams. Another study into using steel to reinforce glued-laminated beams was by Bulleit et al. (1989) who embedded steel reinforcing bars designed for concrete in wood flake board and then used it as a laminate. Two sets of beams were prepared: dry beams and moisture-cycled beams. The dry beams showed stiffness and strength increases and the moisture-cycled beams showed

stiffness increases but no significant strength increase. The reason given for this was the increased steel stresses caused by the reduction in the wood modulus of elasticity due to increased moisture content, and also due to reduced bond strength between the steel and flake board caused by the increase in moisture. As a form of reinforcement for timber, metallic materials are able to increase both the stiffness and strength of the timber; however other problems do exist as reported by Dagher and Lindyberg (2000). They noted that the material's different stiffness and hygro-expansion rates can lead to incompatibilities between materials, thus concluding that metallic reinforcement was not the best option for reinforcing timber.

2.5 FRP Reinforcement of Timber

More recently, fibre reinforced polymers (FRP) have been used as reinforcement for wood. Research involving small-scale specimens of new solid sawn and glued laminated timbers has been conducted at various institutions in North America and Europe. At the University of Manitoba research has been completed using salvaged timbers using both small and large scale specimens.

2.5.1 Research at Institutions other than the University of Manitoba

Two interesting projects involve solid sawn timbers and carbon fibre reinforced polymers (CFRP) sheets are discussed here. The first by Plevris and Triantafillou (1992) used CFRP sheets bonded to the tension surface of wood beams and columns. The specimens were tested using combined flexural and axial loading methods. It was concluded that small amounts of CFRP can significantly enhance the mechanical properties of timber.

An analysis was also developed and confirmed by the experimental program. The analysis was extended to determining the amount of reinforcement for optimum performance. A similar study by Triantafillou and Deskovic (1992) used prestressed CFRP sheets applied to the bottom of solid sawn timbers. An analytical model was developed for determining the maximum prestressing that could be applied without failure at release and amount of reinforcing for maximum performance. The model was verified with experimental work that showed good satisfactory correlation. The research showed that significant savings could be achieved in materials and cost by using prestressing. It was concluded that prestressing was a viable option for both old and new wood. The study did not address the problem of prestress losses.

A study by John and Lacroix (2000) used CFRP and GFRP to reinforce small solid sawn timbers. A total of 150 tests were completed using three different sheet arrangements with each reinforced specimen being matched with a control specimen for comparison purposes. The results of the research showed that strength increases significantly exceeded those which were predicted by simple models that were used to analyse the specimens. The wood appeared to increase in strength by itself due to the effect of the reinforcement. This was attributed to bridging of local defects and confining action of the FRP reinforcement.

A study aimed at evaluating the potential for commercial development of a glued laminated – GFRP beam was conducted by Hernandez et al. (1997). Two different reinforcing schemes were developed using yellow poplar and GFRP sheets. The first layout consisted of placing a layer on the top and bottom of the beam and the second used two layers on the bottom only. Twelve specimens were tested and the strength values correlated well with an analysis based on ASTM D3737. The experimental work showed an 18%

increase in stiffness, 26% increase in strength with a 3% GFRP volume fraction. Problems with delamination were observed indicating the need for greater attention to bonding. It was concluded that it was feasible to commercially produce a wood – GFRP composite beam.

A study involving only shear reinforcement was conducted by Triantafillou (1997) using small solid sawn timber and CFRP. In this project, different layouts of CFRP sheets placed horizontally, vertically or in both directions were experimented within the critical shear zones of the beam. To induce shear failure the cross-section of the beam was narrowed in the shear zones. A simple analysis was developed based on transformed section. This analysis reasonably predicted the strengths that were found in the experimental portion of the project. It was concluded that horizontal sheet orientation produced the best results.

An experimental project in support of a strengthening project on a gymnasium was conducted by Ehsani et al. (2004). This project was both a shear and flexural strengthening project involving CFRP strips and bi-directional CFRP sheets. Before rehabilitating the glued laminated floor beams of the gymnasium, a brief laboratory project was completed in which a single strengthened specimen was tested and compared to a single control specimen. The repair consisted of adding a 75mm wide CFRP strip to the bottom of the beam and then inserting 38 mm wide strips into grooves near the top of the timber. Following this, a two way CFRP sheet was wrapped on the sides and bottom of the beam. A 67% increase in strength was found over the control specimen as well as increases in stiffness and ductility. Following the experimental work, the repair was applied to 21 beams in the gymnasium. This method of repair resulted in cost savings over other options to achieve the required strength increases.

2.5.2 Research at the University of Manitoba

At the University of Manitoba, three research projects have been completed involving GFRP rods and old creosote treated Douglas-fir bridge stringers. The first project involved reinforcing for only flexure while the others dealt with combined effects of flexural and shear strengthening.

The first project was by Gentile (2000) and involved testing 22 half-scale timbers and 4 full size bridge stringers. In this project three different reinforcing ratios were experimented with using GFRP rods placed in grooves on the tension face of the beam. An analytical model was developed based upon the results of the experimental work. Improvements in strength of 18 to 46% were found with a change in failure mode from brittle tension to ductile compression. It was concluded that the GFRP bridged over local defects in the timber and allowed higher nominal stresses.

The second research program into timber strengthening was by Eden (2002) and started out as a shear strengthening project and developed into a combined shear and flexural strengthening project. The project involved testing 50 small scale specimens and 2 full scale timber bridge stringers. The stringers were strengthen in shear using GFRP dowels placed in holes drilled from the bottom of the stringer combined with GFRP rods placed in grooves on the tension face. The analytical model developed by Gentile (2000) was used to predict strength and when compared to the experimental results it was found to be conservative. Similar findings to Gentile (2000) were found: increased strength and ductility; change of failure mode from tension to compression; and a reduction in variability. It was concluded that the GFRP dowels and rods cause the stringer to act as a truss and bridged over local defects. An interesting addition to this work was a life cycle cost analysis comparing the use

of FRP to strengthen timber bridges versus other options. The analysis confirmed the financial feasibility of this method of repair.

The most recent project at the University of Manitoba was completed by Amy (2004) which started as a flexural strengthening project similar to Gentile (2000) with shear strengthening similar to Eden (2002) being added to the program as it developed. Twenty eight timbers with daps were tested. Dap failure is common and was the reason for adding the shear strengthening in later phases of the research. Flexural strengthening by itself was not recommended for dapped beams. Using both flexural and shear strengthening resulted in significant increases in strength. This research also combined the results of the two previous projects at the University of Manitoba and found that using these techniques resulted in a 5^{th} percentile modulus of rupture that was 66% greater than CSA (1994) design value. The analytical model developed by Gentile (2000) was found to need adjustment to fit data from this study. This was due to the increase in sample size and changes in failure mode when dapped beams were considered. Similar overall conclusions to Gentile (2000) and Eden (2002) were made.

2.5.3 Ongoing Research at the University of Manitoba

Currently research is continuing at the University of Manitoba involving GFRP sheets. This research is examining the use of the sheets as flexural reinforcement as well as shear reinforcement. Similar specimens to the specimens tested for this thesis have been tested with promising results. To further isolate the shearing action of timber and directly determine the forces in the GFRP sheets a setup similar to the ASTM D143-94 shear block tester, but on a much larger scale, is being developed. Results are expected in 2005.

CHAPTER 3 EXPERIMENTAL PROGRAM

3.1 OVERVIEW

To determine the feasibility of using GFRP sheets as a means of rehabilitating and strengthening timber bridges in shear, an experimental program was undertaken that consisted of testing 37 specimens that were smaller but typical of timber stringers used for bridges in the Province of Manitoba. Two strengthening schemes were investigated, vertical and diagonal sheets, as shown in Figures 3.1 and 3.2 respectively. Ten specimens were used as control, five specimens were used to investigate a vertical sheet reinforcing scheme and 21 specimens were used for a diagonal sheet reinforcing scheme. A test setup was developed, in which each end of the specimen could be tested separately. This resulted in doubling the size of the data set.

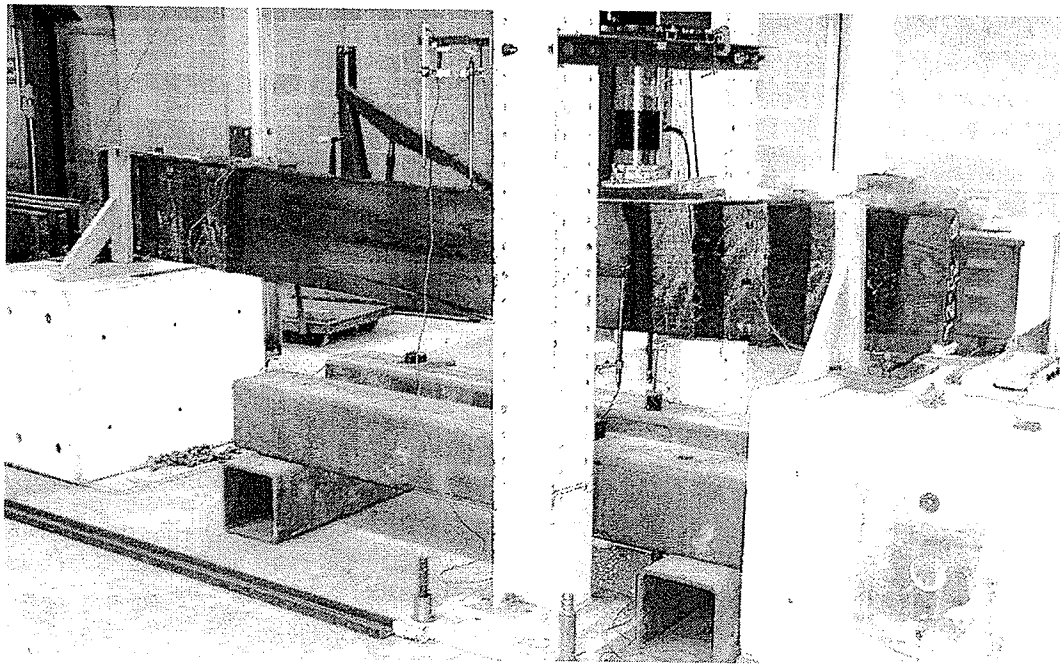

Figure 3.1 Vertical sheet specimen in test set-up

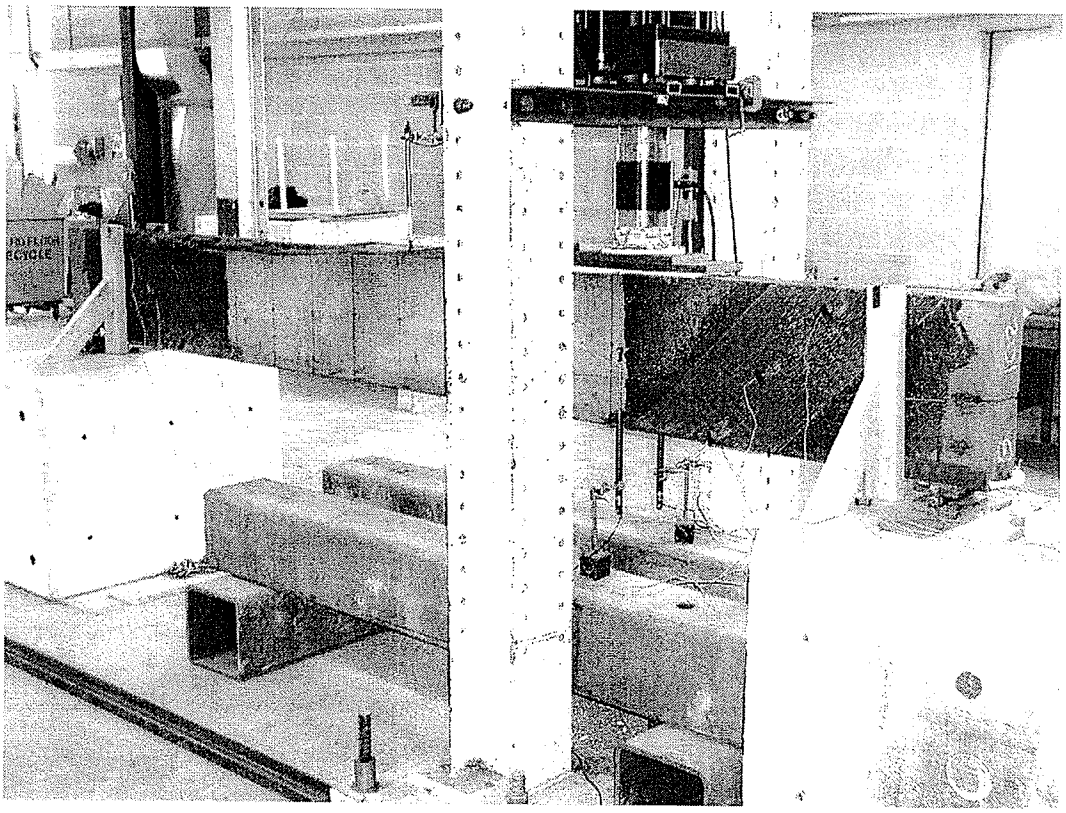

Figure 3.2 Diagonal sheet specimen in test set-up

This chapter is divided into five parts dealing with materials used, reinforcing schemes, specimen preparation, test set-up, and instrumentation.

3.2 MATERIALS

3.2.1 Timber

The timber stringers for the experimental program were acquired from the Bridges and Structures Branch of Manitoba Department of Transportation and Government Services. The stringers were salvaged from a dismantled bridge that had been in service for about 40 years. The typical stringer size was 100 mm wide, 400 mm deep and 3654 mm long, the latter two dimensions shown in Figure 3.3. Details of all stringers, including lengths of splits and rehabilitation schemes, are shown in Figures 3.4, 3.5 and 3.6. The timbers were rough sawn

Douglas fir and had been pressure treated with creosote. A dap is typically cut into the ends of the stringers used in the province (Figure 3.3) and except for specimen C10 (Figure 3.4), all specimens had daps. The typical dap size was 19 mm deep by 230 mm long with the exceptions being shown on Figure 3.6. Typically the top of the stringers were in very bad shape due to nails used to attach the bridge deck. The wood bridge deck typically deteriorated allowing water to penetrate to the stringers via rusted nails, resulting in the wood on top of the stringers to degrade to a depth of 25 to 50 mm. The size of specimens used in this project was based on the availability of timber, it being noted these stringers were smaller in size than the typical timber bridge stringers in Manitoba. Despite being smaller, these specimens allowed for comparisons with real life bridges because they had not been resawn or ripped, had deteriorated with time, were of roughly similar age and had been pressure treated with creosote.

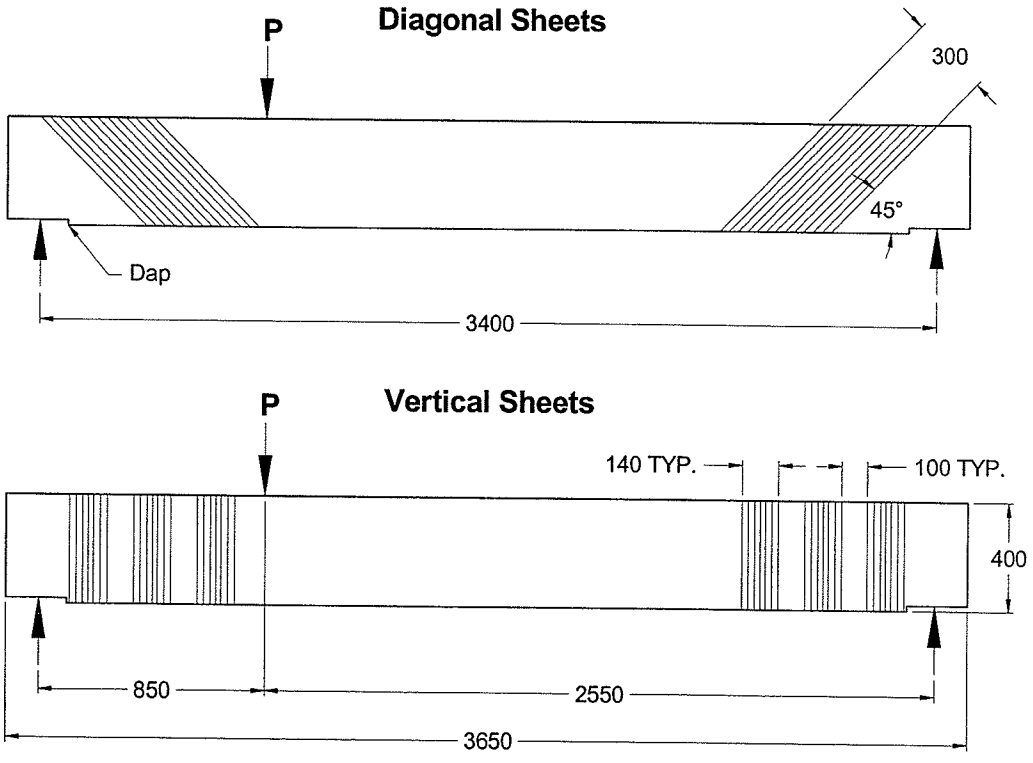

Figure 3.3 Diagonal and vertical sheet reinforcing schemes (all dimensions in mm)

Originally, the timber was of select structural grade, but during the course of time had generally degraded to the 'reject' grade. There are many characteristics that are used in the determination of a timber's grade, such as checks, holes, pockets, rate of growth, shake, skips, slope of grain, splits, stain, torn grain, wane and knots. The grade of a timber may change over time due to changes in these characteristics. Some of these characteristics do not change with time such as slope of grain, rate of growth and knots. However, characteristics such as checks, shakes and splits may develop with time due to changes in moisture content. In this research project the characteristic for downgrading of the timbers was the development of horizontal splits, which were usually longer than one quarter length of the stringer. A split is defined by National Lumber Grades Authority (2002) as "A separation of the wood through the piece to the opposite surface or to an adjoining surface due to tearing apart of the wood cells." According to the National Lumber Grades Authority (2002), when splits are longer than half the depth of the stringer, being 200 mm for specimens under consideration, and go through the entire cross-section, the grade of timber is downgraded to No. 1. When the splits exceed the depth of the stringer in length (400 mm) or are longer than 1/6 the length of the stringer (600 mm) and go through the entire cross-section, the timber is downgraded to No.2. When the splits exceed twice the depth (800 mm) or are longer than 1/6 the length of the stringer (600 mm) and go through the entire cross-section the stringer is not considered suitable for structural applications, i.e. reject, but could still be considered as standard or utility grade. The timbers were graded according to National Lumber Grades Authority (2002) grading rule 130, Beams and Stringers. The stringers used in the experimental program fall between two different national grading rules and the larger size rule was chosen since it corresponds with the real life timbers. Eight out

of the ten control specimens had degraded to the reject grade, while the two other specimens could still be regarded as select structural. All specimens strengthened with vertical sheets and 16 of 21 diagonal sheet specimens were of reject grade. Three of the other 5 diagonal sheet specimens were select structural and the last two were No. 2. A listing of the each specimen's grade is shown in Tables 3.1, 3.2, and 3.3 along with the names of files in which the test data are stored. The location and depth of the splits are shown in Figures 3.4, 3.5 and 3.6.

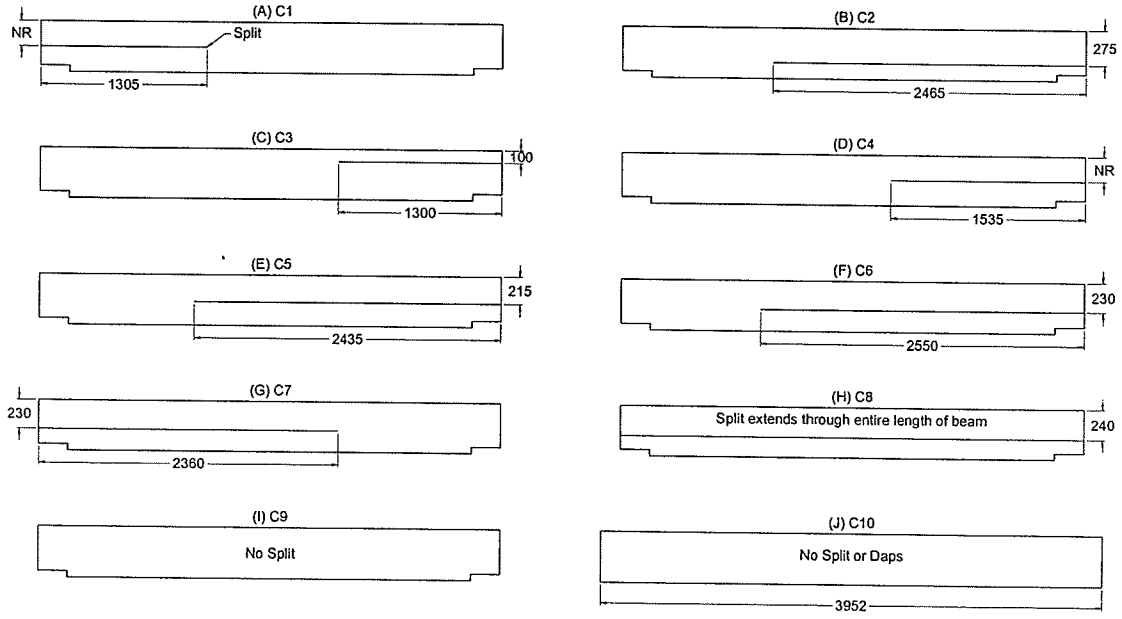

Figure 3.4 Diagrams showing location of splits and deviations from the standard specimen size for control specimens (NR = Not Recorded, all dimensions in mm)

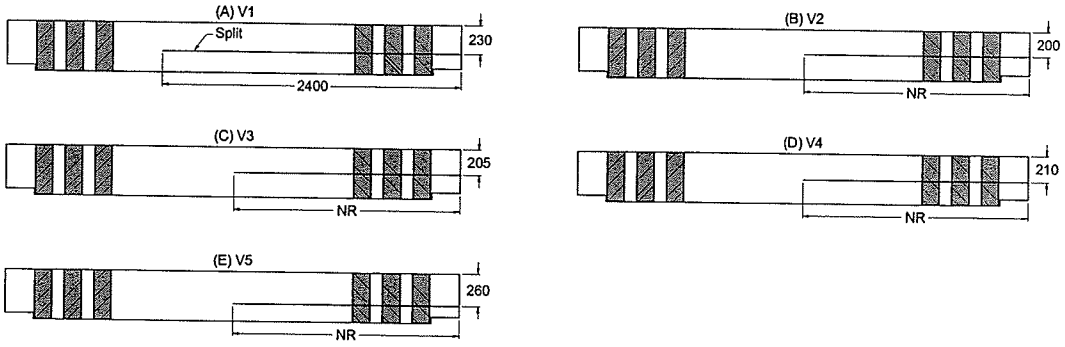

Figure 3.5 Diagrams showing location of splits and deviations from the standard specimen size for vertical sheet specimens (NR = Not Recorded, all dimensions in mm)

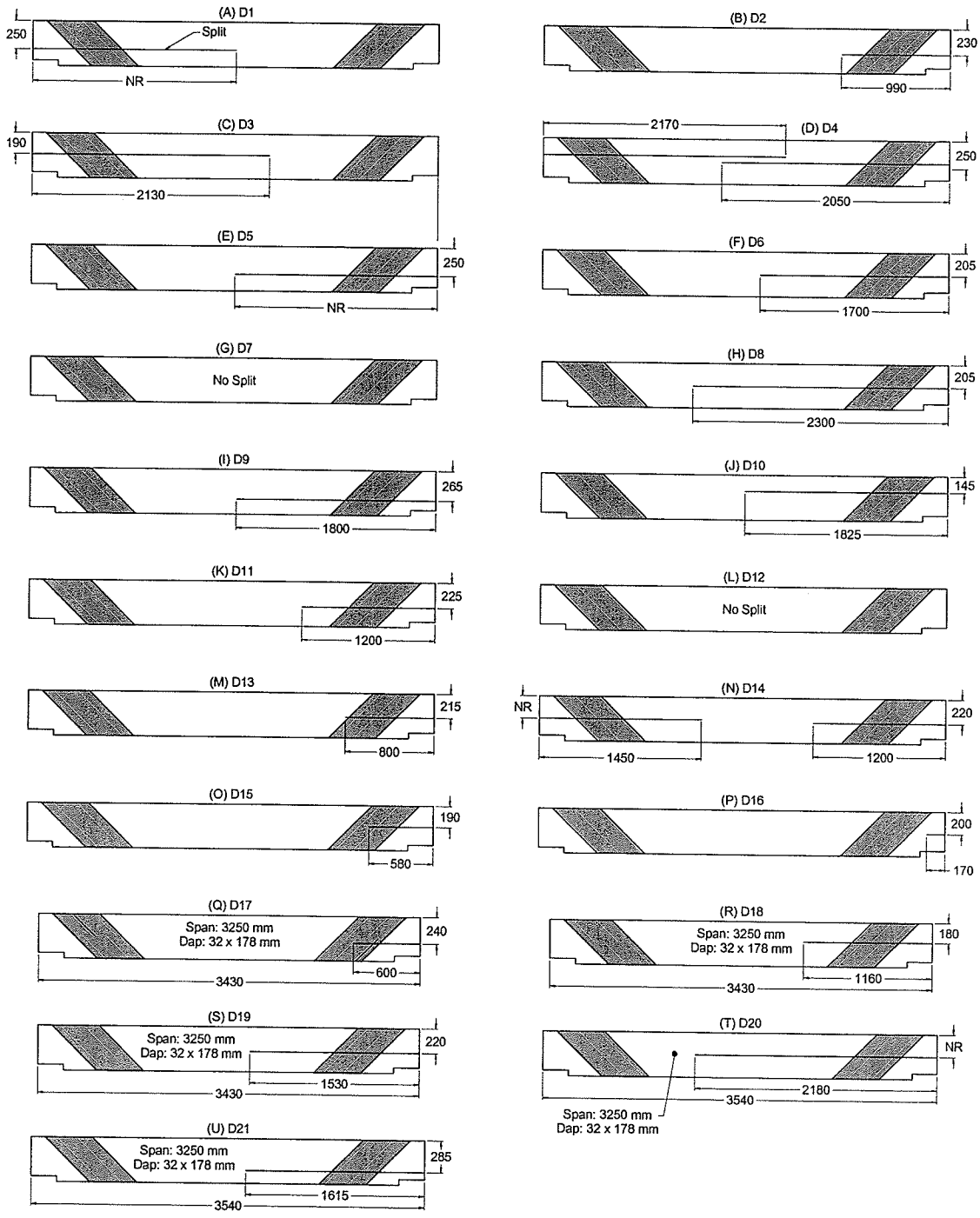

Figure 3.6 Diagrams showing location of splits and deviations from the standard specimen size for diagonal sheet specimens (NR = Not Recorded, all dimensions in mm)

Table 3.1 Control specimen grades

Specimen Designation	Computer File Name	Grade
C1	Y2-19	Reject
C2	Y2-25	Reject
C3	Y2-11	Reject
C4	Y2-12	Reject
C5	Y2-33	Reject
C6	Y2-9	Reject
C7	Y2-4	Reject
C8	Y2-5	Reject
C9	Y2-29	Select Structural
C10	B-15	Select Structural

Table 3.2 Vertical GFRP sheet specimen grades

Specimen Designation	Computer File Name	Grade
V1	Y2-22	Reject
V2	Y2-13	Reject
V3	Y2-10	Reject
V4	Y2-32	Reject
V5	Y2-8	Reject

Table 3.3 Diagonal GFRP sheet specimen grades

Specimen Designation	Computer File Name	Grade
D1	Y2-14	Reject
D2	Y2-101	Reject
D3	Y2-16	Reject
D4	Y2-103	Reject
D5	Y2-102	Reject
D6	Y2-109	Reject
D7	Y2-112	Select Structural
D8	Y2-111	Reject
D9	Y2-114	Reject
D10	Y2-105	Reject
D11	Y2-108	Reject
D12	Y2-107	Select Structural
D13	Y2-110	Reject
D14	Y2-113	Reject
D15	Y2-106	#2
D16	Y2-115	Select Structural
D17	Y1-116	#2
D18	Y1-117	Reject
D19	Y1-03	Reject
D20	Y3-03	Reject
D21	Y3-104	Reject

3.2.2 FRP Strengthening System

The stringers were strengthened using Master Builders MBrace™ Composite Strengthening System, which was designed for strengthening and rehabilitating concrete structures. This system is able to use a variety of fibres such as carbon, aramid and glass. In this experimental project, a uni-directional glass fibre sheet, MBrace™ EG 900 was used. This system usually consists of a primer, epoxy putty filler, a saturant and a top coating. The saturant is a 100% solids amine-cured epoxy and is designed for low-temperature cure. For the current project, it was necessary to only use the primer and saturant. The properties of

the two relevant components of the MBrace™ fibre reinforcement are listed in Table 3.4. Vector Construction Group in Winnipeg, Manitoba carried out the strengthening operation.

Table 3.4 GFRP mechanical properties

Material	Nominal Thickness	Ultimate Tensile Strength	MOE	Rupture Strain
	mm	MPa	MPa	%
EG 900	0.353	1520	72400	2.1
MBrace™ Saturant LTC	-	14	1138	5.3

3.3 Reinforcing Schemes

The initial phase of the experimental research, carried out to determine the preferred orientation of the GFRP sheets, consisted of testing:

a) Ten un-strengthened timber stringers as control specimens,

b) Five stringers with vertical GFRP sheets wrapped around the bottom of the stringer (Figure 3.7a), and

c) Five stringers with diagonal GFRP sheets wrapped onto the bottom of the stringer (Figure 3.7b).

Once the preferred sheet orientation had been determined -- diagonal as shown in chapter 4 -- a second group of sixteen stringers were strengthened and tested. This second group was further divided into two parts. The first eleven specimens were prepared without wrapping the GFRP sheets around the bottom (Figure 3.7c). The last five specimens were also prepared without wrapping around the bottom but an extension sheet was added later in response to dap failure problems that had developed in the previous eleven specimens (Figure 3.7d and 3.7e). The additional GFRP sheets extended 100 mm up the side of the

stringer on the original sheet. The bottom portion wrapped around the bottom of the stringer and was overlapped by the sheet coming from the other side.

The test samples were denoted as "C" for control specimens, "V" for vertical sheet specimens and "D" for diagonal sheet specimens. Each individual specimen was given a number that corresponded to the order in which the tests were completed. Two tests were conducted on each specimen and these are denoted by an "A" for the solid end test, i.e. the solid end of the beam was closer to the load point than the split end, and "B" for the split end test. As an example C3B refers to the third control specimen tested and the split end was closer to the load point.

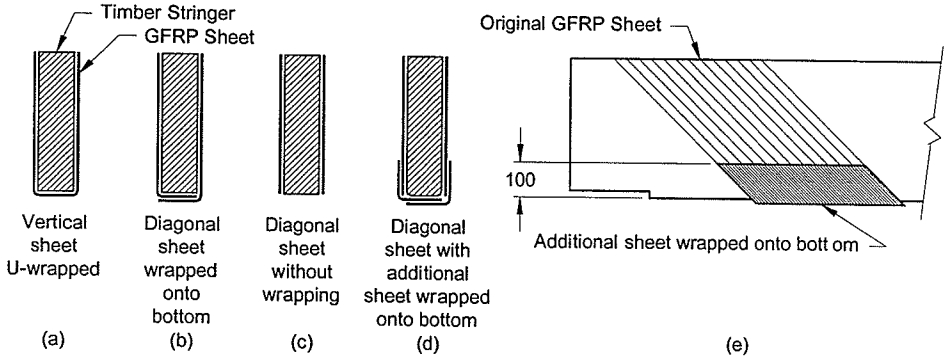

Figure 3.7 Details of stringer reinforcing schemes

The diagonal reinforcing scheme consisted of sheets placed at a 45 degree angle to the beam axis. The GFRP sheets used in the research are manufactured in rolls with a 600 mm width. To avoid wastage, a sheet width that evenly divided into the roll width was chosen, being 300 mm. Further, the 300 mm wide sheet also fit in the space between the support and quarter span loading point. The starting position for the diagonal sheets was at a point on the top edge of the stringer directly above the support.

3.4 SPECIMEN PREPARATION

The weathered timber stringers had accumulated dust and debris, and usually had soiled surfaces. The first step of surface preparation was to lightly brush the stringers with a soft bristle brush while vacuuming up the generated dust. In the first stage the sheets were wrapped without rounding the edges in an effort to avoid disturbing the creosote filled wood. However, due to limitations of the GFRP sheets ability to bend around sharp corners, the sheets were unable to maintain contact with the wood within 25 mm of the edges. In the second group the sheets were not wrapped onto the bottom, however, this was not successful and when the additional sheet was added, the edges of the timber were rounded to a radius of 12.7 mm to enable the GFRP sheet to maintain contact with the surface.

In the first stage of the research, prior to the application of the GFRP sheets on two of the specimens, the horizontal split in the timber was closed using a pipe clamp as shown in Figure 3.8. The other specimens either did not require split closure or the splits were left open. In the second stage of the research all the specimens, except for two, that had horizontal splits had the splits closed using a pipe clamp and then held closed using a lag bolt from the bottom of the specimen. The lag bolts were 12.7 mm by 300mm long, galvanized steel and required a 50 mm diameter washer to prevent crushing of the wood. They were placed 300 mm from the end of the specimen and required a 12.7 mm diameter pilot hole drilled to the depth of the split and then a 10 mm diameter hole was drilled to the full 300 mm depth from the bottom of the pilot hole as shown in Figure 3.9. The lag bolt was intended to close the splits but was not able to create enough force and the thus the pipe clamp was used. The intent of only placing lag bolts from the bottom of the beam was to simulate conditions during a real bridge rehabilitation project where access to only the

bottom of the beam would be available. In field use, a mechanical device would have to be developed, a possible example of which is shown in Appendix C, which can clamp onto the side of the beam and pull the split closed. The two exceptions in which lag bolts were not used had splits too high on the beam to be closed by the 300 mm lag bolt. These specimens had the split closed using the pipe clamp which were left in place until the saturant had cured enough to hold the split closed with the sheets.

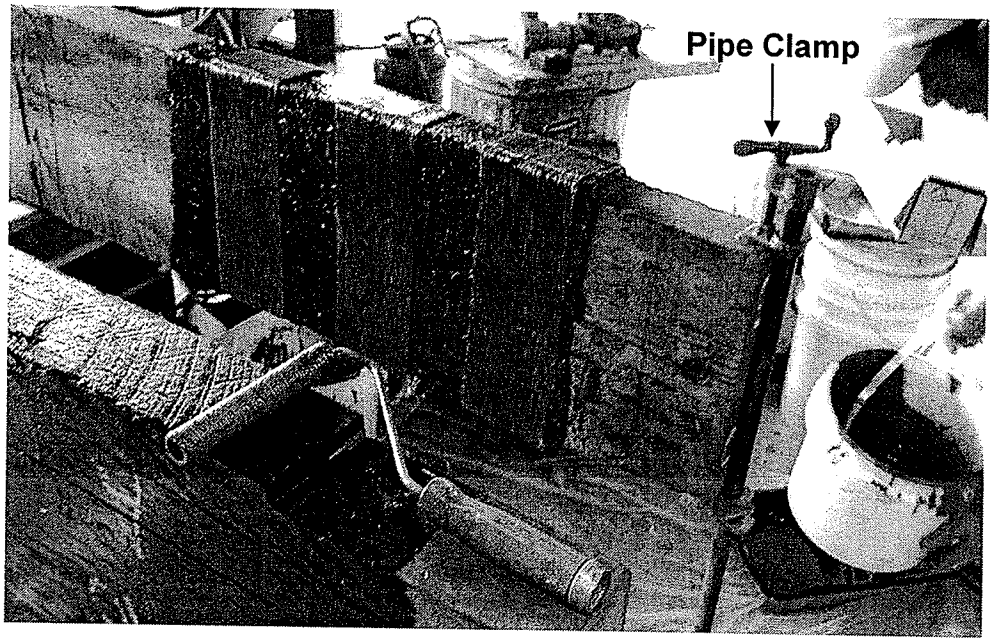

Figure 3.8 Picture showing pipe clamp used to close splits

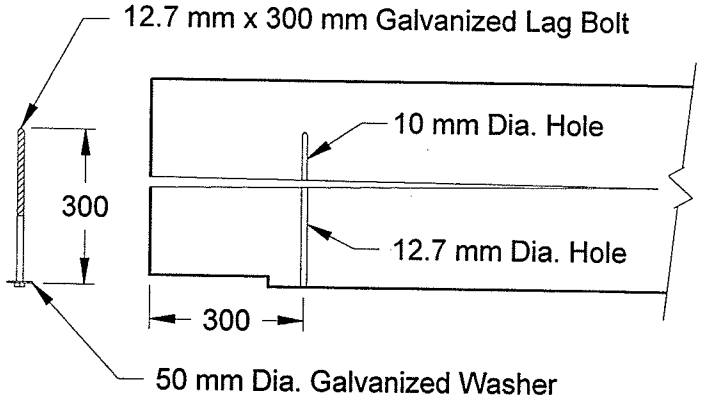

Figure 3.9 Placement detail of lag bolt used to hold splits closed

The first step of the sheet application was applying the primer with a short nap roller (Figure 3.10). Following the primer, a coat of saturant was applied with a short nap roller (Figure 3.11) and then the sheet was placed on the saturant (Figure 3.12) followed by embedding it into the saturant using a grooved steel roller (Figure 3.13). A second coat of saturant was applied (Figure 3.14) to finish the application which is shown in Figure 3.15. The beams were then allowed to cure for a minimum of 7 days before testing. In the second stage of installation, when the additional sheet was added to the original sheet, it was deemed unnecessary to apply primer to the original sheet to achieve proper bond.

Figure 3.10 Applying primer

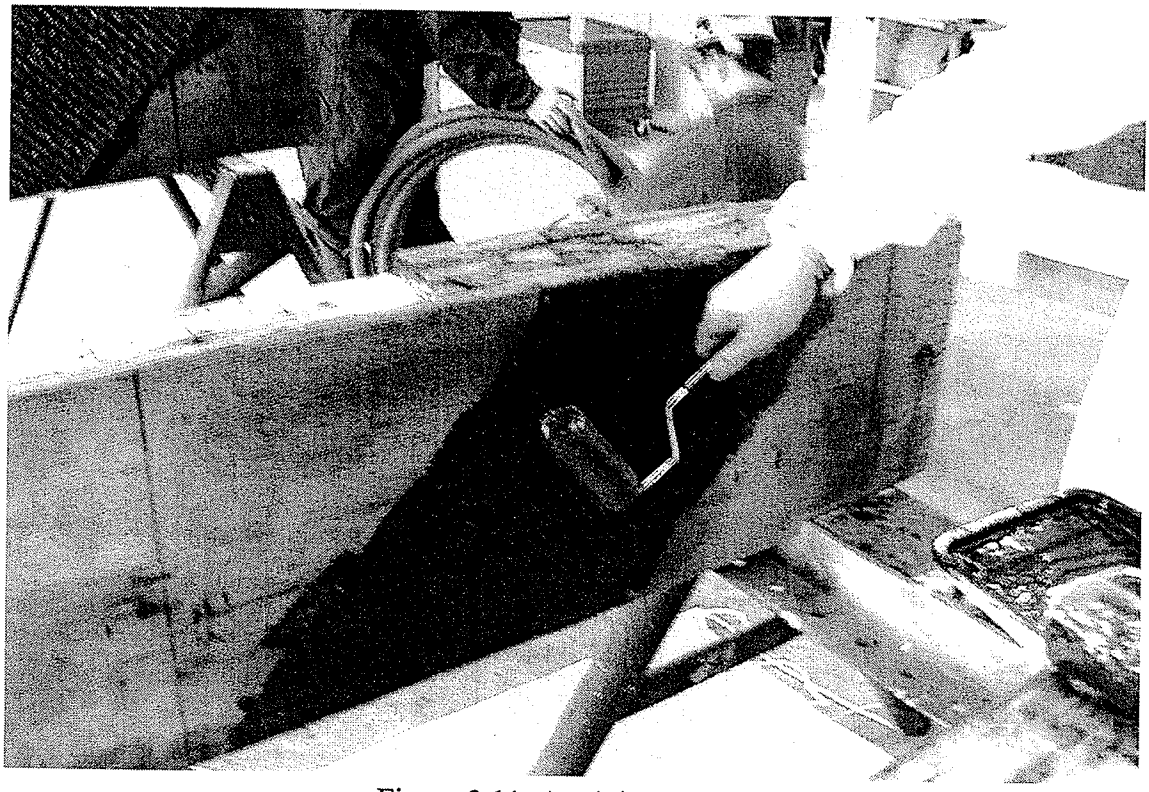

Figure 3.11 Applying saturant

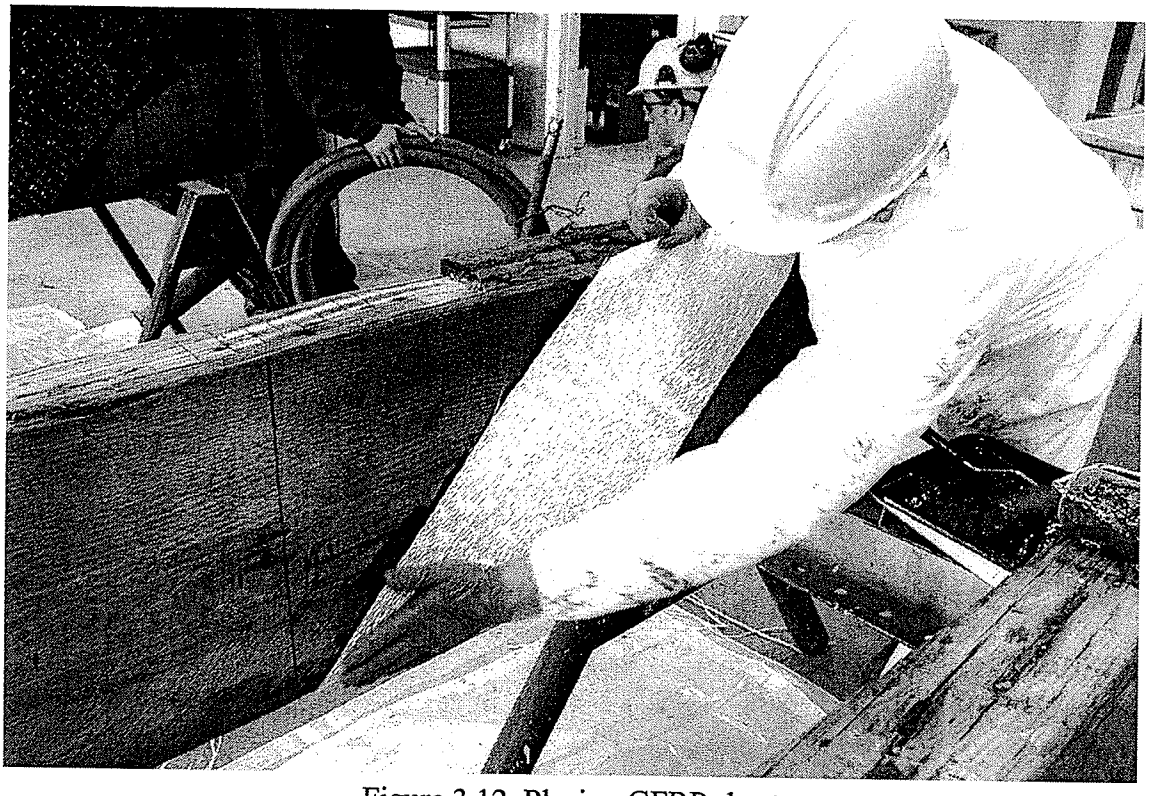

Figure 3.12 Placing GFRP sheet

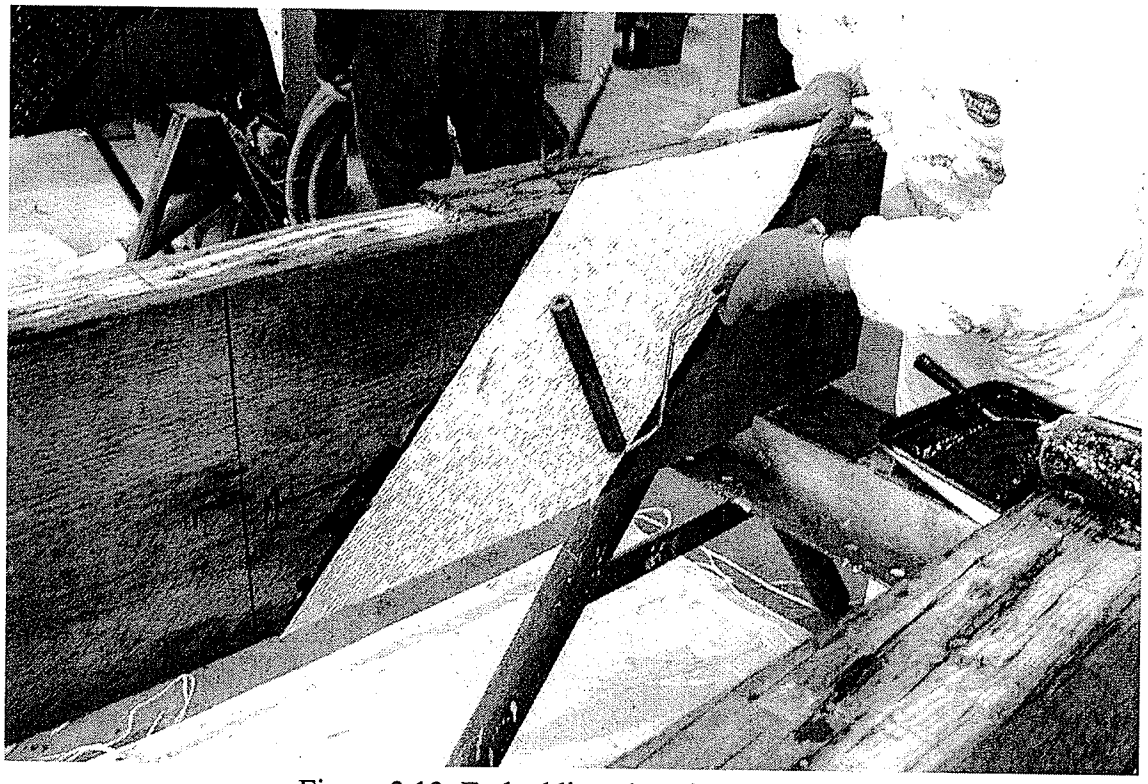

Figure 3.13 Embedding sheet into saturant

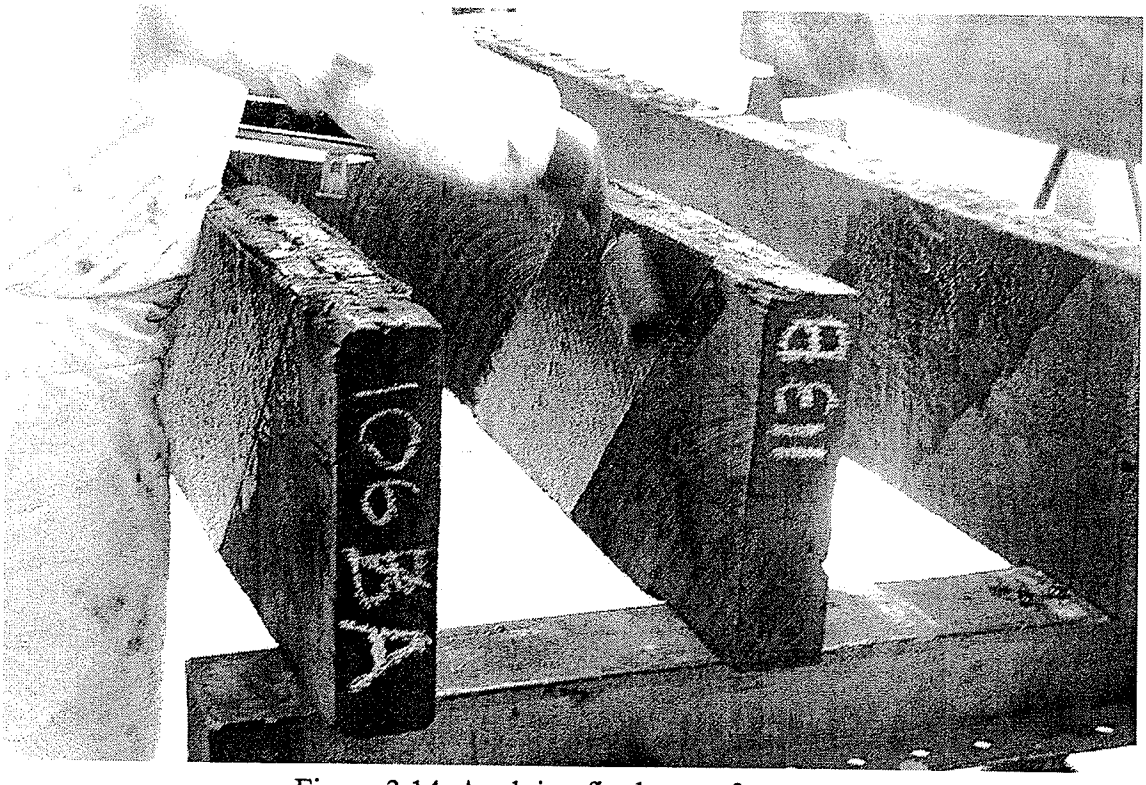

Figure 3.14 Applying final coat of saturant

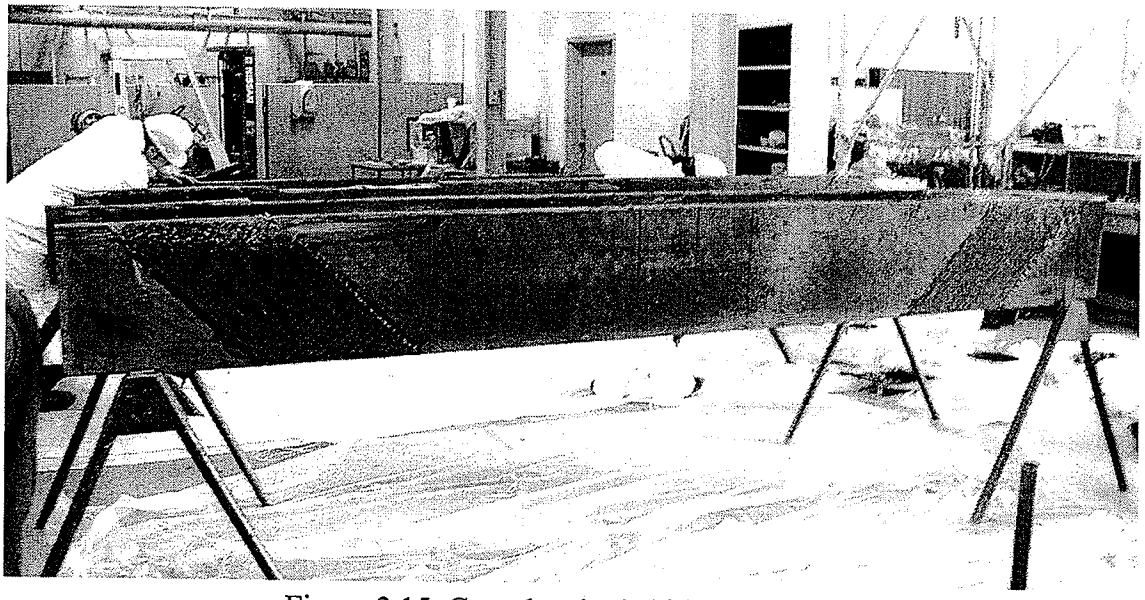

Figure 3.15 Completed rehabilitated stringer

3.5 TEST SET-UP

As can be seen in Figure 3.3, the stringers were loaded at quarter span in order to generate high shear stresses but low flexural stresses. This scheme of testing allowed a second shear test to be performed at the opposite end of the stringer. The testing of the same stringer for two shear tests was important because full-scale timber stringers, removed from an existing bridge, are costly and difficult to obtain.

The test span was 3400 mm and the centre of the concentrated load was 850 mm from the centre of the nearer support, as shown in Figure 3.3. The beams were tested under a displacement control set-up with a rate of displacement of 4 mm per minute, allowing for the maximum load to be reached in approximately 10 minutes as prescribed by ASTM D198-99.

The bearing supports used were 220 mm long which is a little less than the dap length size and allowed for adjustment room. At the load point a 500 mm long steel plate was used to distribute the load. A large plate was necessary at the load point because wood on top of the stringer had degraded, and thus has little bearing strength.

3.6 INSTRUMENTATION

The instrumentation for the research program consisted of 125 mm linear variable deflection transducers (LVDTs) to measure deflections and strain gauges to measure strains in the GFRP sheets in the direction of the fibres. As shown in Figure 3.16, the deflections were measured at three locations along the stringers, with an LVDT placed on either side of the stringer at each location. The deflections were measured directly under the load point, at mid-span and at the point of maximum deflection, located 200 mm from the mid-span of the stringer towards the loading point. The LVDTs were calibrated before the testing program began and periodically throughout the experimental work. To calibrate the LVDTs, they were connected to a computer data acquisition (DAQ) system and then attached to a micrometer that could accurately displace the LVDT's shaft. The LVDT was displaced in small increments while recording the voltage change to calibrate them. The precision of LVDT's was 0.1875 mm (±0.15% of 125 mm full displacement).

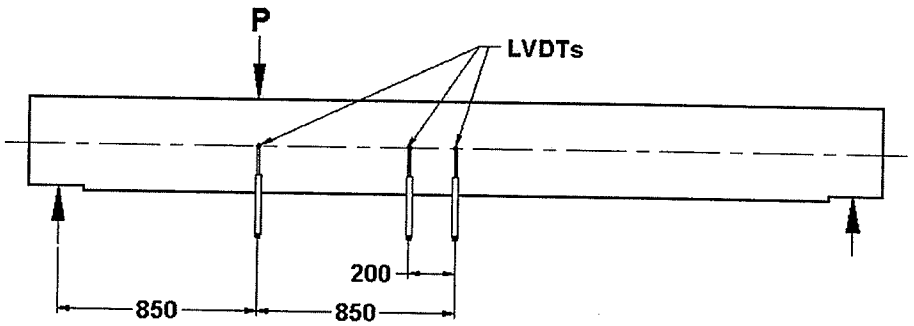

Figure 3.16 LVDT locations (all dimensions in mm)

Several different arrangements for strain gauge locations were investigated in an effort to optimize placement and number of gauges versus the time and money required to install them. Eight different configurations were used for diagonal sheet specimens and two configurations for vertical sheet specimens. A listing of the strain gauge layouts and the

corresponding specimens that they were used on are shown on Table 3.5. For the first vertical sheet specimen, V1, where three closely-spaced strips were applied (Figure 3.17(A)), three gauges were placed on the middle strip on both ends and sides. Three additional strain gauges were placed on each of the outer strips on one side of the solid end of the specimen to determine the variation between the GFRP strips. On the remaining vertical sheet specimens, 3 strain gauges were placed on the middle strip with additional strain gauges placed at mid-height on the outer strips as shown in Figure 3.17(B). The diagonal sheet specimens are shown in Figures 3.18 and 3.19. In all configurations the gauges were placed along the centre line of the sheet in the direction of the fibres. On layout #2 shown on Figure 3.18(B), two additional rows of strain gauges were added 50mm away from the edge of the sheet in the direction of the fibres. This was done to investigate the variation of strains on the sheets and was done only on one side of the specimen at the split end. At first three strain gauges were used on each sheet; however an investigation of five strain gauges per sheet was done on D6 and D7 to better understand the strain profile, after which it was decided that the gauges near the end of the fibres were not needed because they typically showed low strains. From specimen D8 three strain gauges were used on the solid end of the specimen and one strain gauge at the split end near the split but not right on it since the gauge would get damaged during loading when the split starts to move. On the last six diagonal sheet specimens, an additional gauge was added 50 mm from the bottom of the sheet to determine if higher than expected strains were occurring near the bottom of the sheet that were causing dap failure. The various strain gauge locations were chosen to determine the most optimum sensor arrangement so that the variation of the strain along the length of the sheets in subsequent tests could be observed without missing the maximum strains.

The readings from the LVDTs and strain gauges were recorded at one second intervals through out the test using the DAQ.

Table 3.5 Listing of strain gauge layouts and their corresponding specimens

Sheet Orientation	Strain Gauge Layout	Specimens
Diagonal	1	D1,D3,D4,D5
	2	D2
	3	D6,D7
	4	D10,D11,D12,D15
	5	D8,D9,D13
	6	D14
	7	D16,D17
	8	D18,D19,D20,D21
Vertical	1	V1
	2	V2,V3,V4,V5

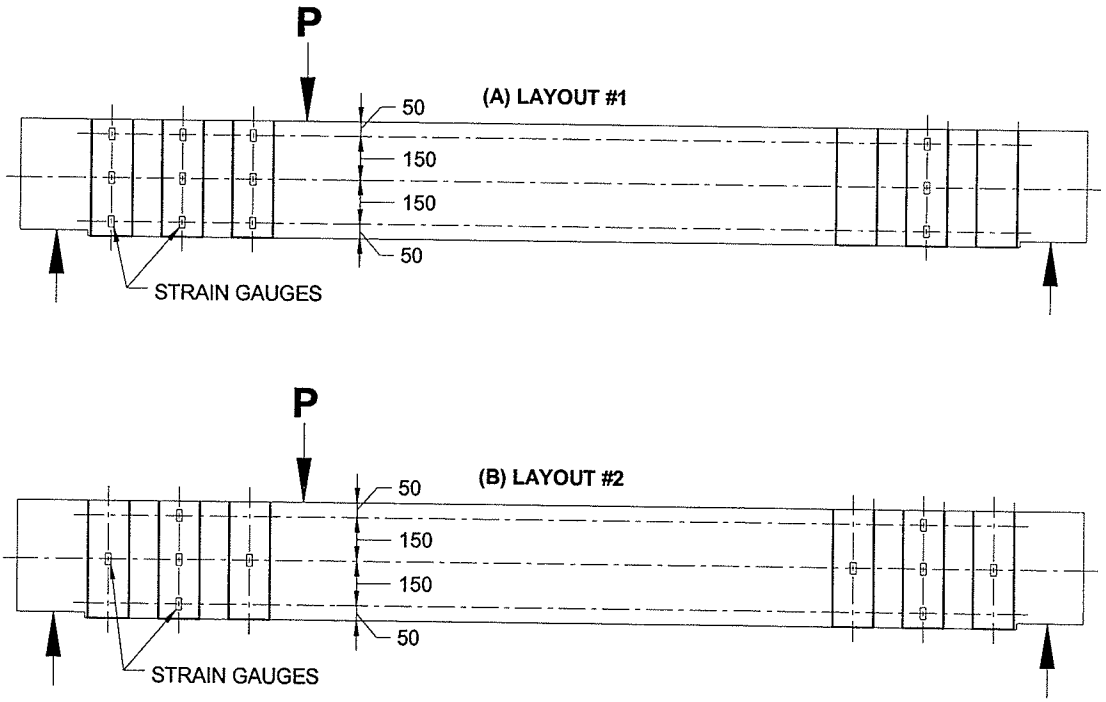

Figure 3.17 Vertical sheet strain gauge layouts (all dimensions in mm)

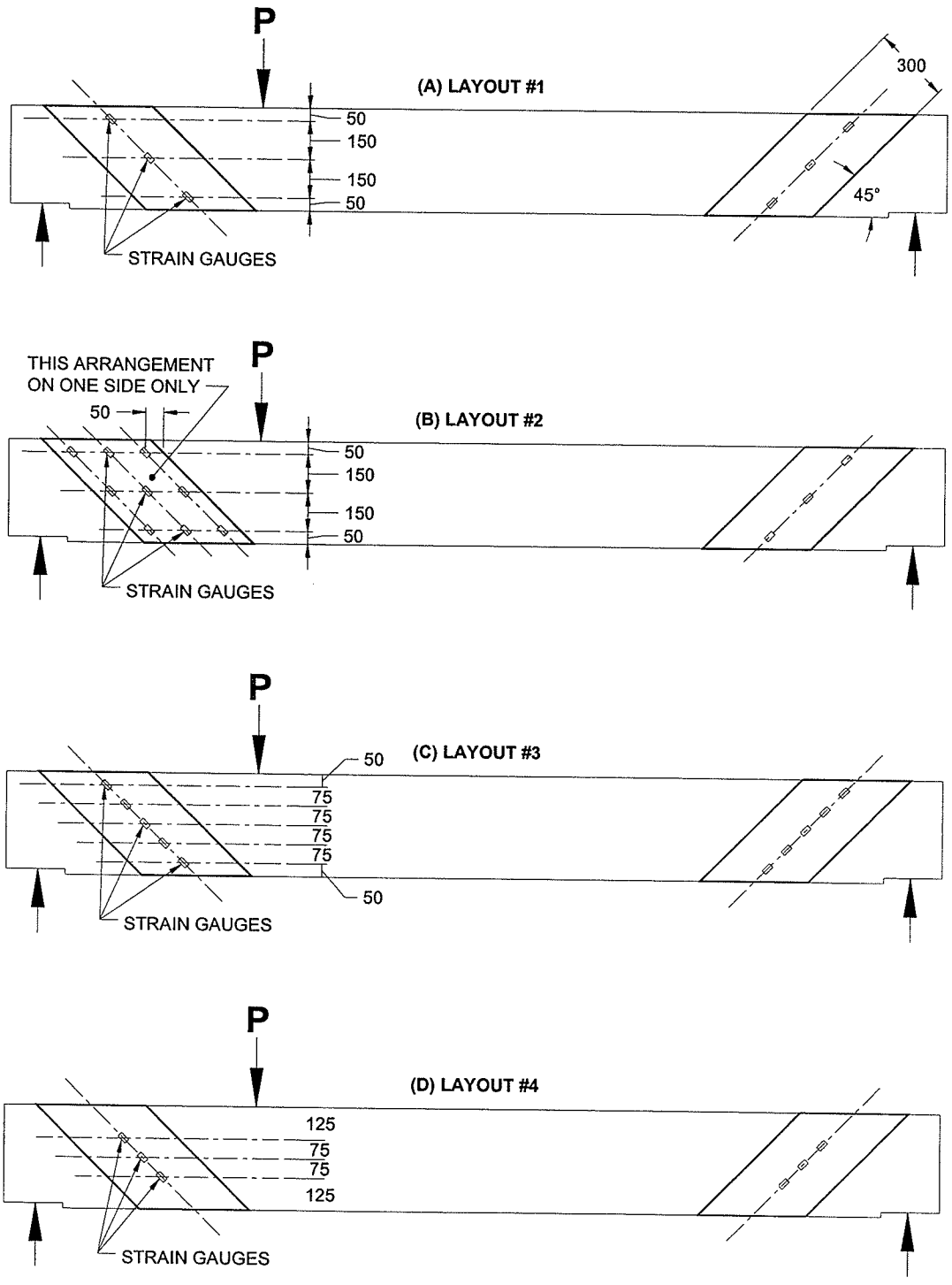

Figure 3.18 Diagonal sheet strain gauge layouts 1 to 4 (all dimensions in mm)

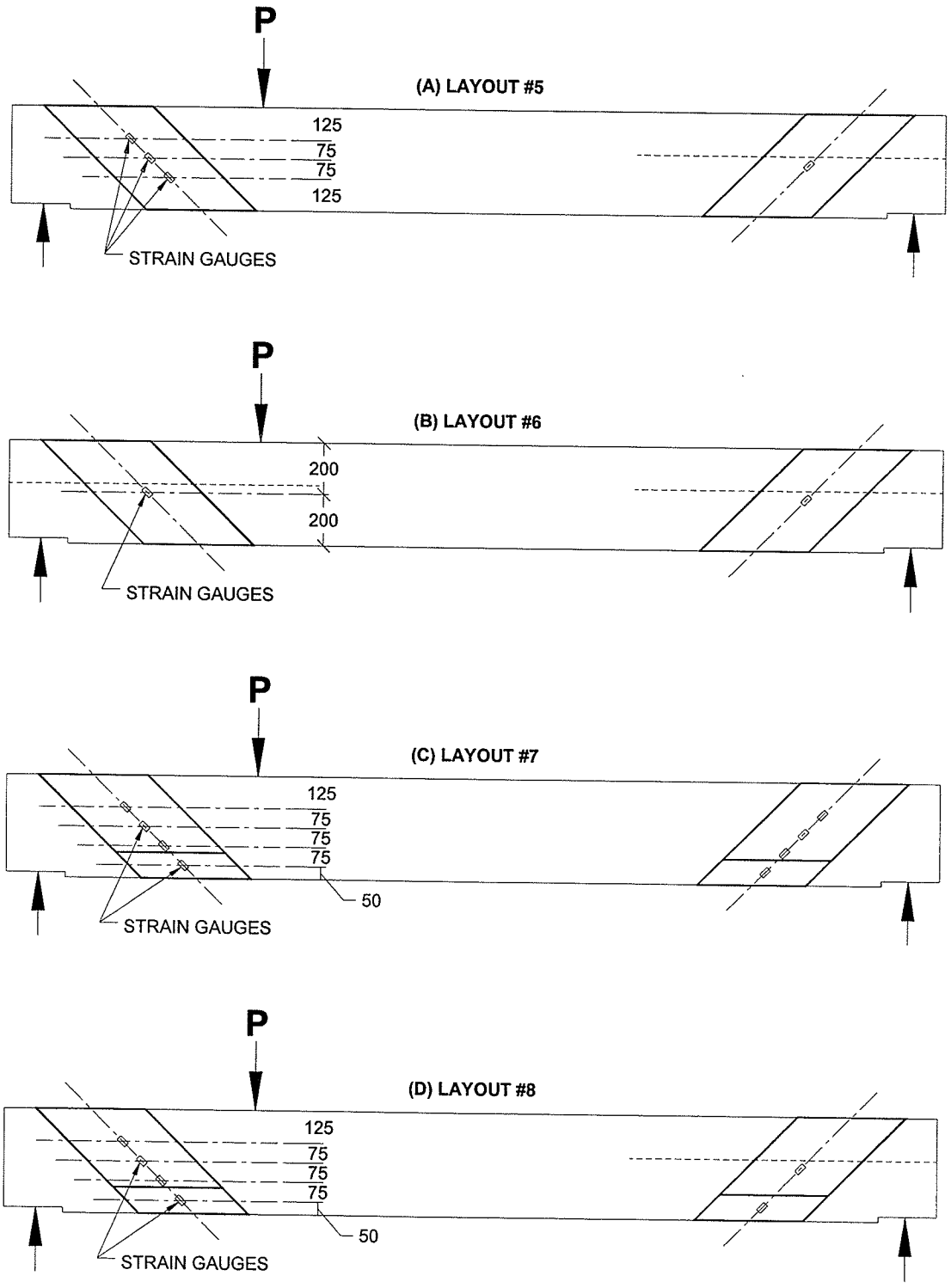

Figure 3.19 Diagonal sheet strain gauge layouts 5 to 8 (all dimensions in mm)

CHAPTER 4 EXPERIMENTAL RESULTS AND DISCUSSION

4.1 Overview

This chapter details the results of the experimental program. The test data collected was used to determine the performance of the two reinforcing schemes in relation to the control specimens. To be reviewed are the load/deflection behaviour, ultimate load, shear stress, flexural stress, stiffness, stresses in the GFRP sheets, modes of failure and performance of the sheets during the test.

4.2 Load-Deflection Behaviour

The load-deflection curves for all tests are shown in Appendix A, where both tests on each specimen are shown on one chart. The control specimen load-deflection curves show a large variation in stiffness and strength. Typically, the specimens acted linearly until cracking at about a load of 40 to 50 kN after which the stiffness of the beam started to decrease. With further increase in load some of the samples started to show signs of bearing problems. This was exhibited by inspection of the load-deflection curves, when a plateau had developed that signified that further load cannot be carried by the beam. The bearing failure at the load point is a result of the weak state of the wood fibres on the top of the beam or at the supports. All stringers had been salvaged from old bridges, and therefore the wood was significantly weathered in some cases.

There were 2 tests performed on each stringer. Typically the first test, which, except for two specimens, was performed on the solid end first, showed better results than the second test. The first of these two specimens in which the split end was tested first,

specimen C1 (Figure 4.1), performed better during the first test than during the second test despite the split, however the stiffness was lower. The second specimen, C7 (Figure 4.2), performed better during the second test as expected because the solid end was being tested. The beams frequently would have sudden drops in load when timber cracked, but would then regain the load and continue to higher loads showing that timber has the ability to redistribute load. The source of the cracking was difficult to determine from visual inspection and thus appears that it is internal. Any cracking of the stringer that was visually apparent usually resulted in the failure of the specimen. This shows that it is possible to have damaged beams that cannot be determined by visual inspection. One control specimen that showed cracking and continued to sustain substantially higher loads was C10 shown in Figure 4.3. The load drop at approximately 60 kN was the beginning of shear failure. Despite the beam shearing the load was redistributed and much higher loads were attained.

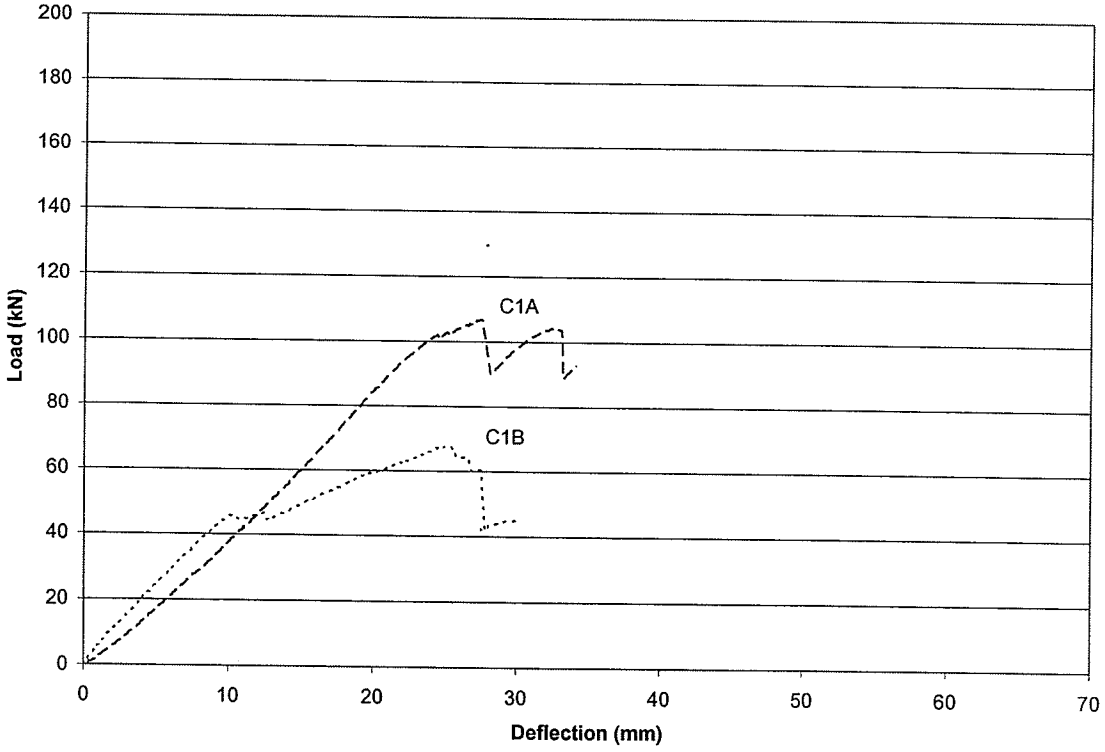

Figure 4.1 Load-Deflection curves for control specimen C1 (Y2-19)

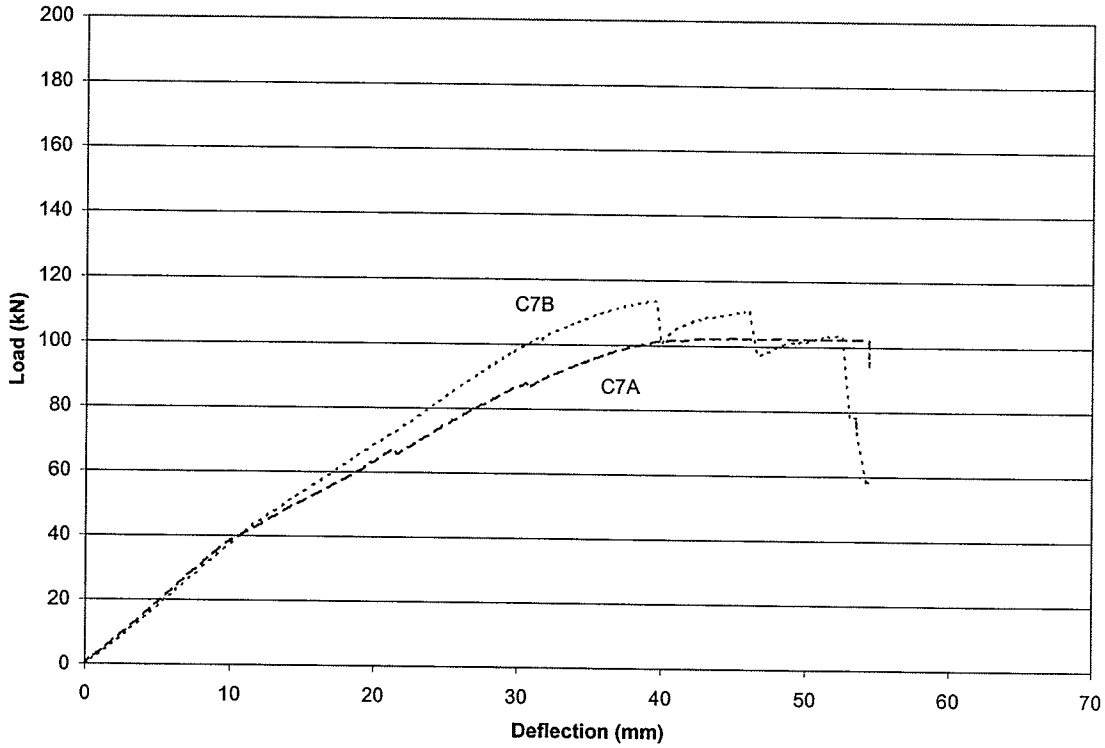

Figure 4.2 Load-Deflection curves for control specimen C7 (Y2-4)

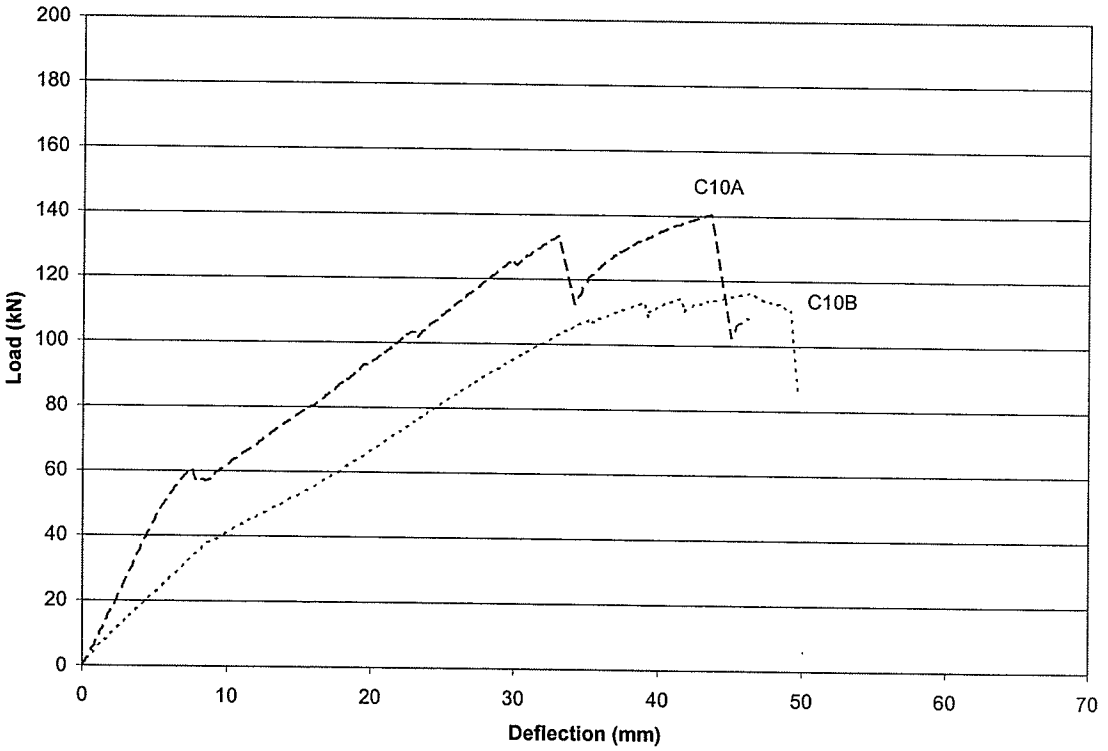

Figure 4.3 Load-Deflection curves for Control Specimen C10 (B15)

The upper and lower bounds of the load-deflection behaviour of control specimens are compared in Figure 4.4 with those of corresponding specimens strengthened with vertical (group V) and diagonal (group D) GFRP sheet specimens. The vertical sheet specimens' load-deflection behaviour exhibited large variability, showing that the typical variability was not improved using this strengthening technique. It can be seen in Figure 4.4 that vertical sheets are not effective in improving their stiffness. There was a marginal improvement in strength for the beams in group V in comparison with control beams, especially in lower timbers represented by the lower bound curve in Figure 4.4. The upper bound curve for V group was identical with that of control samples. The diagonal sheet specimens, group D, showed an improvement in stiffness as can be seen in Figure 4.4 by the shift in the curves to the left and upwards. Further, the ultimate strength is also shown to have improved. However the best specimens of from groups C and V are able to perform similarly to the lower bound of group D specimens. The group D specimens also displayed a large variability in ultimate load but the stiffness was less variable. The improvement over the groups C and V is evident from Figure 4.4, where the lower bound curve for group D is close to the upper bound curve of C and V samples.

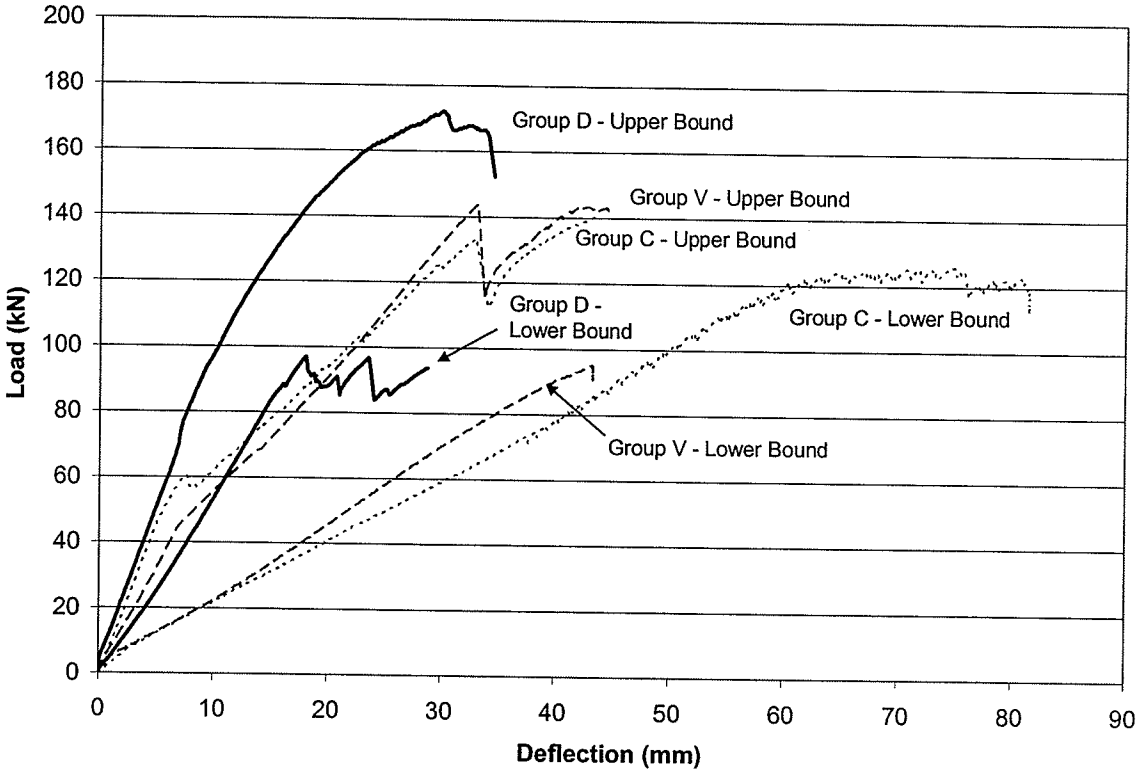

Figure 4.4 The effect of vertical and diagonal sheets on beam behaviour

The load-deflection curves for group V specimens given in Appendix A show that in four out of five specimens the first tests conducted on a specimen performed better by reaching higher ultimate loads and showing greater stiffness than the second tests. On specimen, V1, with results plotted in Figure 4.5, the second test reached a higher ultimate load than the first test but with a lower stiffness. The first test on four of the specimens was conducted on the solid end, thus it would be expected that they should perform better than during the second test, this was the case except for specimen V1, which as noted was stiffer but reached a lower ultimate load. The other specimen, V2, was tested on the split end first and performed better in this test despite the second test being on the solid end. The second tests on each of the specimens exhibited greater deformability; however these tests were left to run longer than the first tests because the first test was stopped shortly after ultimate load was reached to avoid damaging the beam excessively. Generally the vertical sheet specimens

acted linearly at first; however two specimens, V1A and V3A (Figures 4.5 and 4.7), had sharp declines in their curves at relatively low loads, approximately 20 and 45 kN loads respectively, and continued linearly at a lower stiffness. It seems that the seating of the testing assembly was responsible for this behaviour. In all vertical sheet specimens, except V2B (Figure 4.6) and V1B (Figure 4.5), the load levelled off towards the end of the test indicating possible bearing failure.

Strengthening with diagonal sheets had two effects: (a) the slope of the load-deflection curves is increased, thus indicating a marked improvement in the stiffness of the stringers, and (b) the area under the load-deflection is increased significantly, thus confirming a large increase in the deformability of the beams.

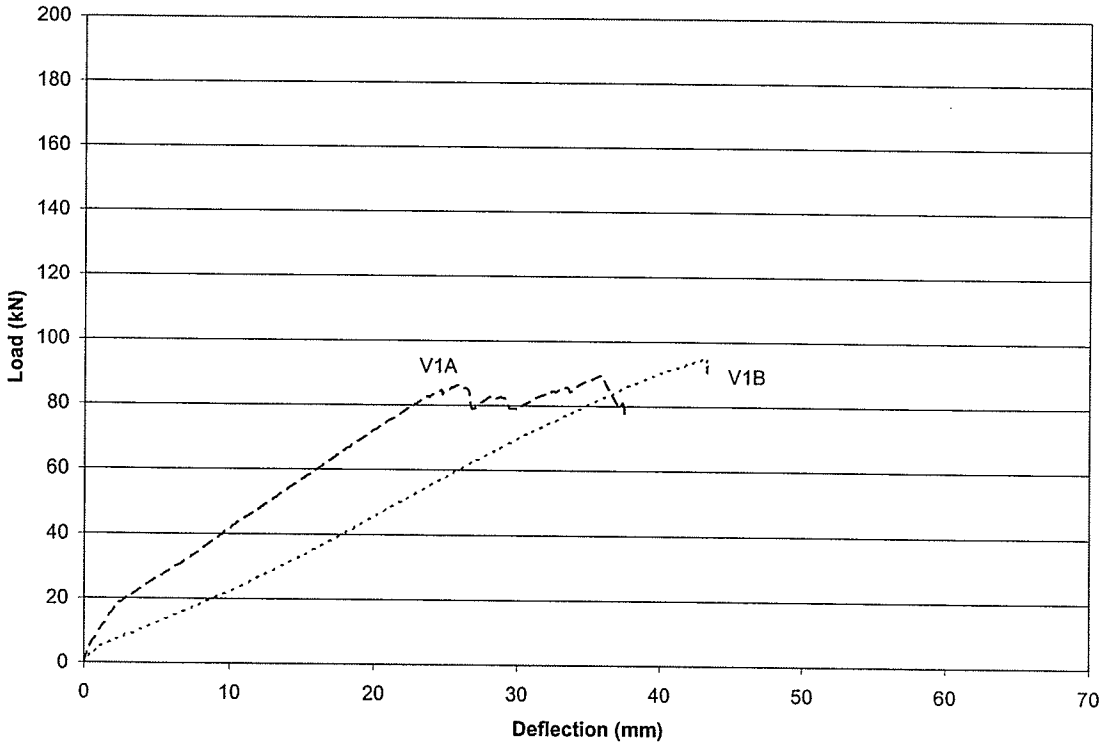

Figure 4.5 Load-Deflection curves for vertical sheet specimen V1 (Y2-22)

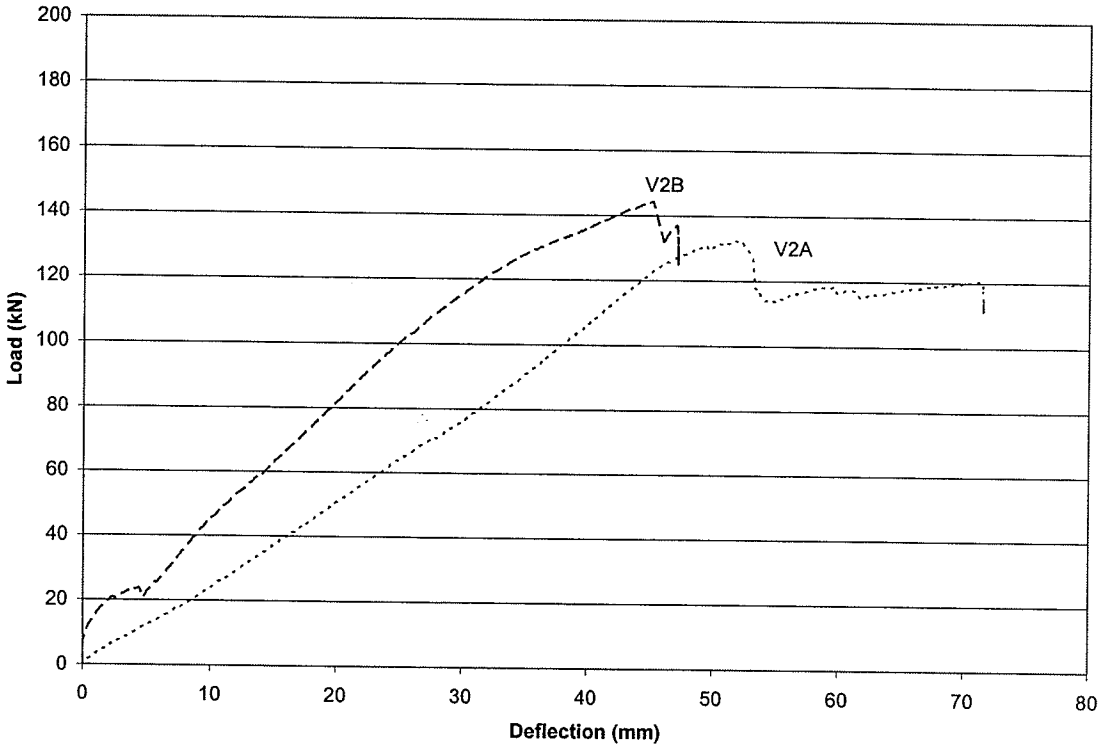

Figure 4.6 Load-Deflection curves for vertical sheet specimen V2 (Y2-13)

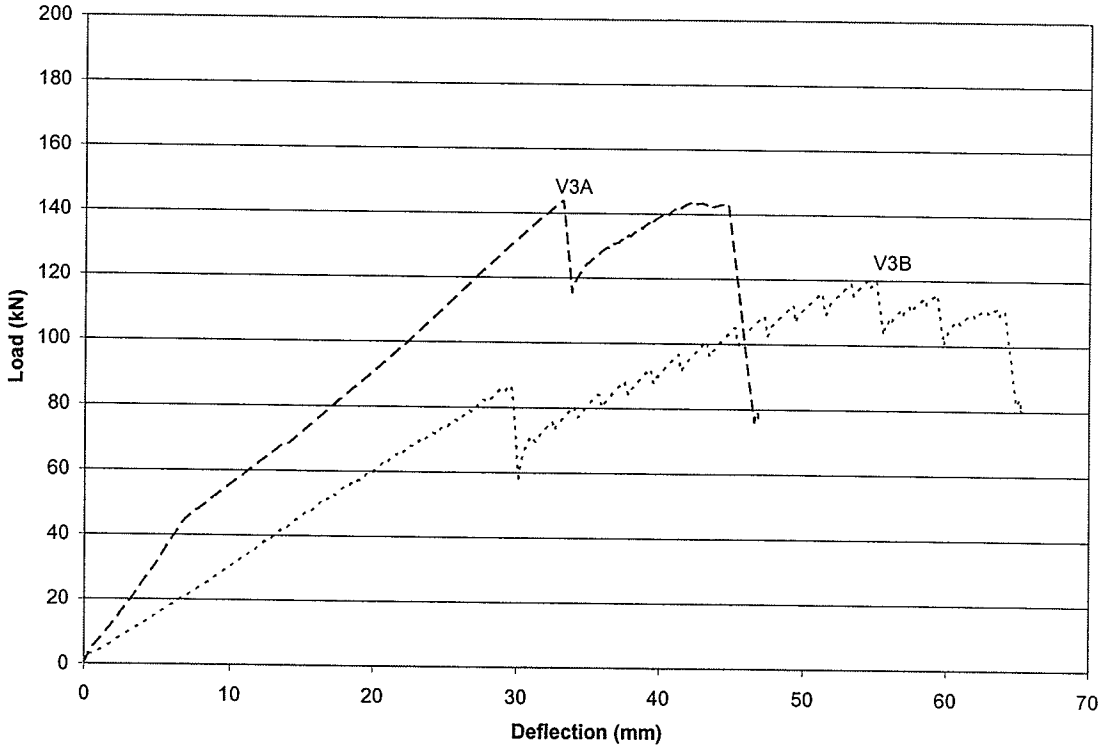

Figure 4.7 Load-Deflection curves for vertical sheet specimen V3 (Y2-10)

The first test on diagonal specimens was always run on the split end first, thus the second test conducted on the solid end was expected to run nearly as well or better than during the first test. This was confirmed by testing, although in general the first test was slightly better than the second. The second test on the diagonal sheet specimens was allowed to run longer after ultimate load was reached and shows the greater deformability of beams with GFRP sheets.

The diagonal sheet specimens generally acted linearly up to about 80 kN load level beyond which the stiffness of the beam began to drop. Some beams experienced a horizontal plateau of the curve indicating a bearing type failure. Tests D1B and D4A (Figures 4.8 and 4.9) acted bi-linearly at first increasing stiffness at approximately 15 kN; and D4B and D5B (Figures 4.9 and 4.10) did not act in a linear fashion at the beginning of the test showing that the stiffness was varying until about 60 kN where stiffness began acting in a linear fashion. These anomalies are because the existing shear splits were not closed tightly during preparation.

The load deflection curves for diagonal sheet specimens show a reduction in the variability of timber specimens but still show a wide variety of behaviour. The diagonal sheet specimens displayed the ability of timber to redistribute load. Many of the curves reveal instances where a crack in the timber has occurred resulting in a loss of load followed by the specimen regaining most of or the entire load and continuing on to higher loads. With the GFRP sheets this may be due to the stresses in the wood being transferred to the sheets after the wood has been damaged.

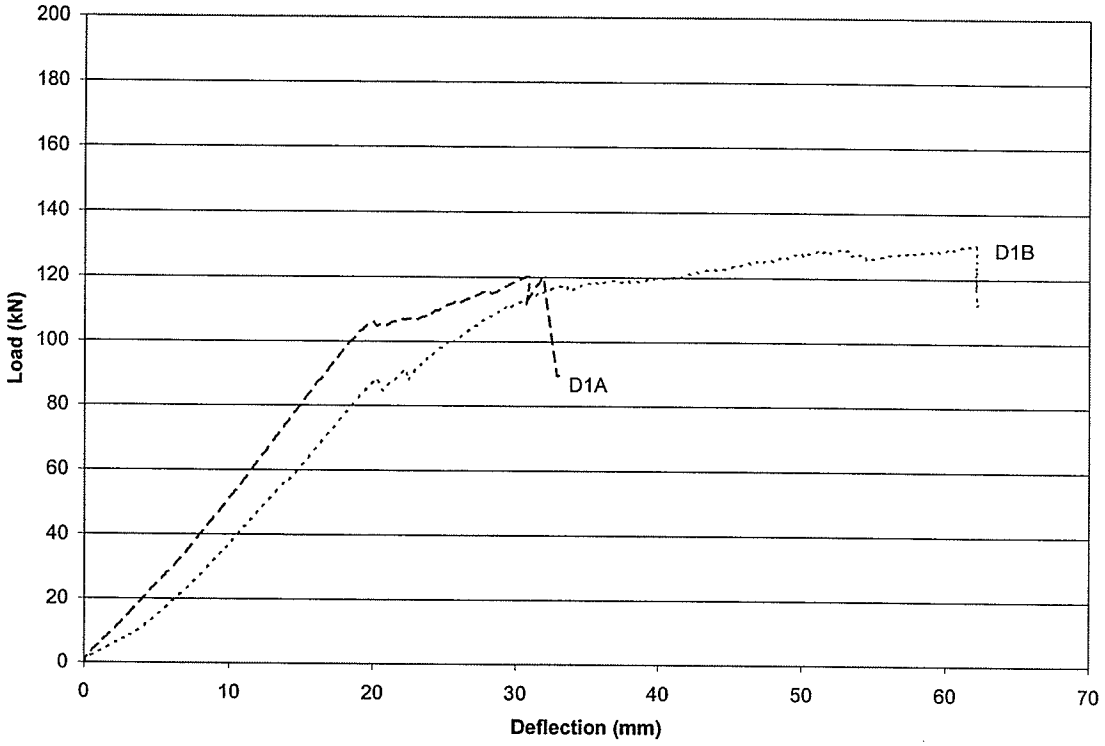

Figure 4.8 Load-Deflection curves for diagonal sheet specimen D1 (Y2-14)

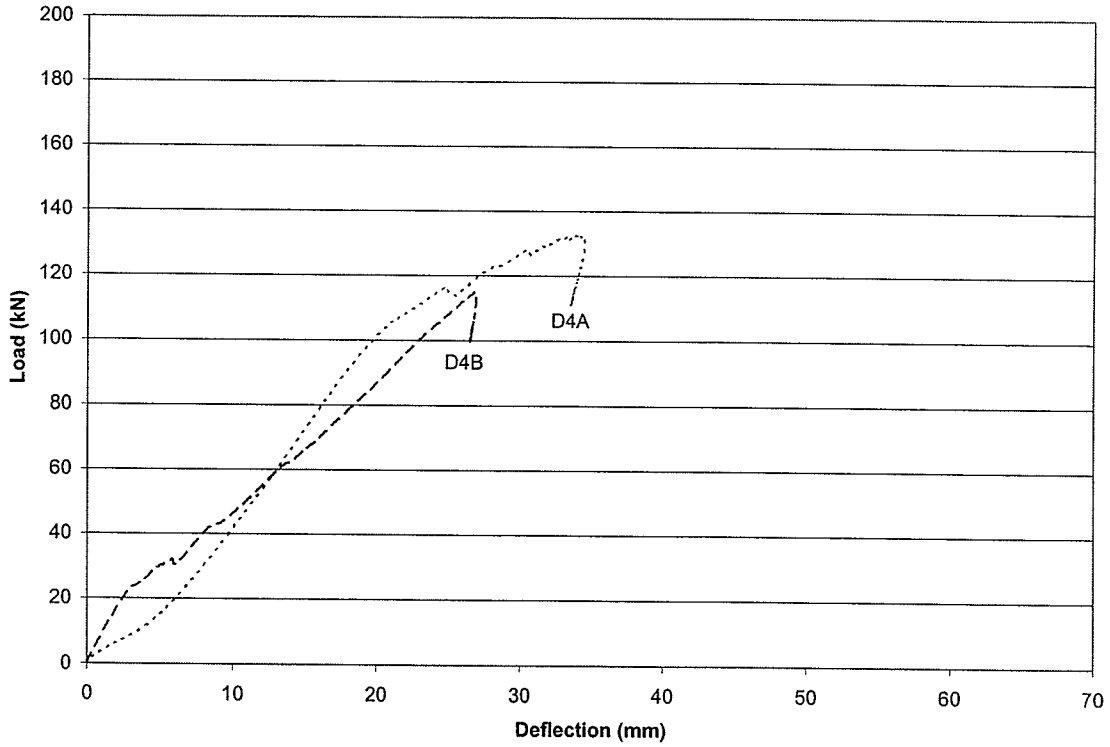

Figure 4.9 Load-Deflection curves for diagonal sheet specimen D4 (Y2-103)

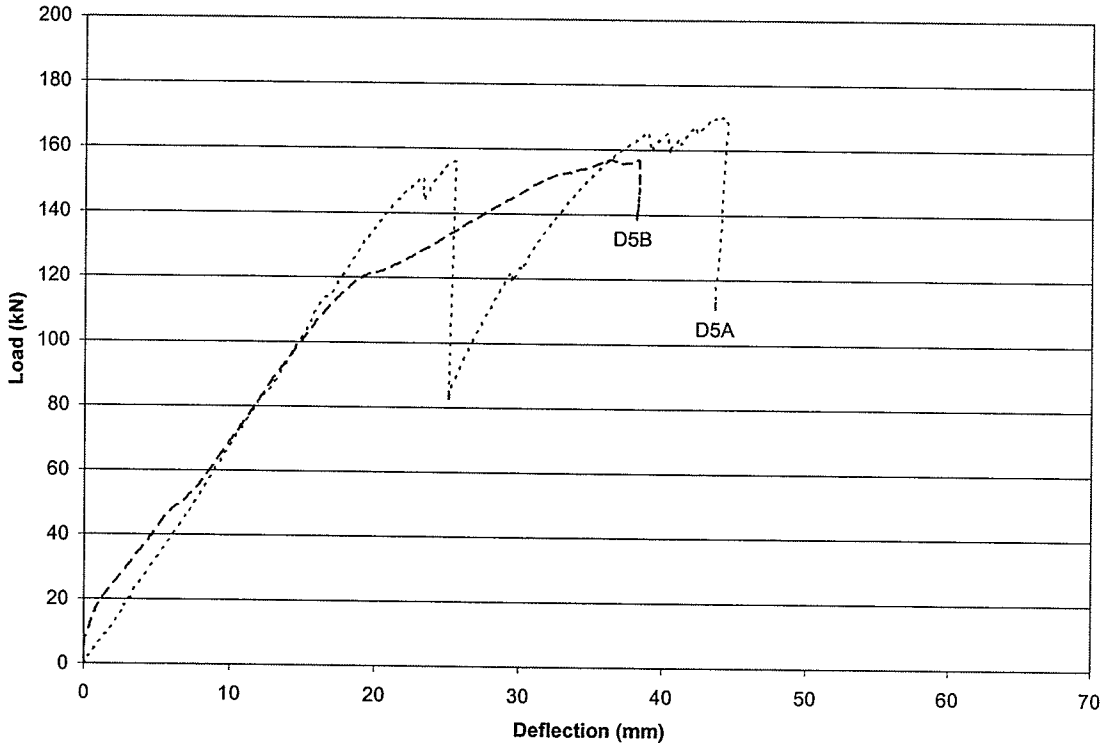

Figure 4.10 Load-Deflection curves for Diagonal Sheet Specimen D5 (Y2-102)

4.3 ULTIMATE LOAD

Control stringers without strengthening were tested to failure to establish a strength base line. A total of 10 stringers were tested at each end, thus giving a set of 20 failure loads. The ultimate loads for control specimens are listed in Table 4.1 along with some relevant information. The average failure load of the control specimens was 102.5 kN, the lowest load was 54.1 kN, and the highest 140.5 kN. The large difference between the lowest and highest loads shows the large variability in the properties of timber, and thus highlights the difficulty in establishing reliable strength data especially for previously damaged samples. The standard deviation was 22.3 kN resulting in a coefficient of variation of 21.7%.

Similar to the control specimens, the strengthened stringers were also tested to failure at each of their ends. The ultimate loads for vertical sheet specimens are listed shown in Table 4.2. The ten tests on five specimens with vertical GFRP sheets led to an average

failure load of 119.3 kN, indicating a 16.4% increase over the control specimens. The minimum ultimate load on these specimens was 83.1 kN, while the maximum load was 165.1 kN. The standard deviation was 27 kN giving a coefficient of variation of 22.6%, a slight increase over the control specimens.

Table 4.1 Experimental results for control specimens

Specimen Designation	Grade	Ultimate Load	EI^{Final}	Failure Mode	Maximum Shear Stress	Maximum Flexural Stress
		kN	($x10^9$ kNmm^2)		MPa	MPa
C1A	Reject	106.8	2.44	Dap	3.00	25.5
C1B	Reject	67.6	2.07	Dap	1.90	16.2
C2A	Reject	104.3	2.70	LP Bearing	2.93	24.9
C2B	Reject	107.4	2.43	Not noted	3.02	25.7
C3A	Reject	130.8	3.06	Shear	3.68	31.3
C3B	Reject	90.9	2.38	Dap	2.56	21.7
C4A	Reject	79.9	3.09	Flexure	2.25	19.1
C4B	Reject	75.2	2.22	Flexure	2.12	18.0
C5A	Reject	115.0	2.80	Shear	3.23	27.5
C5B	Reject	126.1	2.09	Bearing	3.55	30.1
C6A	Reject	112.5	3.05	LP Bearing	3.16	26.9
C6B	Reject	54.1	1.54	LP Bearing	1.52	12.9
C7A	Reject	102.5	1.78	LP Bearing	2.88	24.5
C7B	Reject	113.7	1.78	Flexure	3.20	27.2
C8A	Reject	119.4	1.93	Dap	3.36	28.5
C8B	Reject	91.6	1.36	Flexure	2.58	21.9
C9A	SS	115.3	3.66	Bearing	3.24	27.6
C9B	SS	80.4	3.14	Dap	2.26	19.2
C10A	SS	140.5	4.28	Shear	3.95	33.6
C10B	SS	116.4	1.93	Shear	3.27	27.8
Average		102.5	2.49		2.88	24.5

Where EI^{Final} = Stiffness after application of GFRP sheets, calculated using Equation 4.3, maximum shear stress is calculated using Equation 4.1, maximum flexural stress calculated using Equation 4.2, and LP = Load Point.

The ultimate loads for diagonal sheet specimens wrapped and non-wrapped are shown in Tables 4.3 and 4.4 respectively. The average failure load for the 40 tests on 21 specimens with diagonal GFRP sheets (two of the specimens were only tested once due to excessive damage caused by the first test) was 137.5 kN, an increase of 34.1% over the control specimens, and a 15.3% increase over the specimens with vertical sheets. The range of failure loads had also increased in relation to the control specimens to a minimum of 79.9 kN and a maximum of 194 kN. The standard deviation was 28.6 kN resulting in a coefficient of variation of 20.8%, a slight decrease from the control specimens.

Table 4.2 Experimental results for vertical sheet specimens

Specimen Designation	Grade	Ultimate Load	$EI^{Orig(1)}$	$EI^{Final(2)}$	Failure Mode	Maximum[3] Shear Stress	Maximum[4] Flexural Stress
		kN	($x10^9$ $kNmm^2$)	($x10^9$ $kNmm^2$)		MPa	MPa
V1A	Reject	89.6	1.35	1.38	Flexure	2.52	21.4
V1B	Reject	95.3	1.06	0.98	Shear	2.68	22.8
V2B	Reject	144.4	1.94	2.18	Flexure	4.06	34.5
V2A	Reject	132.6	3.09	1.78	Flexure	3.73	31.7
V3A	Reject	143.9	2.39	2.93	Flexure	4.05	34.4
V3B	Reject	120.1	2.23	1.37	Flexure	3.38	28.7
V4A	Reject	103.9	3.46	3.54	Bearing	2.92	24.8
V4B	Reject	83.1	3.02	2.02	Bearing	2.34	19.9
V5A	Reject	165.1	2.50	2.02	Flexure	4.64	39.5
V5B	Reject	114.7	2.58	1.98	Flexure	3.22	27.4
Average		119.3	2.36	2.02		3.35	28.5

Where, EI^{Final} = Stiffness after application of GFRP sheets, EI^{Orig} = Stiffness before application of GFRP sheets, both calculated using Equation 4.3, maximum shear stress is calculated using Equation 4.1, and maximum flexural stress calculated using Equation 4.2.

The cumulative strength distributions for the three sets of stringers are plotted in Figure 4.11, in which it can be seen that both strengthening schemes improve the strength of the stringers. The plots also show that the diagonal sheet scheme provides a clear

improvement over the vertical sheet scheme. If a 10th percentile failure load was taken as a measure of the shear strength of the stringers, then the un-strengthened control specimens would have a failure load of nearly 74 kN. The corresponding failure loads for stringers strengthened with vertical and diagonal GFRP sheets would be nearly 84.7 kN and 100.8 kN, respectively. This observation confirms that strengthening with vertical and diagonal sheets will increase the specified shear strength of the stringers by about 14.4 and 36.2 %, respectively.

Table 4.3 Experimental results for wrapped diagonal sheet specimens

Specimen Designation	Grade	Ultimate Load	EI^{Orig}	EI^{Final}	Failure Mode	Maximum Shear Stress	Maximum Flexural Stress
		kN	($x10^9$ $kNmm^2$)	($x10^9$ $kNmm^2$)		MPa	MPa
D1A	Reject	120.2	1.82	2.97	Flexure	3.38	28.7
D1B	Reject	130.6	2.04	2.09	Bearing	3.67	31.2
D2B	Reject	103.3	2.50	2.88	Bearing	2.91	24.7
D2A	Reject	127.9	3.55	3.08	Dap	3.60	30.6
D3A	Reject	148.1	2.30	4.42	Debonding	4.17	35.4
D4B	Reject	115.1	1.87	3.29	LP Bearing	3.24	27.5
D4A	Reject	132.6	2.19	2.41	LP Bearing	3.73	31.7
D5B	Reject	156.9	2.77	2.62	LP Bearing	4.41	37.5
D5A	Reject	170.3	3.31	3.60	LP Bearing	4.79	40.7
D17B	#2	171.8	3.53	3.99	Bearing	4.76	40.4
D17A	#2	173.2	4.18	3.23	Debonding	4.80	40.8
D18B	Reject	122.4	2.72	4.26	Flexure	3.39	28.8
D19B	Reject	159.1	2.00	4.01	LP Bearing	4.41	37.4
D19A	Reject	140.8	2.44	2.25	Bearing	3.90	33.1
D20B	Reject	137.0	2.09	3.53	Bearing	3.85	32.8
D20A	Reject	100.8	2.39	2.62	Bearing	2.83	24.1
D21B	Reject	141.9	2.55	3.81	LP Bearing	3.93	33.4
D21A	Reject	193.6	2.88	3.45	Bearing	5.36	45.6
Average		141.4	2.62	3.25		3.95	33.6

Table 4.4 Experimental results for non-wrapped diagonal sheet specimens

Specimen Designation	Grade	Ultimate Load	EI^{Orig}	EI^{Final}	Failure Mode	Maximum Shear Stress	Maximum Flexural Stress
		kN	($x10^9$ $kNmm^2$)	($x10^9$ $kNmm^2$)		MPa	MPa
D6B	Reject	172.1	2.22	4.35	Bearing	4.84	41.1
D6A	Reject	146.2	2.83	3.20	Debonding	4.11	34.9
D7B	SS	144.9	3.67	4.45	Bearing	4.08	34.6
D7A	SS	146.5	3.40	3.73	Bearing	4.12	35.0
D8B	Reject	97.0	1.16	2.44	Dap	2.73	23.2
D8A	Reject	99.9	1.47	1.47	*	2.81	23.9
D9B	Reject	131.4	1.81	3.51	Debonding	3.70	31.4
D9A	Reject	118.4	2.77	2.98	LP Bearing	3.33	28.3
D10B	Reject	167.8	2.86	4.65	Bearing	4.72	40.1
D10A	Reject	194.0	3.73	3.59	Dap	5.46	46.4
D11B	Reject	160.6	2.24	3.84	Bearing	4.52	38.4
D11A	Reject	140.9	3.23	3.08	Dap	3.96	33.7
D12B	SS	161.8	3.33	4.00	Dap	4.55	38.7
D12A	SS	118.8	3.18	2.38	Flexure	3.34	28.4
D13B	Reject	158.9	3.04	4.02	Bearing	4.47	38.0
D13A	Reject	170.5	3.73	3.96	Bearing	4.80	40.8
D14B	Reject	119.4	1.92	3.61	Dap	3.36	28.5
D14A	Reject	91.7	1.63	1.87	Dap	2.58	21.9
D15B	#2	117.3	3.25	3.60	Dap	3.30	28.0
D15A	#2	90.7	2.89	2.15	Dap	2.55	21.7
D16B	SS	126.3	3.24	3.93	Dap	3.55	30.2
D16A	SS	79.1	3.44	2.75	Flexure	2.23	18.9
Average		134.3	2.77	3.34		3.78	32.1

* Reached limit of testing machine's stroke

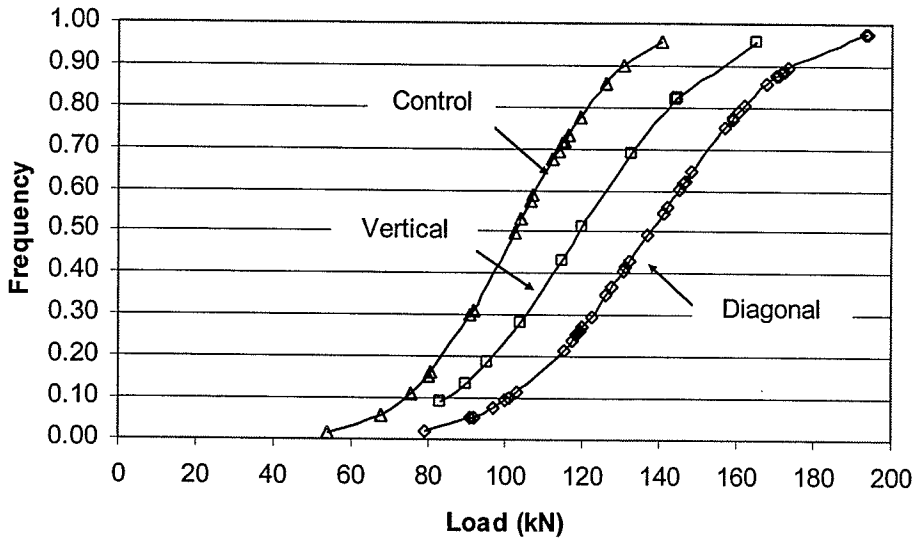

Figure 4.11 Cumulative ultimate load distributions.

Comparing the first and second tests of the same specimen it was found that the average ultimate load of control specimens decreased by 18% between the two tests, with a 42% increase in the standard deviation. The vertical sheet specimens showed a decrease in average ultimate load of 15.7 % but the standard deviation decreased by 37 %. For the diagonal sheet specimens there was a 3.3 % decrease in average ultimate load, however the standard deviation changed substantially between the first and second tests, with a 49 % increase.

Dividing the diagonal sheet specimens into wrapped and un-wrapped groups, compared to the control stringers the wrapped specimens increased average ultimate load by 6.2 % with 38% increase in standard deviation. The average ultimate load for un-wrapped specimens decreased by 10.3 % with an increase in standard deviation of 46 %. It is therefore recommended that sheets be always wrapped onto the bottom of the stringer.

Dividing the data according to their grades allows for an alternative perspective. For the control specimens the reject stringers attained an average load of 99.9 kN. The reject

grade specimens with vertical sheets reached 119.3 kN and the diagonal specimens reached a load of 139 kN. This means an increase in ultimate load of 19.4% and 39.1%, respectively, over control specimens (Figure 4.12).

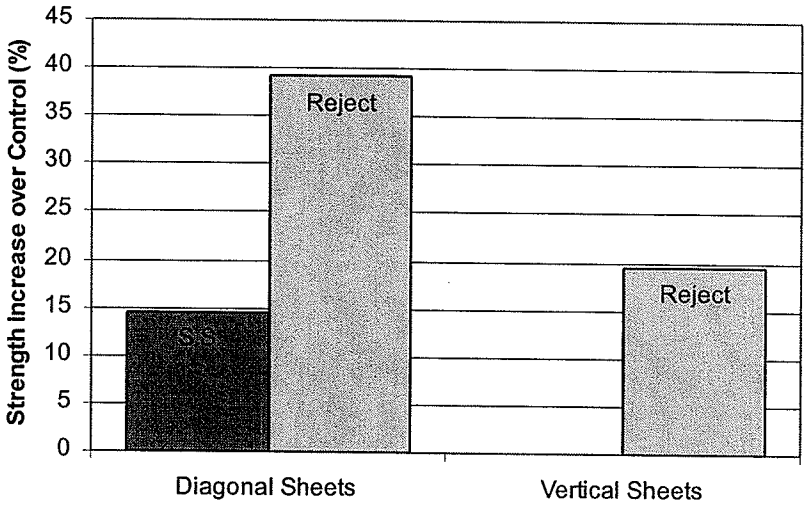

Figure 4.12 Strength increases over control by reinforcing type and grade.

The control beams of select structural grade reached an average ultimate load of 113.2 kN while the diagonal sheet specimens failed at 129.6 kN, an increase of 14.5%. There was no select structural specimen with vertical sheets. The increase in the capacity of select structural specimens is substantially less than that for reject specimens, showing that this reinforcement technique provides more benefit for lower grade stringers than for higher grades. Similar conclusions were also found by Gentile et al. (2002) indicating that the modulus of rupture can increase by up to 50% for weaker samples and by 20% for the stronger samples.

4.4 Shear Stress

Despite using a test setup that creates greater shear to flexure stresses and testing samples with pre-existing horizontal splits, shear failure was rare. Calculating the shear

strength is thus not possible, however calculating the shear stress at ultimate load does provide minimum values. The shear stress (τ) is calculated using the following equation,

$$\tau = \frac{VQ}{Ib} \qquad \text{(Equation 4.1)}$$

where V = shear force due to loading, Q = first moment of area above horizontal plane at stringer depth of interest, generally mid-depth , I = moment of inertia, and b = width of member. The calculated maximum shear stresses for all the specimens are shown in Tables 4.1, 4.2 and 4.3. The average shear stress for control specimens, specimens with vertical and diagonal sheets at failure was 2.9 MPa, 3.3 MPa, and 3.8 MPa, respectively. At the 5^{th} percentile level, the control samples attained 1.9 MPa, the vertical 2.1 MPa, and the diagonal 2.5 MPa shear stress at ultimate load.

To account for the damage done to the beams in the first test the data was divided up into two sets, first test and second test on a stringer. Looking only at the first test for control specimens, which was conducted on the solid end of the beam, the average shear stress was 3.17 MPa. The minimum value was 2.25 MPa and the maximum value was 3.95 MPa. The highest value was recorded on specimen C10A which had a grade of select structural and failed in shear, therefore this value is a true indication of the shear strength of that specimen. The horizontal split began to appear in the tested end at a load of approximately 60 kN, leading to shear failure at 140.5 kN. The average shear stress on the first tests of the vertical sheet specimens was 3.64 MPa an increase of 14.8%. These tests were conducted on the solid end on 4 out of 5 specimens. The minimum and maximum shear stresses were 2.52 and 4.64 MPa. For the diagonal sheet specimens the average first test shear stress was 3.92 MPa, an increase of 23.7 %. These tests were conducted on the split end of the beam first, thus the

increase is not as great as it would be if the tests were conducted on the solid end. The minimum and maximum values recorded were 2.73 and 4.84 MPa, respectively.

The Canadian Highway Bridge Design Code (CAN/CSA-S6-00) specifies a value of 0.9 MPa for the shear strength of all grades of Douglas fir. Although it appears that even the control specimens attained stresses greater than the specified value, the specified value is based on the occurrence of splits, rendering most designs overly conservative. By closing the split and using diagonal GFRP sheets to ensure that the stringer acts as a beam without splits, shear failures have been eliminated and other modes of failure may occur. The minimum shear stress from the diagonal sheet specimens, which was obtained from a test on a severely damaged specimen, was 2.2 MPa.

4.5 Flexural Stress

Very few of the specimens failed in flexure and therefore it is not possible to determine the modulus of rupture. However, it is possible to calculate the flexural stress at the maximum load to determine attainable stress levels. The flexural stress (σ) was calculated using the following equation,

$$\sigma = \frac{My}{I} \qquad \text{(Equation 4.2)}$$

where M = bending moment, y = distance from neutral axis to extreme fibre and I = moment of inertia. The average flexural stress at maximum load for the control specimens was 24.5 MPa, while the vertical sheet and diagonal sheet specimens reached stresses of 28.5 MPa and 32.8 MPa, respectively. This corresponds to flexural stress increases of 15.1% and 33.9%, respectively. At the 5^{th} percentile level the flexural stress for control specimens was 15.7 MPa and the vertical and diagonal specimens reached 17.9 and 21.6 MPa, respectively. This

resulted in increases of 14% and 37.6% over control specimens. The 5th percentile value for the diagonal specimens was greater than the CAN/CSA-S6-00 select structural flexural stress of 19.5 MPa.

4.6 STIFFNESS

The flexural stiffness (EI) was calculated for all the beams and is shown in Tables 4.1, 4.2, 4.3 and 4.4. A pre-repair stiffness test was completed on all beams selected for strengthening so that a direct comparison of the stiffness before and after strengthening could be evaluated. The flexural stiffness was calculated using the following equation:

$$EI = \left(\frac{P}{\delta}\right)\frac{a^2b^2}{3L} \qquad \text{(Equation 4.3)}$$

where,

EI = flexural stiffness
P = load
a,b = distance from support to load point (Figure 4.13)
L = span
δ = deflection

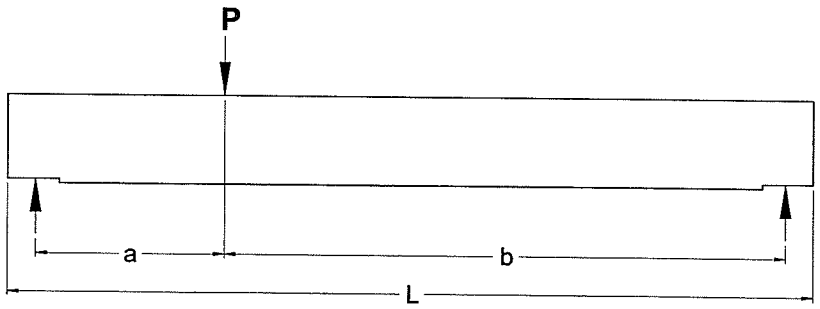

Figure 4.13 Diagram showing variables used for calculating stiffness.

To use this equation it is necessary to find the average P/δ value from the experimental load/deflection curve. This was done by fitting a linear trend line to the

load/deflection plot between 10 and 40 kN, and then determining the slope of that line to obtain the P/δ value.

Theoretically the flexural stiffness should not increase with shear strengthening repair. However the GFRP sheets tied the top and bottom of the stringers together, effectively increasing the moment of inertia and therefore the stiffness. Data analysis confirmed that increases occurred from the pre-repair tests (EI_{ave}^{orig}) to the final tests (EI_{ave}^{final}). It is recalled that each beam was subjected to two tests; one on the split end and one on the solid end, however the solid end may have been damaged by the first test. The first tests of the vertical sheet specimens showed a 3.5% increase in stiffness, while the second tests on the now somewhat damaged stringers, showed a decrease of 32%. For the diagonal specimens the first test showed an increase of 47.8%, while the second test revealed stiffness decreased by 2.5%. A summary of the stiffness values is shown in Table 4.5.

Table 4.5 Stiffness values divided into grades and, first and second tests

Specimen Type	Grade	Test	EI_{ave}^{orig}	COV	EI_{ave}^{final}	COV	$EI_{ave}^{orig} / EI_{ave}^{final}$
			($x10^9$ kNmm^2)	%	($x10^9$ kNmm^2)	%	
Control	Reject	First	-	-	2.61	19.7	-
		Second	-	-	1.98	19.6	-
		Both	-	-	2.30	23.7	-
	SS	First	-	-	3.97	10.9	-
		Second	-	-	2.53	33.8	-
		Both	-	-	3.25	30.7	-
	All Grades	First	-	-	2.88	25.9	-
		Second	-	-	2.09	24	-
		Both	-	-	2.49	29.7	-
Vertical	Reject	First	2.33	33.4	2.41	24.6	1.04
		Second	2.40	34.4	1.63	27.2	0.68
		Both	2.36	32	2.02	37.4	0.85
Diagonal	Reject	First	2.24	21.7	3.64	18.1	1.62
		Second	2.73	27	2.83	25.9	1.04
		Both	2.47	26.5	3.26	24.4	1.32
	#2	First	3.39	5.8	3.80	7.2	1.12
		Second	3.54	25.9	2.69	28.5	0.76
		Both	3.47	15.8	3.24	24.4	0.94
	SS	First	3.41	6.6	4.13	6.9	1.21
		Second	3.34	4.2	2.95	23.6	0.88
		Both	3.38	5.1	3.54	22.7	1.05
	All Grades	First	2.52	26.4	3.72	16.3	1.48
		Second	2.91	25.3	2.84	24.5	0.97
		Both	2.71	26.6	3.30	23.7	1.22

4.7 GFRP Sheet Strains

Each beam typically had a split at one end while the other end was unsplit or solid. It was expected that the split end of the beam will have greater horizontal movement between the split portion of the beam and will therefore pull on the sheets creating larger strains.

Thus it is necessary for clarity to distinguish between the split and solid ends of the beam when referring to strains.

The vertical sheet specimens frequently showed negative strains in the sheets indicating that the sheets were in compression. In other cases very low positive strains were recorded. Overall the strains varied substantially thus making interpretation difficult. On specimen V1, where 3 strain gauges were placed on each strip on one side, the strains showed no consistency between the gauges on each strip or at each level of the three separate sheets. The performance of these sheets was generally poor and therefore the strains were not analysed in detail.

In contrast to the vertical sheet strain gauges, the strain gauges on the diagonal sheet specimens provided useful information. During the test on the split end of the specimens it was found that near the failure load, the axial strains in the diagonal GFRP sheets on the tested end of the specimen at the top and bottom were typically less than 1,000 μstrain, with the gauges at the bottom consistently showing larger strains than those at the top. The gauges at ±75 mm of the centreline showed strains for the gauge above the centreline on average 2,400 μstrain, and for below the centreline, 3,600 μstrain. The axial strains at the middle of the sheets were the largest, with an average of 5,000 μstrain and ranging from 2,000 to 17,000 μstrain. The latter high strains were observed in only a few cases. The rupture strain of the GFRP sheets is 20,000 μstrain, thus on average approximately 25% of the capacity of the sheets was used. The strains in the solid end of beams during the split end test typically averaged less than 1,000 μstrain with the greatest value at the centre of the sheet.

When testing the solid end of the specimens the strains at the split end were approximately 3,500 μstrain, while the solid end experienced 2,500 μstrain. It would be expected that the tested end would develop greater strains due to the higher shear; however, the splits caused the damaged end to have greater differential movement and thus created greater stresses in the sheets.

Shown in Figure 4.14 are the strain profiles for specimen D7, with 5 strain gauges placed on each GFRP sheet. The strain profiles are shown for three load levels of 60 and 100 kN, which are the un-factored and factored loads that correspond approximately to a CL-625 design truck, and also ultimate load on the specimen. Figure 4.14A shows the strains in the solid end of the beam while the split end was tested and reveals that without a split the profile is similar to the traditional shear stress distribution according to beam theory. Figure 4.14B shows the profiles for the split end during split end test, and shows that there is a spike in the profile near the split showing that the split causes strain concentrations. Figures 4.14C and D are for the solid end test with the solid and split end profiles shown respectively. These charts show similar patterns to Figures A and B. The strains in the split end during solid end test are lower than the strains of the split end during split end test as expected because shear is lower. Solid end strains in Figure 4.14C are greater because of the greater shear in that end of the beam in comparison to the first test. Strain profiles for the rest of the diagonal sheet specimens are shown in Appendix B for specimens that had sufficient data to reproduce a test profile.

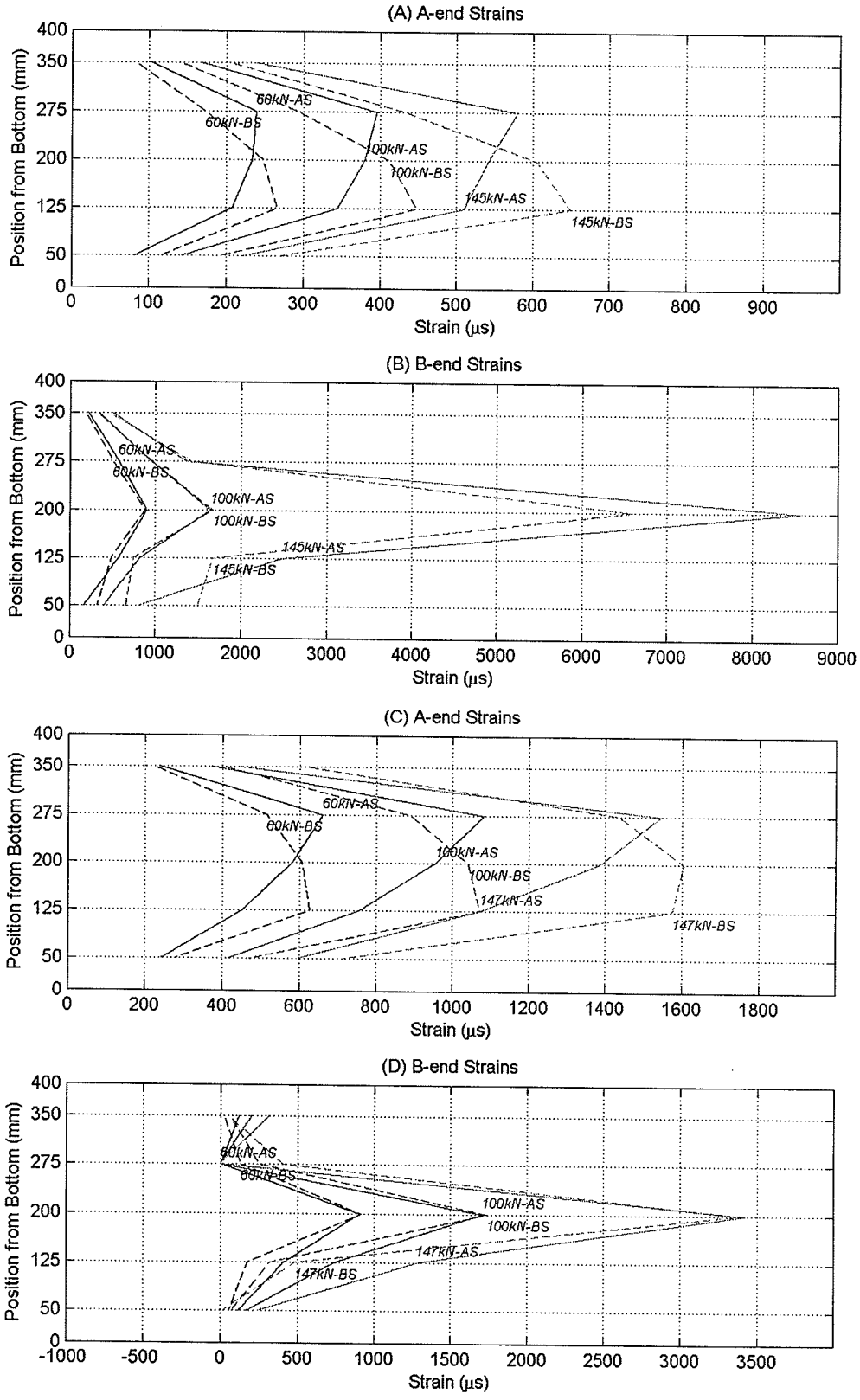

Figure 4.14 Strain profile on sheets for D7 (Y2-112). (A) & (B) are for split end (B-end) test and (C) & (D) are solid end (A-end) test

4.8 FAILURE MODES

While the individual failure modes for all specimens are shown in Tables 4.1, 4.2 and 4.3, a summary of the observed failure modes is shown in Table 4.6. The control specimens failed in a wide variety of modes such as flexure, shear, dap splitting, and bearing failure at the support and/or under load point (LP bearing parallel to grain). Examples of shear and dap splitting failure are shown in Figures 4.15 and 4.16, respectively. Shear failure is characterised as horizontal shear failure parallel to grain, while dap failure is always initiated at the corner of the dap and propagates parallel to the grain until mid-span of the beam. The vertical sheet specimens consistently failed in flexure, showing that the sheets prevented shear failure but allowed flexural failure. An example of flexural failure is shown in Figure 4.17. The stringers used for the project had originally wooden decks nailed into them. The nail connections, and possibly moisture trapped between the deck and top of stringers, resulted in the deterioration of the top portion of the stringers, making it difficult to apply concentrated loads without bearing failure. Since they were subjected to generally higher loads than the other specimens, most specimens with diagonal GFRP sheets experienced bearing failure under the load or at the support. An example of bearing failure at the load point is shown in Figure 4.18 and a support bearing failure is shown in Figure 4.19. The other significant failure mode was dap splitting. However, the high number of dap splitting failures only occurred on specimens that did not have the sheets wrapped onto the bottom of the specimen. In Figure 4.20, the diagonal sheet specimens are divided into two groups to show the effect of wrapping the sheets onto the bottom. The low incidence of shear and flexural failures in the specimens with diagonal sheets, shown in Figure 4.20, confirms the

effectiveness of diagonal sheets in increasing the load carrying capacity of stringers to such an extent that they were forced to fail in bearing.

Table 4.6 Summary of Failure Modes

Type of Failure	Control Specimens	Vertical Sheet Specimens	Diagonal Sheet Specimens		
			Non-Wrapped	Wrapped	Total
Bearing	2	2	7	7	14
LP Bearing	4	-	1	6	7
Debonding	-	-	2	2	4
Dap	5	-	9	1	10
Flexure	4	7	2	2	4
Shear	4	1	-	-	-
Undetermined	1	-	-	-	-
Reached maximum machine deflection	-	-	1	-	1

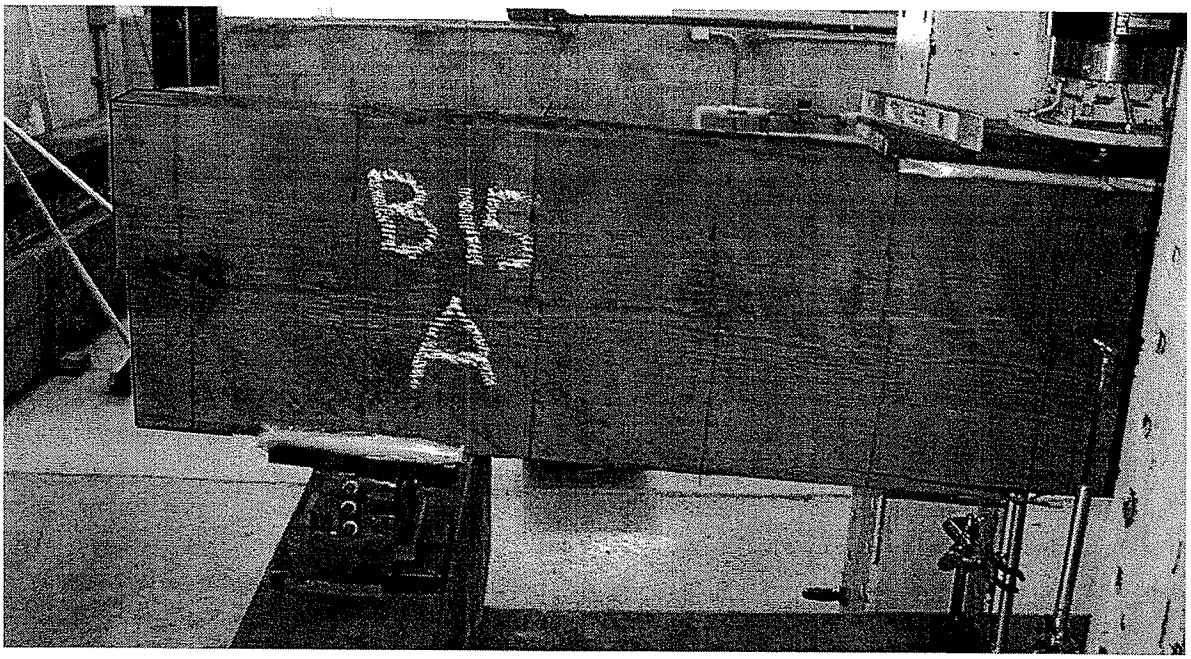

Figure 4.15 An example of shear failure on specimen C10A (B15A)

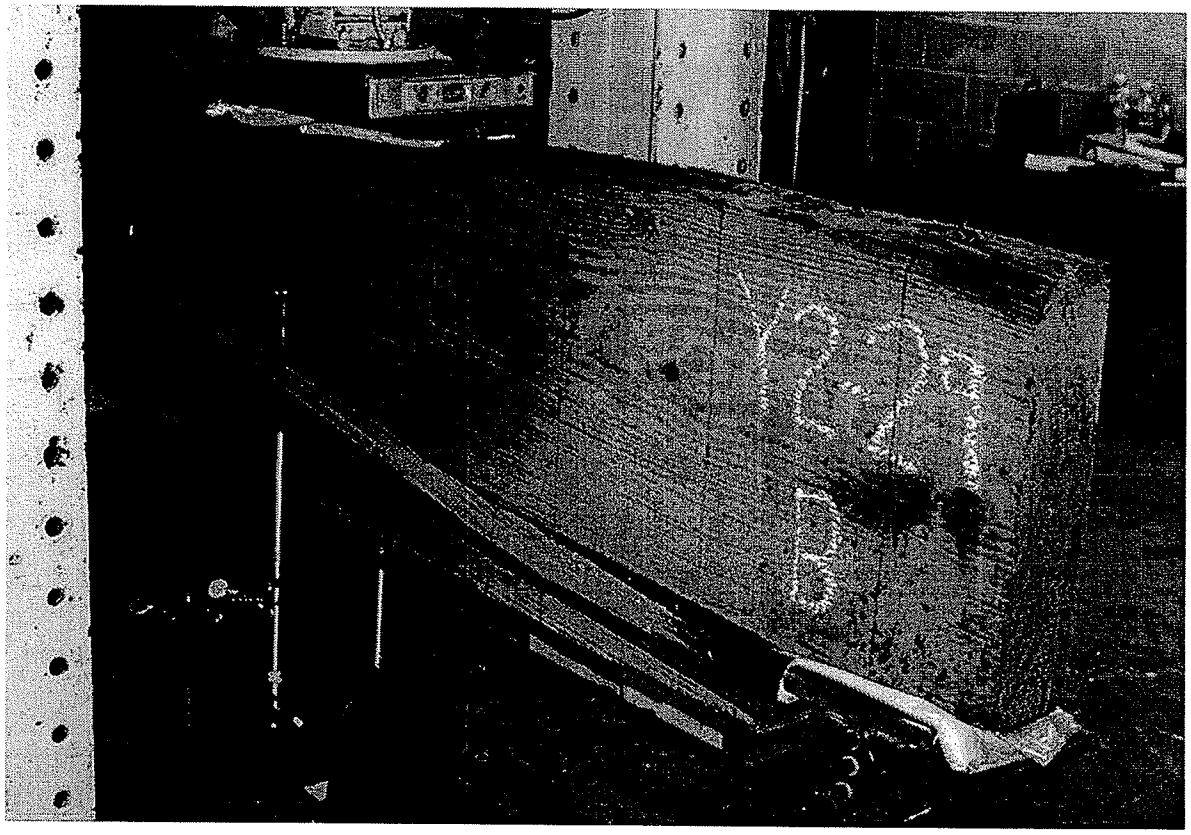

Figure 4.16 Example of dap splitting failure on specimen C9B (Y2-29B)

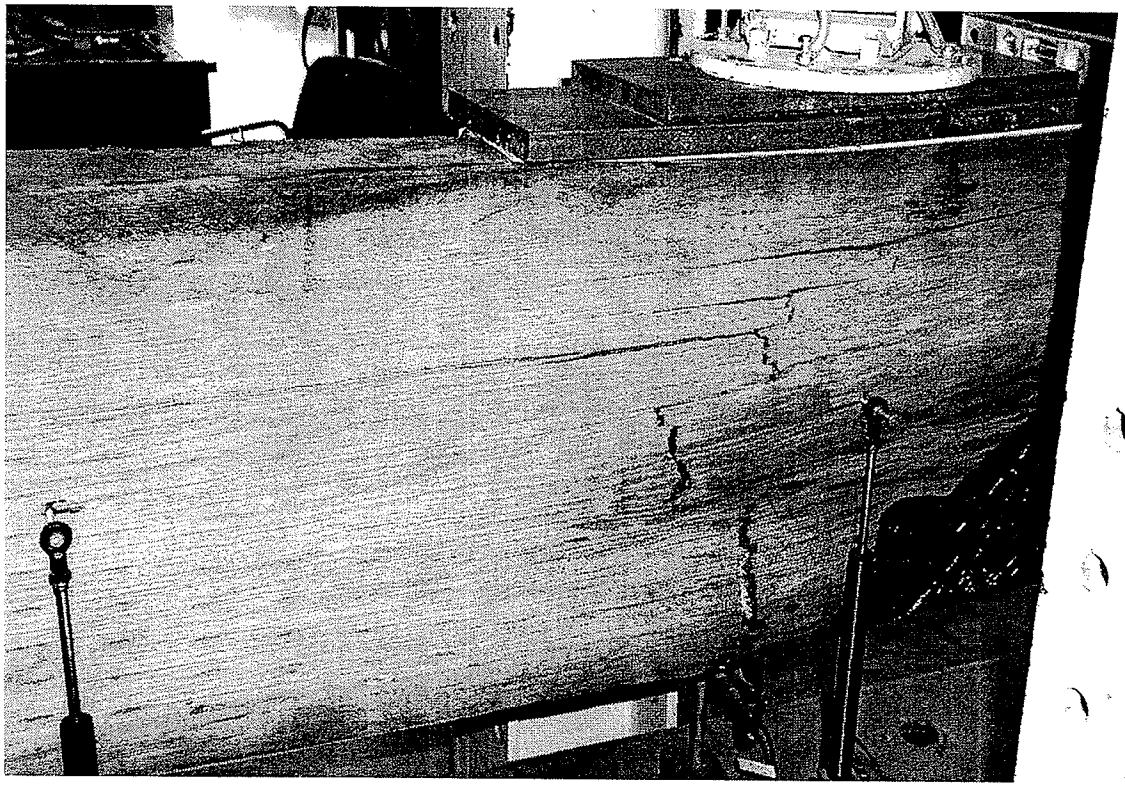

Figure 4.17 Example of flexural failure on specimen D18B (Y1-117B)

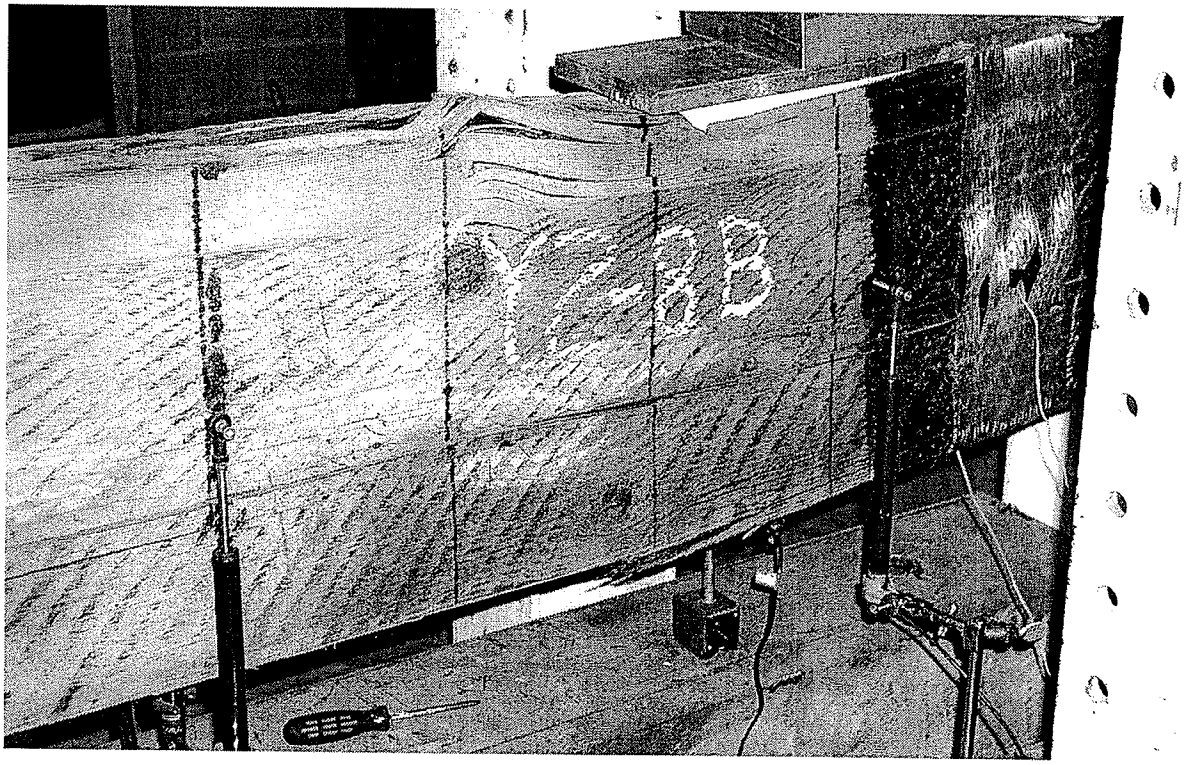

Figure 4.18 An example of bearing failure at the load point on V1B (Y2-08B)

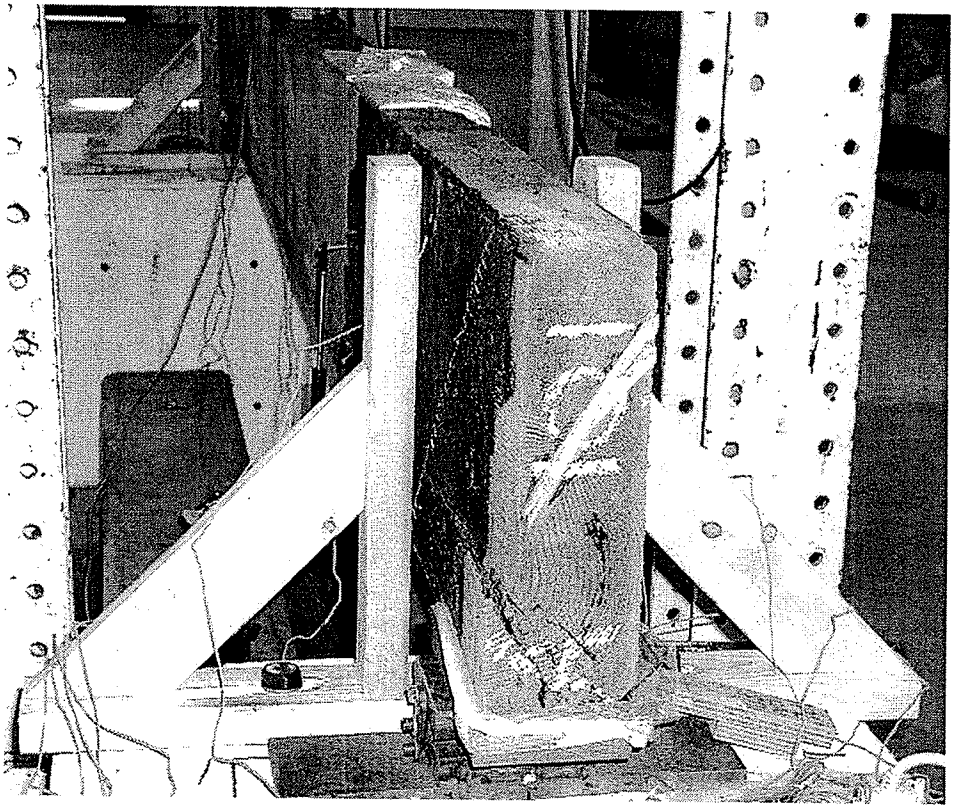

Figure 4.19 Example of bearing failure at the support on C2A (Y2-101A)

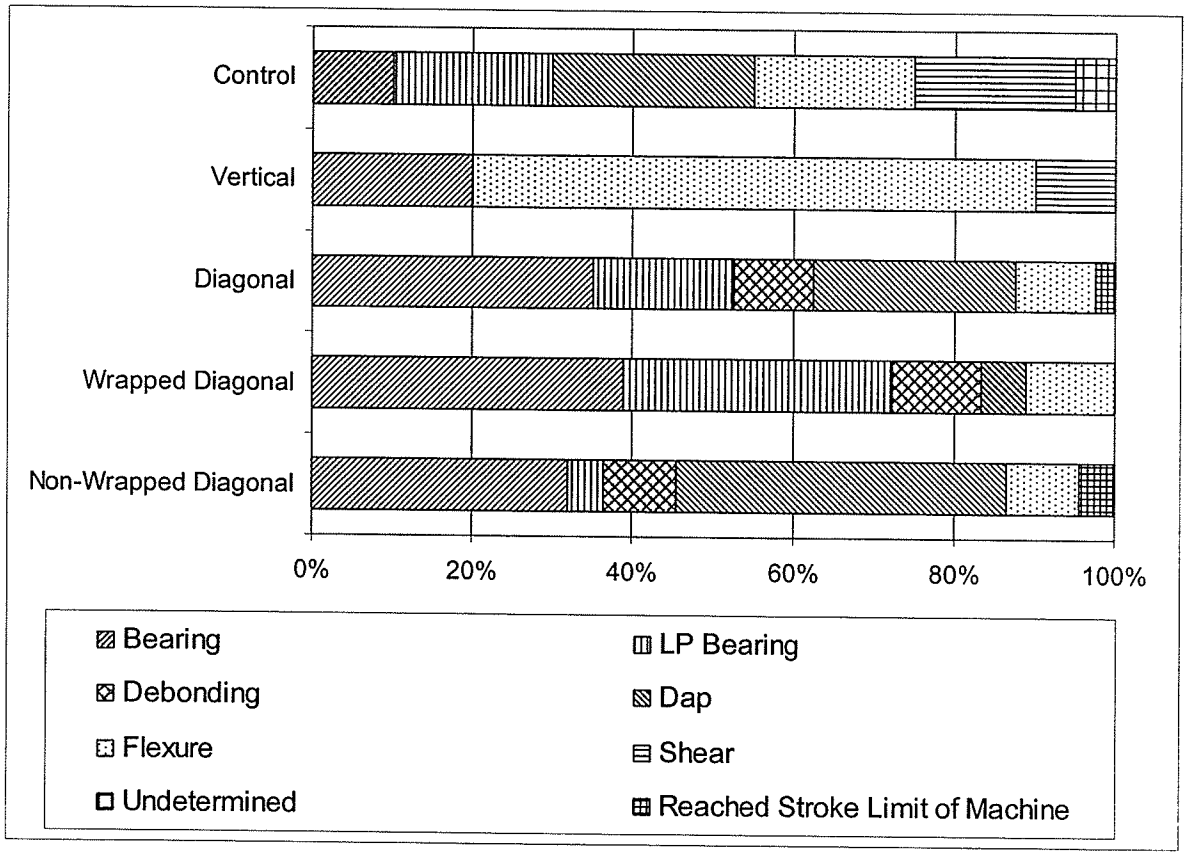

Figure 4.20 Failure Modes

4.9 Sheet Performance During the Test

As the specimens with open horizontal splits were loaded, compressive strains were frequently observed in the vertical GFRP sheets. In these specimens, a complex interaction took place between the closing of the splits and a relative horizontal movement of the two parts of the stringer, above and below the split. With sliding along the horizontal splits the sheets eventually began to tilt and tended to tear up leading to damage to the strain gauges (Figure 4.21). The peeling off of the sheets was also observed in the diagonal sheets but on a much smaller scale and after considerable horizontal displacement. The peeling off of diagonal sheets was due primarily to the gap at the split. Closing the gap allowed the fibres to remain straight near the gap and enabled them to resist the shear forces between the top

and bottom of the sheet. It was concluded that the peeling of the sheets depended upon the presence and extent of the gap at the splits. Specimens with wider splits tended to allow greater movement, which led to the tearing up of the sheets.

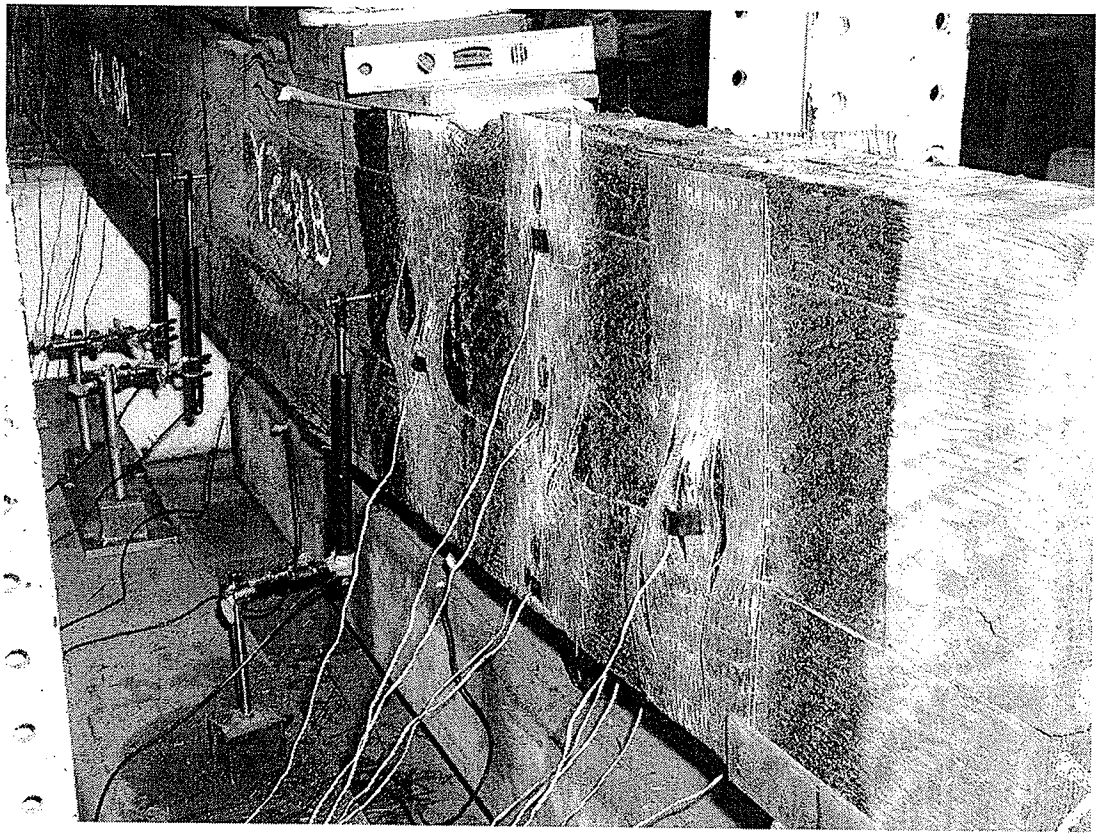

Figure 4.21 Vertical sheet specimen with sheets raised by shearing action

4.10 VERTICAL VERSUS DIAGONAL SHEET ORIENTATION

The performance of the sheets as discussed in the previous section indicates that the diagonal sheet orientation is preferred. The vertical sheet specimens had a 16.4% increase in average ultimate load over control while the diagonal sheet specimens improved by 34.1%. Comparing the initial stiffness with the final stiffness, the stiffness for the first test on vertical sheet specimens only increased 3.5% while the diagonal sheet specimens increase 47.8%. The greater improvements in average ultimate load and stiffness of the diagonal sheets versus the vertical sheet specimens also suggest the superiority of diagonal sheets. Further the

vertical sheets showed negative sheet strains indicating that they were in compression or peeled off and wrinkled, because of which these sheets were not used to their best advantage. These reasons thus confirm that the diagonal sheet orientation is superior to the vertical orientation.

4.11 Moisture Content

The moisture content of the specimens was determined according to ASTM D4444-92and measured using a resistance type hand-held moisture meter Delmhorst J-2000 with 25 mm insulated pins. The readings were taken on both sides of the beam in two rows 100 mm from the top and bottom at 500mm from the ends and at mid-span for a total of 12 readings per stringer which were then averaged. The readings were taken shortly after the tests were completed. For 17 of the diagonal sheet specimens the moisture content readings were also recorded at the time of the initial stiffness tests. The moisture content for all the specimens is noted in Tables 4.7, 4.8 and 4.9 along with the specific weights.

Table 4.7 Moisture content and specific weight of control specimens

Specimen	Moisture Content	Specific Weight
	%	kN/m^3
C1	15.5	6.35
C2	19.7	6.45
C3	17.7	5.73
C4	17.1	6.30
C5	17.5	7.01
C6	17.5	5.95
C7	20.2	5.04
C8	16.3	5.42
C9	15.3	5.83
C10	14.8	6.37
Average	17.2	6.04

Table 4.8 Moisture content and specific weight of vertical sheet specimens

Specimen	Moisture Content	Specific Weight
	%	kN/m^3
V1	21.3	6.55
V2	18.9	7.67
V3	17.9	7.01
V4	13.1	5.58
V5	16.4	6.83
Average	17.5	6.73

Table 4.9 Moisture content and specific weight of vertical sheet specimens

Specimen	MC @ Time of Stiffness Test	MC @ Time of Final Test	Specific Weight
	%	%	kN/m^3
D1	19.1	16.1	5.95
D2	20.5	15.3	5.04
D3	21.6	17.9	7.31
D4	19.7	14.8	6.10
D5	-	19.4	6.34
D6	23.6	19.3	5.88
D7	21.5	19.2	5.88
D8	25.9	20.4	6.08
D9	30.5	24.5	5.83
D10	-	18.9	6.66
D11	30.8	21.8	5.91
D12	19.4	20.0	5.33
D13	27.7	24.3	5.55
D14	32.8	20.9	5.95
D15	26.0	19.2	5.16
D16	26.1	23.6	5.41
D17	17.1	15.7	6.34
D18	22.8	18.3	6.02
D19	15.6	15.0	6.59
D20	-	15.0	5.83
D21	-	16.1	5.55
Average	23.6	18.8	5.94

Prior to working on the specimens, they were stored outside and were not covered in any way. The initial stiffness tests were conducted shortly after they were brought into the laboratory, while the final tests were conducted several months later during which time they were stored indoors. The diagonal sheet specimens show that at the time of the initial stiffness tests the moisture content was higher and by the time the final test was conducted the moisture content had dropped by approximately 20%. Despite the decline in moisture content, the diagonal sheet specimens still had a higher average moisture content, 18.8%, than 17.2% of the control specimens which were tested to failure shortly after being brought into the laboratory. Thus by coincidence the diagonal sheet specimens typically had a higher moisture content than the control group. The vertical sheet specimens showed a similar average moisture content to control specimens of 17.5% despite having been in the laboratory priory to the test.

Theoretically as moisture content of timber increases, the strength should decrease. Madsen (1992) however states that this is only true for the higher strength members of the strength distribution and that at the lower end strength actually marginally increases. A comparison of moisture content to ultimate load was conducted for control, vertical and diagonal sheet specimens but failed to show any increase in strength with lower moisture content as shown in Figures 4.22, 4.23 and 4.24. This suggests that the specimens used in this project were from the lower end of the strength distribution or the observed behaviour resulted from other factors such as damage of the beams. Beams with splits have additional surface area through which moisture can escape.

Madsen (1992) states that the modulus of elasticity is "somewhat sensitive" to moisture content but the stiffness is "not sensitive" to moisture content because of shrinkage.

Detailed measurements of the specimens were not conducted to show that stiffness was not affected. However, the change in stiffness of the first tests conducted on the diagonal sheet beams from the stiffness test to the final test was compared to the change in moisture content. As shown in Figure 4.25, the beams do exhibit an effect on the stiffness due to changes in moisture content. However, the best fit linear trend line is a relatively poor fit of the data set.

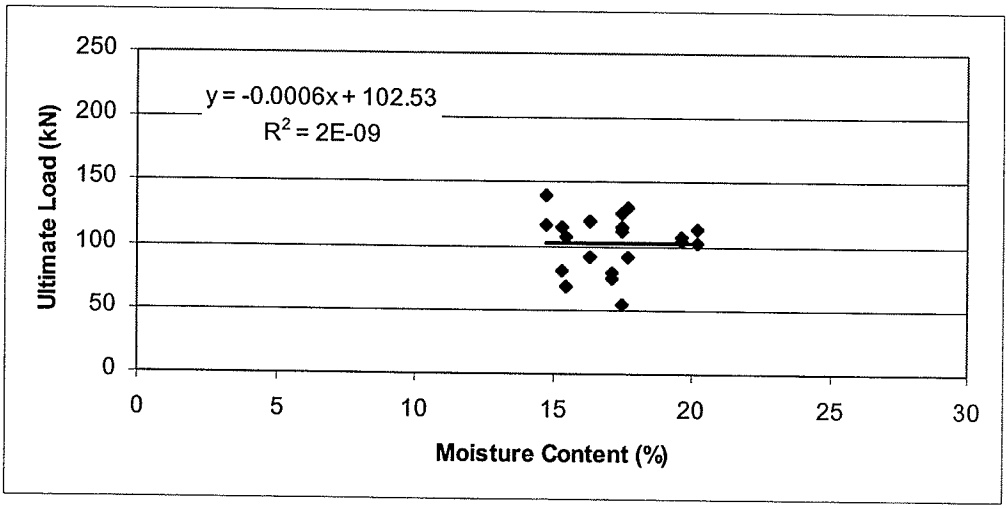

Figure 4.22 Moisture content of control specimens versus ultimate load

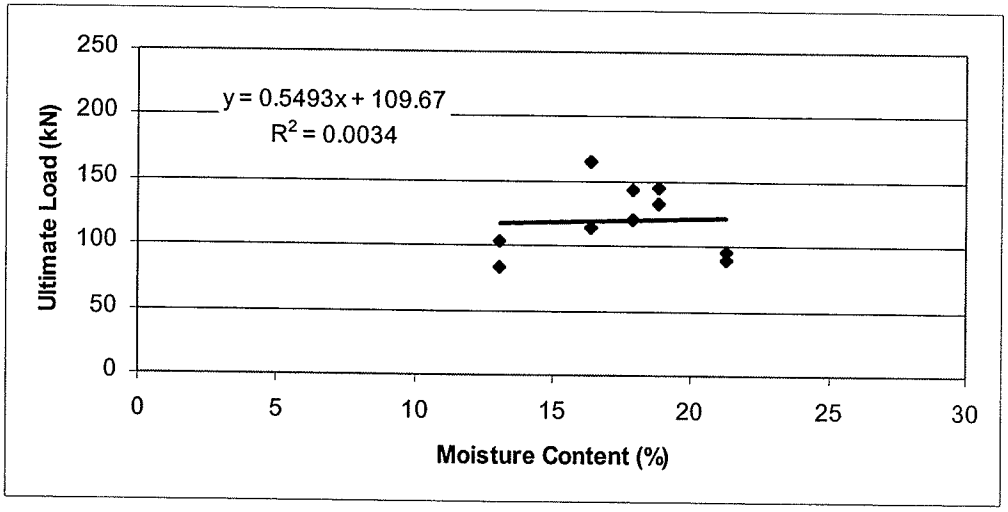

Figure 4.23 Moisture content of vertical sheet specimens versus ultimate load

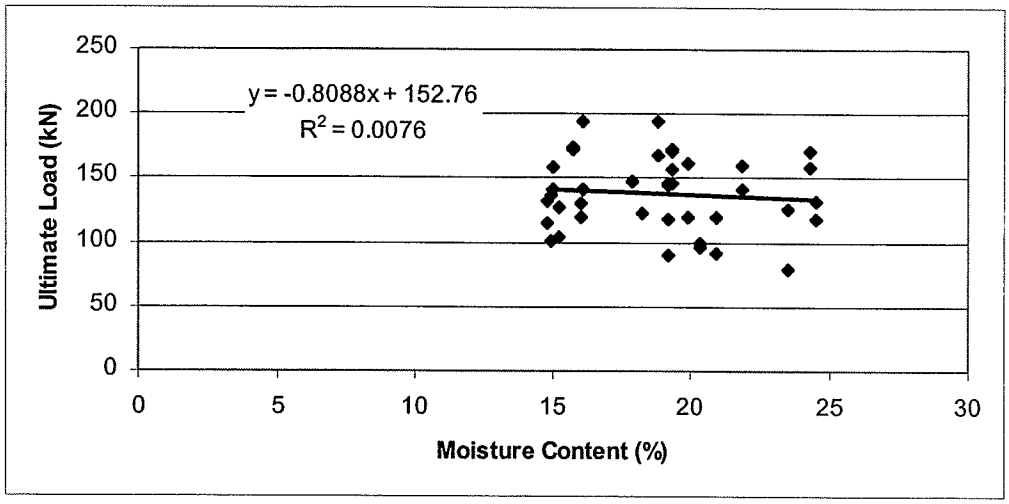

Figure 4.24 Moisture content of diagonal sheet specimens versus ultimate load

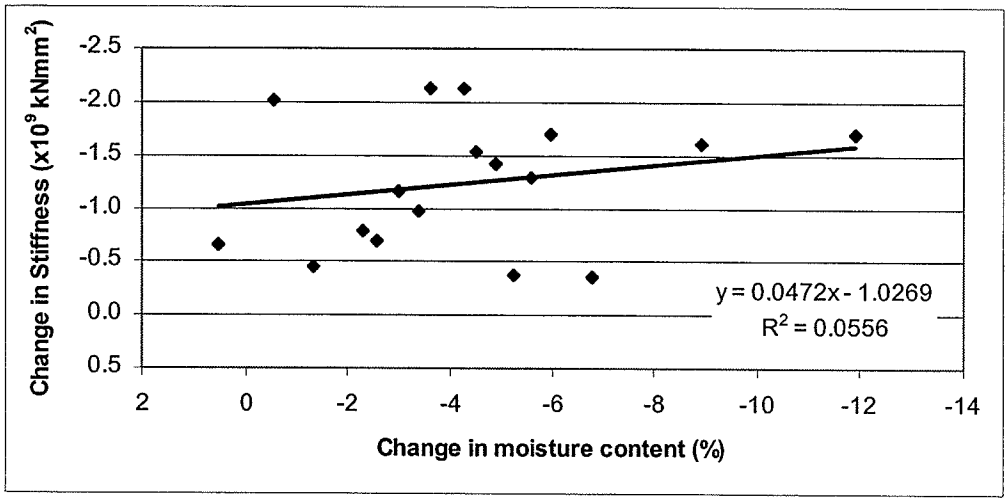

Figure 4.25 Stiffness change for first test specimens from elasticity to final test

4.12 Specific Weight

The specific weight or density of the specimens was calculated to determine if it had any effect on strength. The specific weight for all the specimens is given in Tables 4.7, 4.8 and 4.9. The average specific weight of the control, vertical and diagonal sheet specimens was 6.04, 5.94 and 6.73 kN/m^3, respectively. The specimens ranged from a low specific weight of 5.04 kN/m^3 to a high value of 7.67 kN/m^3, showing the typical large variability of timber properties. The specific weight is plotted against ultimate load in Figures 4.26, 4.27

and 4.28. The control specimens did not show any correlation between unit weight and ultimate load, but the vertical and diagonal sheet specimens showed some correlation. Madsen (1992) states that density is a poor indicator of strength which is indicated in the control specimens, but the repaired specimens show a better correlation which is probably due to the covering up of defects in the timber by the sheets.

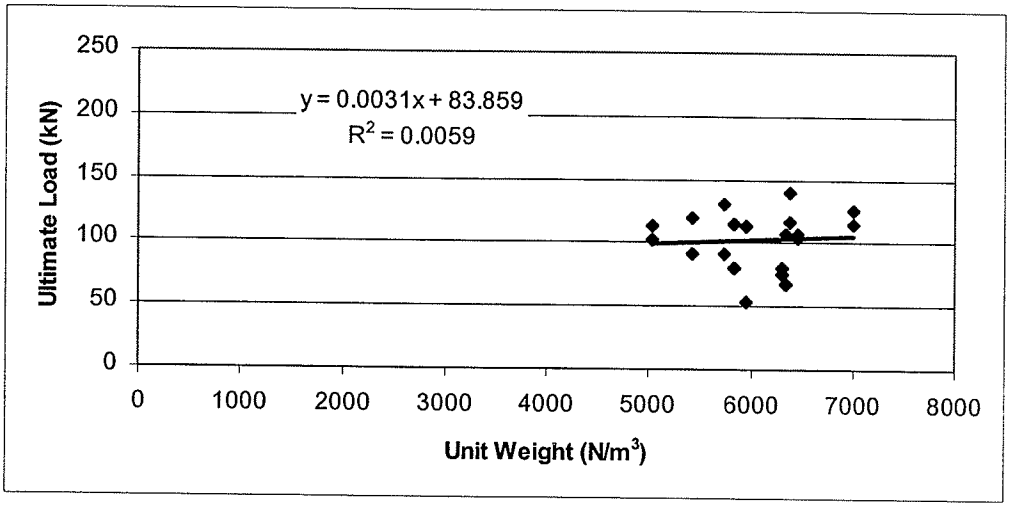

Figure 4.26 Unit weight of control specimens versus ultimate load

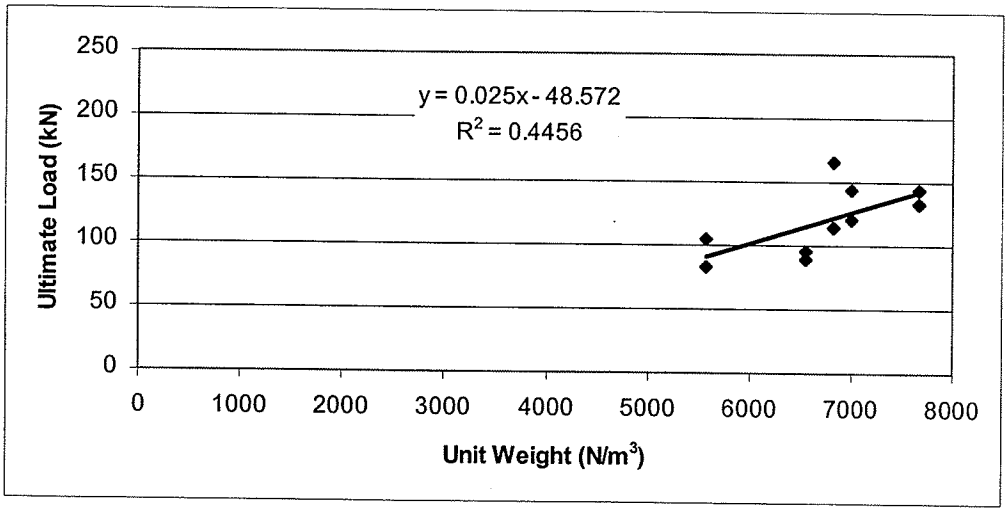

Figure 4.27 Unit weight vertical sheet specimens versus ultimate load

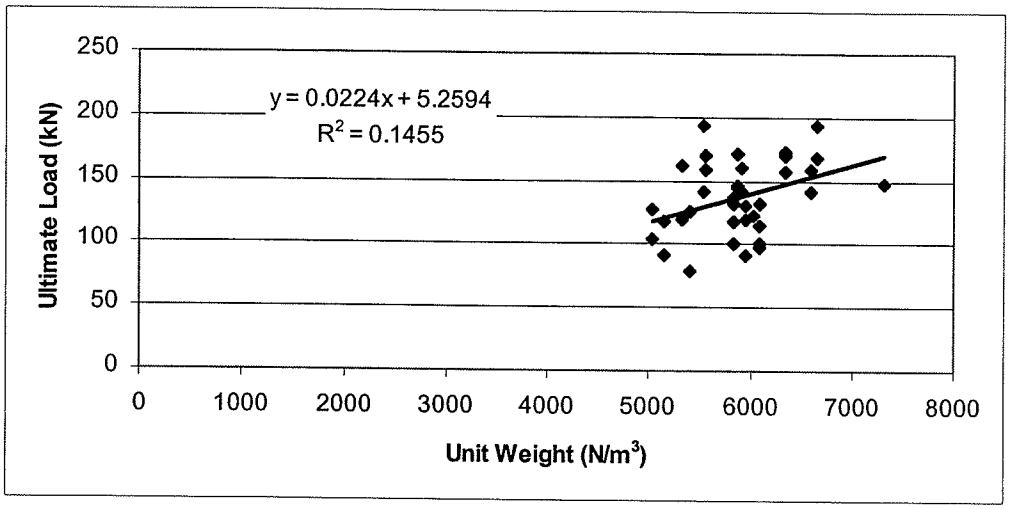

Figure 4.28 Unit weight of diagonal sheet specimens versus ultimate load

CHAPTER 5 DATA ANALYSIS

5.1 RELIABILITY ANALYSIS

As a means of determining the safety of existing and rehabilitated stringers a safety index analysis was performed. The safety index is a method of assessing the probability of failure. It relates the distribution of resistances and loads and compares their overlap that signifies probability of failure. Figure 5.1 shows the mass distributions for shear of control specimens, vertical and diagonal sheet specimens, and truck loadings. The safety index for single components is calculated using the following equation:

$$\beta = \frac{\mu_R - \mu_S}{\left(\sigma_R^2 + \sigma_S^2\right)^{0.5}} \qquad \text{(Equation 5.1)}$$

where, β = safety index, μ_R = mean of resistances, μ_S = mean of load effects, σ_R = standard deviation of resistances, and σ_S = standard deviation of load effects.

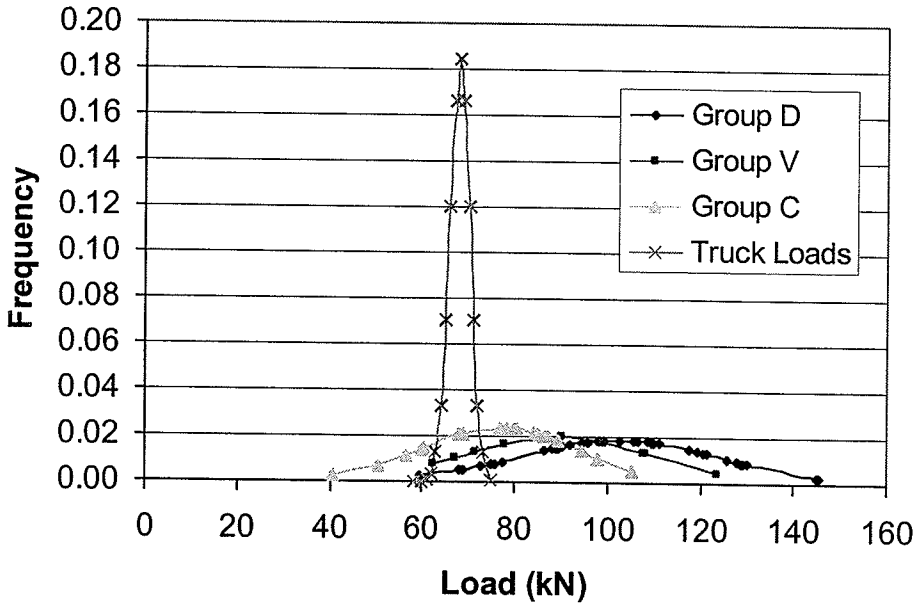

Figure 5.1 Mass distributions of shear

The safety index was calculated for the experimental specimens using a span of 3.4 m, a stringer spacing of 0.6 m, two 3.6 m wide lanes and CL-625 design truck. The safety indices for the control, vertical sheet and diagonal sheet specimens were found to be 0.53, 1.06 and 1.63 respectively. The target safety index for new design is 3.5 although the evaluation section of the Canadian Highway Bridge Design Code, CAN/CSA-S6-00 (CSA, 2000) does permit safety index values as small as 2.5 for evaluation of strengths of existing bridges. The control specimens, as expected, did not reach the target level but neither of the rehabilitating schemes produces an acceptable safety index value either. Re-evaluating previous analysis for 0.4 m stringer spacing, the safety index for control specimens was 1.9, for specimens with vertical sheets it was 2.2 and for specimens with diagonal sheets it was 2.7. An overall improvement of 15% was obtained for samples with vertical sheets and 42% for samples with diagonal sheets over the control beams. There is a need to further examine the safety indices of timber bridges strengthened by varies schemes.

5.2 Contribution of GFRP sheets to Shear Capacity

To determine the contribution of diagonal GFRP sheets to the overall shear capacity of the stringer, the forces in the sheets were calculated from the strains and compared to the shear force due to the applied load at failure. To determine the shear force taken by the GFRP sheets it was necessary to use the strains determined from the strain gauges at the mid-height of the sheets or the gauges at the location of the split, and the stress-strain relationship as shown in equation 5.2,

$$\sigma = E\varepsilon \qquad \text{(Equation 5.2)}$$

where σ = stress in the GFRP sheets at mid-height of the stringer, E = modulus of elasticity of the GFRP sheets, and ε = average strain recorded in sheets on both sides of the beam

during test. The next step is to determine the force in the sheets parallel to the grain, F_{GFRP}, using the following equation:

$$F_{GFRP} = n\,t\,w\,\sigma\,(\cos\theta) \qquad \text{(Equation 5.3)}$$

where n = number of layers of sheets per stringer (in this application 1 sheet per side was applied and therefore a value of 2 was used), t = thickness of GFRP sheet, w = width of GFRP sheet, σ = stress in GFRP sheets from Equation 5.2, and θ = angle of GFRP sheet with the horizontal plane, 45° for this application.

To calculate the total longitudinal shear force in the composite stringer it is necessary to calculate the shear stress at the mid-depth of the beam using equation (4.1). The longitudinal shear force, F_{vl}, is calculated as follows,

$$F_{vl} = \tau\, b l_v \qquad \text{(Equation 5.4)}$$

where τ = shear stress, b = beam width and l_v = longitudinal shear length. To determine the contribution of the sheets, the force in the sheets, F_{GFRP}, was divided by the longitudinal shear, F_{vl}.

An example calculation is shown for specimen D2B at a load of 60 kN. The recorded strains on the sheets on either side of the beam at mid-height for B-end were 0.001495 and 0.001260, as shown in the strain profile on Figure 5.2.

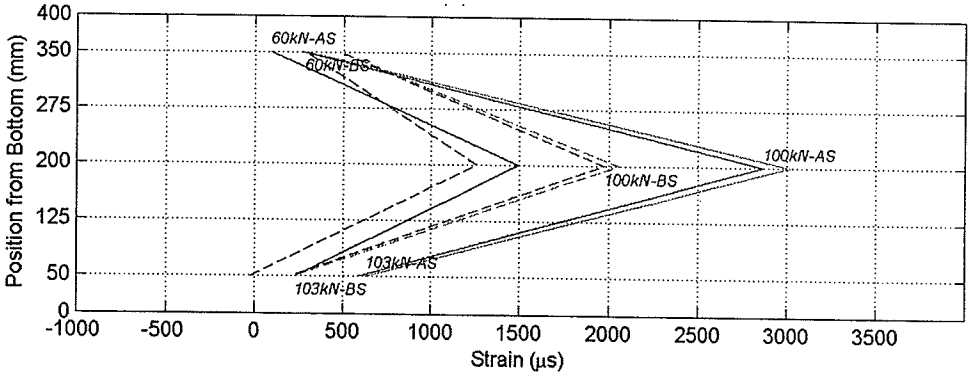

Figure 5.2 Strain profile on GFRP sheets for D2B (Y2-101B). A-side is indicated by solid lines and B-side by dashed lines.

The first step is to use Equation 5.2 to calculate the average stress in the sheets,

$$\sigma = E\varepsilon = 72{,}400\ MPa * \left(\frac{0.001495 + 0.001260}{2}\right) = 99.73\ MPa$$

The shear force parallel to the sheets, F_{GFRP}, is calculated using the average stress calculated above with n = 2, t = 0.353 mm, w = 300mm and θ = 45°,

$$F_{GFRP} = n\,t\,w\sigma(\cos\theta) = 2 * (0.353mm) * (300mm) * (99.73MPa) * (\cos 45) = 14936\ N$$

The next step is to calculate the shear stress on the horizontal plane of interest, which for this specimen is at mid-depth, using Equation 4.1, where V = 45,000 N, Q = 2,000,000 mm^3, I = 533,333,333 mm^4 and b = 100 mm,

$$\tau = \frac{VQ}{Ib} = \frac{45{,}000N * 2{,}000{,}000mm^3}{533{,}333{,}333mm^4 * 100mm} = 1.69\ MPa$$

This stress is used to calculate the longitudinal shear, F_{vl}, using Equation 5.4 and b = 100 and l_v = 850 mm,

$$F_{vl} = \tau\, bl_v = 1.69MPa * 100mm * 850mm = 143{,}437.5\ N$$

Therefore, the percent contribution for this case is:

$$\frac{F_{GFRP}}{F_{lv}} = \frac{14936\,N}{143{,}437.5\,N} * 100 = 10.4\%$$

These calculations were completed at three different load levels and for both ends of all specimens when valid strains were available for both sides of the beam. The average contribution of the sheets at the three load levels is shown in Table 5.1. The results show that the GFRP sheets in the split end of the beams contributes to the shear capacity more than at the solid end. For the tests conducted on the split end of the beam, the sheets on the solid end contributed 6% of the shear force in that end of the beam while at the split end the contribution was 12% at a 60 kN load. The reason for this difference is that the split allows

movement between the top and bottom of the beam with respect to each other. This movement reduces the frictional force available for horizontal shear resistance and allows the GFRP sheets to take up the forces in the beam. Without the differential movement, such as in the solid end of the beam, the sheets only take the forces due to tension and compression in the bottom and top of the beam. At the 97.5 kN load level a significant increase in the sheet contribution occurred for split end sheets when the split end was being tested, but did not occur for the solid end of the beam. This is due to the continuing movement of the top and bottom of the beam increasing the horizontal gap between them and thus the stresses on the sheets. In the solid end there was no gap and thus the contribution remains approximately the same, noting that the contribution is not changing significantly but the forces are always increasing with load. This marginal increase also occurred for both the solid and split end sheets when the solid end was tested. An interesting observation is that the split end sheets took a substantial part of the shear force during the solid end test. This can be explained by the lower normal force applied to the split, reducing the frictional resistance and forcing the sheets to take a greater proportion of the shear force. However at 97.5 kN load level the increase in sheet contribution that was seen for the split end test did not occur as would be expected. The contribution of the sheets at the maximum load for each of the specimens was also calculated. The sheets in the split end during the split end test showed a marginal increase in contribution from the 97.5 kN load level while the solid end during the split end test and both the solid and split end sheets during the solid end test showed greater increases. This is because the beams had become damaged at the ultimate load and were relying on the sheets to hold them together, thus taking greater loads. The split end on the other hand was already taking a significant part of the load due to the split

which represents damage to the beam. Thus it should be noted that the sheets are most effective when the frictional forces are exceeded such as when a split is present. It should be emphasised that the sheets are holding the beam together preventing shear failure.

Table 5.1 Contribution of sheets to overall shear capacity

Load	Split End Test		Solid End Test	
	Solid End Gauges	Split End Gauges	Solid End Gauges	Split End Gauges
kN	%	%	%	%
60	6.3	12.0	6.0	31.6
97.5	7.0	16.6	6.5	32.3
Max.	9.6	17.8	8.9	39.0

5.3 Analysis using Triantafillou Method

An attempt to predict the shear strength of reinforced timber beams was made by Triantafillou (1997). In this method the maximum shear stress in a section, τ_{max}, is used,

$$\tau_{max} = \frac{3V}{2bd} \qquad \text{(Equation 5.5)}$$

where V = shear, b = width of cross-section and d = depth of cross-section. This is then modified by a factor 'r' which is developed by a transformed section analysis, i.e.,

$$r = \frac{\left(1 + n\,{}^{h}/_{h_{frp}}\,\rho_{frp}\right)\left[1 + n\left({}^{h_{frp}}/_{h}\right)^{2}\rho_{frp}\right]}{\left(1 + n\,{}^{h_{frp}}/_{h}\,\rho_{frp}\right)} \qquad \text{(Equation 5.6)}$$

where n = E_{FRP}/E_{wood}, h = depth of beam, h_{frp} = depth of GFRP sheets and ρ_{frp} = reinforcement ratio. Equation 5.5 is rearranged to solve for shear as follows.

$$V = \frac{2bh\tau}{3} r \qquad \text{(Equation 5.7)}$$

Equation 5.7 is used to predict the strength of the beams. In order to use it, a decision has to be made on what to use for three of its parameters: τ, E_{wood}, and ρ_{frp}. The first parameter, τ, is the shear strength of wood. In Eden (2002) the Canadian Highway Bridge Design Code, CAN/CSA-S6-00 (CSA, 2000) design value of 0.9 MPa was used and was then adjusted for size using Clause 9.7.2. For this research the average shear stress from the control specimens was used because it better reflects the actual shear strength of the timber. However, it should also be noted that since the specimens typically did not fail in shear, this value is a conservative estimate of the shear strength. The average shear strength from the control specimens was 2.9 MPa. To calculate the modular ratio, n, it is necessary to decide what value of E_{wood} to use. For this analysis it was decided to use the modulus of elasticity from the elasticity tests conducted on the specimens prior to applying the reinforcement. However, for the purposes of design there would not be any elasticity tests conducted and the modulus of elasticity from the Canadian Highway Bridge Design Code (CAN/CSA-S6-00) will be used based on the grade stringers. The modulus of elasticity for the GFRP sheets, E_{frp}, is taken from the manufacturer's literature as 72.4 GPa. Finally the reinforcement ratio needs to be determined. Triantafillou (1997) calculated the ratio in the vertical plane. However, the horizontal plane is critical for shear and for these calculations the plane between the support and loading point was used.

$$\rho_{frp} = \frac{2tw/\sin\theta}{bl_v} \qquad \text{(Equation 5.8)}$$

In Equation 5.8, t = thickness of the GFRP sheet (0.353 mm), w = width of sheet (300 mm), θ = angle of GFRP sheet to horizontal plane, b = width of specimen and l_v = horizontal shear

length between the support and the loading point. The results are tabulated in Table 5.2 where only the first test on the specimens is shown since the pre-repair modulus on the opposite end of the beam is no longer valid because of the damage to the beam caused by the first test.

The results show that except for two cases this method conservatively estimates the shear capacity. The first exception was specimen D2B which failed in bearing at the support and the second was specimen D8B which experienced a dap failure, but also exhibited the weakest pre-repair elasticity for diagonal sheet specimens. On average the experimental results were 1.278 times greater than the Triantafillou analysis with a standard deviation of 0.219 and coefficient of variation of 17.1%. The greatest difference between experimental and analytical values was 58%. This analytical prediction is reasonably good and not overly conservative as it was in Eden (2002) where the CSA-S6-00 design value (f_v = 0.9 MPa) was used as the shear stress. It should also be noted that the specimens were not failing in shear and that the shear used for comparison is that at the maximum load, thus the actual shear strength is higher and these results are conservative.

Table 5.2 Comparison of analytical shear capacity to experimental

Specimen Designation	Pre-Test MOE	Experimental Shear	Analytical Shear	Experimental/ Analytical Shear
	GPa	kN	kN	
D1A	3.41	90.2	83.1	1.085
D2B	4.69	77.5	81.5	0.950
D3A	4.31	111.1	81.9	1.356
D4B	3.51	86.3	83.0	1.041
D5B	5.19	117.7	81.1	1.451
D6B	4.16	129.1	82.1	1.573
D7B	6.88	108.7	80.2	1.355
D8B	2.18	72.7	86.4	0.842
D9B	3.39	98.6	83.1	1.186
D10B	5.36	125.8	81.0	1.553
D11B	4.21	120.5	82.0	1.469
D12B	6.25	121.4	80.5	1.508
D13B	5.71	119.2	80.8	1.475
D14B	3.59	89.5	82.8	1.081
D15B	6.10	88.0	80.6	1.092
D16B	6.07	94.7	80.6	1.175
D17B	6.62	126.9	80.3	1.580
D18B	5.11	90.4	81.2	1.113
D19B	3.76	117.5	82.6	1.423
D20B	3.92	102.8	82.4	1.247
D21B	4.79	104.8	81.5	1.286
Average		104.4	81.8	1.278
Std. Dev.		17.1	1.4	0.219
CV		0.16	0.02	0.17

CHAPTER 6 CONCLUSIONS AND RECOMMENDATIONS

6.1 CONCLUSIONS

Damaged timber bridge stringers shear-strengthened with GFRP sheets were investigated with two strengthening schemes incorporating vertical and diagonal GFRP sheets, respectively. It was found that while the use of strengthening improved both the ultimate load and deformability, the vertical sheets tore up easily in the vicinity of the horizontal splits, while the diagonal sheets, primarily subjected to tension, did not tear up from the surface. However, it should be noted that if the horizontal shear splits are open, it is necessary to close them tightly before strengthening to ensure that the sheets do not tear up.

While preparing timber bridge stringers for rehabilitation using GFRP sheets wrapped around the edge, it is essential that the timber edges be rounded to a minimum of 12.5 mm to ensure the sheets are able to properly bond to the surface.

The strengthening scheme with diagonal GFRP sheets performed very well with much larger increases in both the ultimate load and deformability in comparison to vertical sheet specimens. For reject grade specimens an average ultimate load increase was found to be 19.4% for vertical sheet specimens and 39.1% for diagonal sheet specimens. For select structural specimens an average ultimate load increase of 14.5% was found for diagonal sheet specimens, confirming that for higher grade timber the strength increase is lower (Gentile 2000).

A noticeable increase in the flexural stiffness of the beams was observed for diagonal sheet specimens resulting from closing the splits and tying the top and bottom of the beams together allowing the beam to act as a single unit and hence increasing the moment of inertia

of the sections. A stiffness increase of 47.8% was found for the first test on diagonal sheet specimens while the vertical sheet specimens only had 3.5% increase, thus showing the superiority of diagonal sheets over vertical sheets. The stiffness of the beams during the second test tended to decline because of the damage from the first test. This increase was due to the two split beam haves acting as one with the help of the sheets. It was shown that the diagonal scheme was more effective in providing this effectively.

Specimens with vertical GFRP sheets typically experienced flexural failure, whereas the stringers with diagonal sheets had become so strong that they frequently failed in bearing either under the concentrated test load, or at the support. Bond between the GFRP sheets and the creosote timber was not found to be a problem in this research project, however, further research is necessary to ensure that long term bond problems do not occur.

The safety index of beams strengthened using this approach was increased by 42% compared to the control beams. The contribution of the GFRP sheets to the overall shear capacity was calculated. These calculations showed that as expected the sheets on the split end were contributing more to shear strength than sheets on the solid end. This is a result of greater horizontal movement, although restrained, in the split end. The average contribution at a load of 60 kN, which is approximately a CL-625 design truck, was 12% in the split end during loading of the split end while an average contribution of 32% was found when loading the solid end. The sheets on the solid end only contributed on average 6% when loading either end. An analysis based on a method developed by Triantafillou (1997) was completed showing that it was capable to conservatively estimate the shear strengths.

The shear strength of the beams was calculated, and it is recommended that when diagonal GFRP sheets are used in the shear span of Douglas-fir timber bridge stringers, shear

strength of 1.8 MPa may be considered in rehabilitation of existing bridges provided that the minimum requirements provided in the draft provisions for rehabilitation of timber bridges in CAN/CSA-S6-00 Canadian Highway Bridge Design Code are met. These provisions are based on this research, and can be found in Appendix D. The research has shown conclusively that diagonal GFRP sheets are more effective than the vertical sheets in shear-strengthening timber stringers with horizontal splits at their ends. Thus, this technique of rehabilitation for creosote treated timber bridges is recommended for use after durability testing has been completed.

6.2 Recommendations For Future Research

The research detailed in this thesis shows that using GFRP sheets have good potential. However, further research is needed to determine if the method can be optimized. Areas that specifically need to be researched are:

1. Determine the minimum and optimum amounts of reinforcement to achieve appropriate strength improvement.
2. Develop a system that uses a combination of shear and flexural GFRP sheets.
3. Investigate the durability of bonding agents used bond GFRP sheets to creosote treated wood under the effects of temperature and moisture fluctuations.
4. The bond strength between the creosote treated wood and the sheets needs to be determined.
5. Development of analytical methods is needed to further understand the effect of GFRP sheet on the shear capacity.

6. In future research a minimum 5 strain gauges per GFRP sheet is needed to adequately determine the distribution of stresses in the sheets.
7. Further research is needed in determining the shear strength of unstrengthened wood, especially ingrade testing of timbers.

REFERENCES

Amy, K.S. 2004. "Reinforcing Dapped Timber Stringers with GFRP Bars." Master's of Science in Civil Engineering thesis. University of Manitoba, Winnipeg, Manitoba, Canada.

ASTM. (1994). Standard Methods of Testing Small Clear Specimens of Timber, ASTM D143-94. American Society of Testing and Materials, Philadelphia, PA.

ASTM. (1999). Standard Practice for Establishing Structural Grades and Related Allowable Properties for Visually Graded Lumber, ASTM D245-99. American Society of Testing and Materials, Philadelphia, PA.

CSA. Canadian Highway Bridges Design Code, CAN/CSA-S6-00. 2000. Toronto, Ontario, Canada. CSA International.

Brooks, K.M. 2000. Assessment of the environmental effects associated with wooden bridges preserved with creosote, pentachlorophenol, or chromated copper arsenate. Res. Pap. FPL-RP-587. Madison, WI: U.S. Department of Agriculture, Forest Service, Forest Products Laboratory.

Bulleit, W.M., L.B. Sandburg, and G.J. Woods. 1989. Steel-reinforced glued laminated timber. *Journal of Structural Engineering - ASCE.* 115(2): 433-444.

Eden, R.J. 2002. "Strengthening of Timber Bridge Stringers Using GFRP." Master's of Science in Civil Engineering thesis. University of Manitoba, Winnipeg, Manitoba, Canada.

Ehsani, M., M. Larsen and N. Palmer. 2004. Strengthening of Old Wood with New Technology. Wood Science. February: 19-21.

Ethington, R.L., W.L. Galligan, H.M. Montrey and A.D. Freas. 1979. Evolution of Allowable Stresses in Shear for Lumber. General Technical Report, GTR-FPL-23. Madison, WI: U.S. Department of Agriculture, Forest Service, Forest Products Laboratory.

Foschi, R.O., and J.D. Barrett. 1976. Longitudinal shear strength of Douglas-fir. *Canadian Journal of Civil Engineering*. 3: 198-208.

Foschi, R.O., and J.D. Barrett. 1977. Longitudinal shear in wood beams: a design method. *Canadian Journal of Civil Engineering*. 4: 363-370.

Gentile, C.J. 2000. "Flexural Strengthening of Timber Bridge Beams using FRP. Master's of Science in Civil Engineering thesis. University of Manitoba, Winnipeg, Manitoba, Canada.

Gentile, C., D. Svecova, and S.H. Rizkalla. 2002. Timber beams strengthened with GFRP bars – development and application. *Journal of Composites for Construction - ASCE*. 6(1): 11-20.

Hernandez, R., J.F. Davalos, S.S. Sonti, Y. Kim, and R.C. Moody. 1997. Strength and stiffness of reinforced Yellow-poplar glued-laminated beams. Res. Pap. FPL-RP-554. Madison, WI: U.S. Department of Agriculture, Forest Service, Forest products Laboratory.

Huggins, M.W., J.H.L. Palmer, and E.N. Alpin. 1966. Evaluation of the effect of delamination. *Engineering Journal*. February, 32-41.

Johns, K.C. and S. Lacroix. 2000. Composite reinforcement of timber in bending. *Canadian Journal of Civil Engineering*. 27: 899-906.

Keenan, F.J. and Selby, K.A. 1973. The shear strength of Douglas-fir glued-laminated Timber Beams. Publ. 73-01, Dep. Civ. Eng., Univ. Toronto, Toronto, Ont.

Lam, F., H. Yee, and J.D. Barrett. 1997. Shear strength of Canadian softwood structural lumber. *Canadian Journal of Civil Engineering*. 24: 419-430.

Lantos, G. 1970. The flexural behaviour of steel reinforced laminated timber beams. Wood Science. 2(3): 136-143.

Madsen, B. 1992. Structural Behaviour of Timber. Timber Engineering Ltd. North Vancouver, British Columbia, Canada.

National Lumber Grades Authority 2002. Standard Grading Rules for Canadian Lumber 2000. January 1, 2002 ed., New Westminster, British Columbia, Canada.

Newlin, J.A., G.E. Heck, and H.W. March. 1934. New method of calculating longitudinal shear in checked wooden beams. *Transactions of the American Society of Mechanical Engineers*. 739-744.

Peterson, J. 1965. Wood beams prestressed with bonded tension elements. *Journal of the Structural Division - ASCE*. 91(ST1): 103-119.

Plevris, N and T. Triantafillou. 1992. FRP-Reinforced wood as structural material. *Journal of Materials in Civil Engineering – ASCE*. 4(3): 300-317.

Rammer, D.R., Soltis, L.A., and Lebow, P.K. 1996. Experimental shear strength of unchecked solid-sawn Douglas-fir. Res. Pap. FPL-RP-553. Madison, WI: U.S. Department of Agriculture, Forest Service, Forest Products Laboratory.

Triantafillou, T. 1992. Prestressed FRP sheets as external reinforcement of wood members. *Journal of Structural Engineering – ASCE*. 118(5): 1270-1284.

Triantafillou, T. 1997. Shear reinforcement of wood using FRP materials. *Journal of Materials in Civil Engineering – ASCE*. 9(2): 65-69.

APPENDIX A

LOAD-DEFLECTION GRAPHS

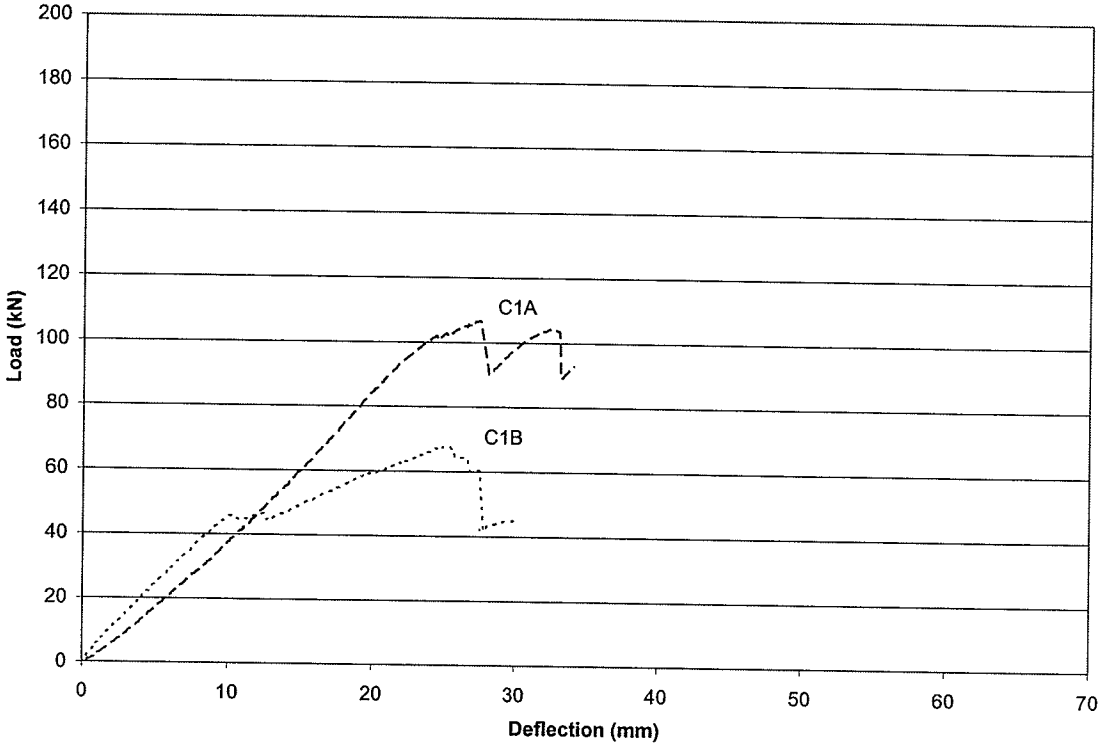

Figure A-1 Control Specimen C1 (Y2-19)

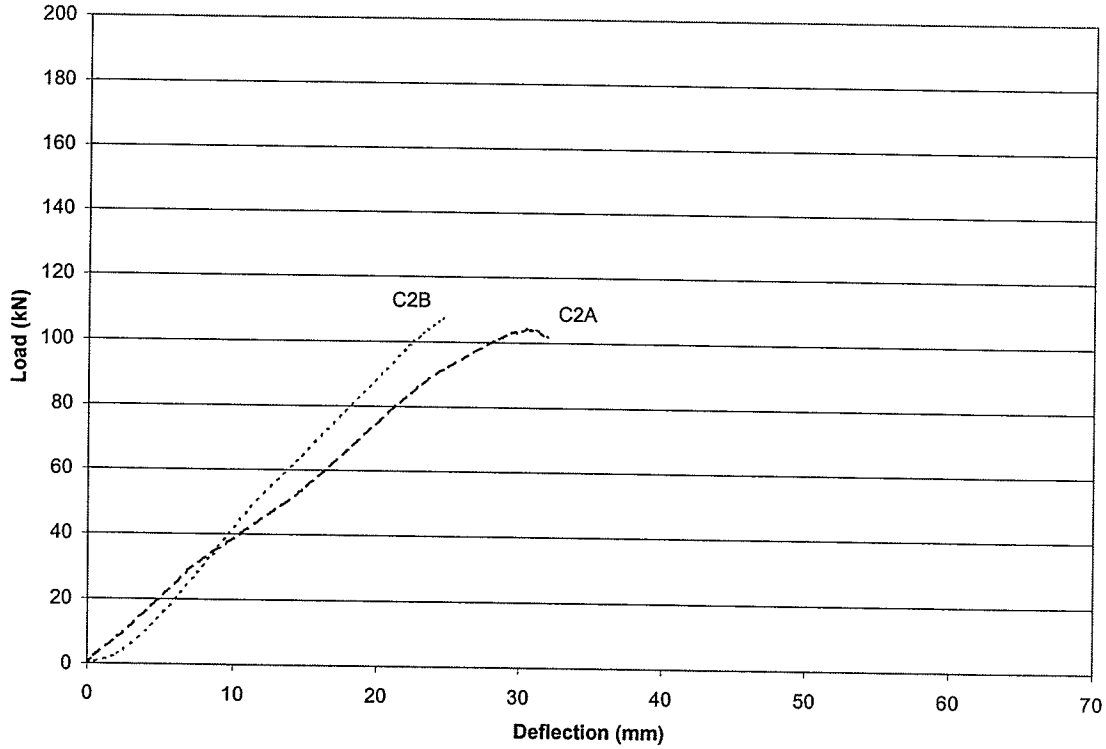

Figure A-2 Control Specimen C2 (Y2-25)

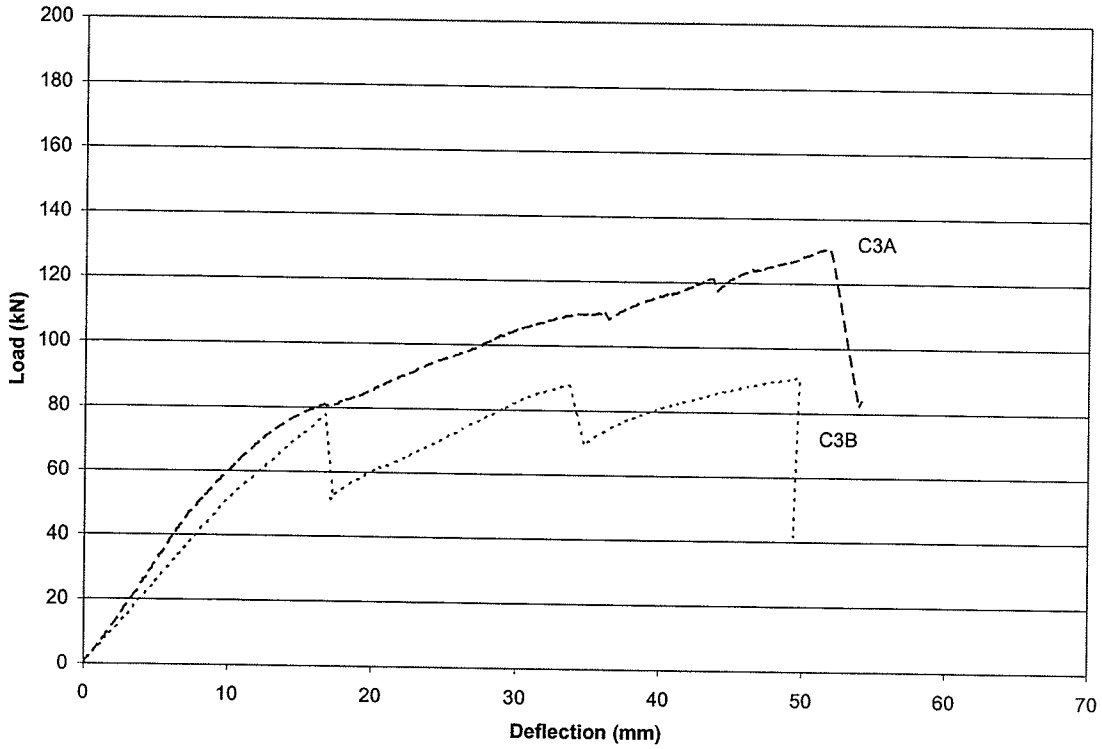

Figure A-3 Control Specimen C3 (Y2-11)

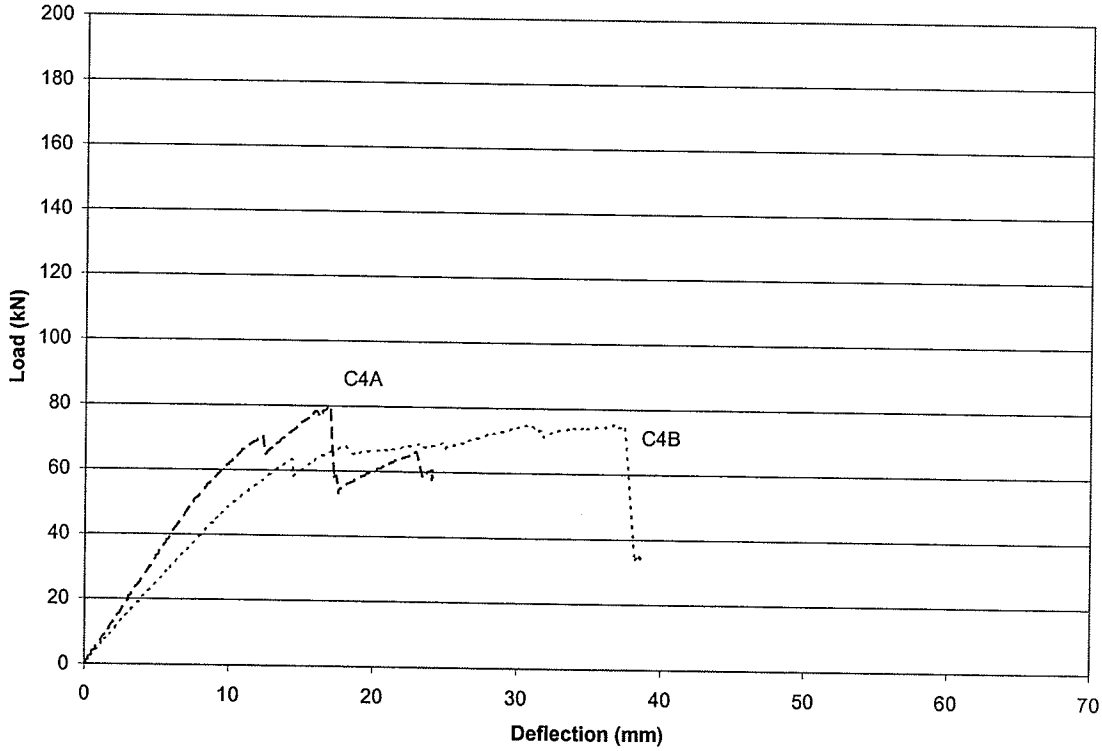

Figure A-4 Control Specimen C4 (Y2-12)

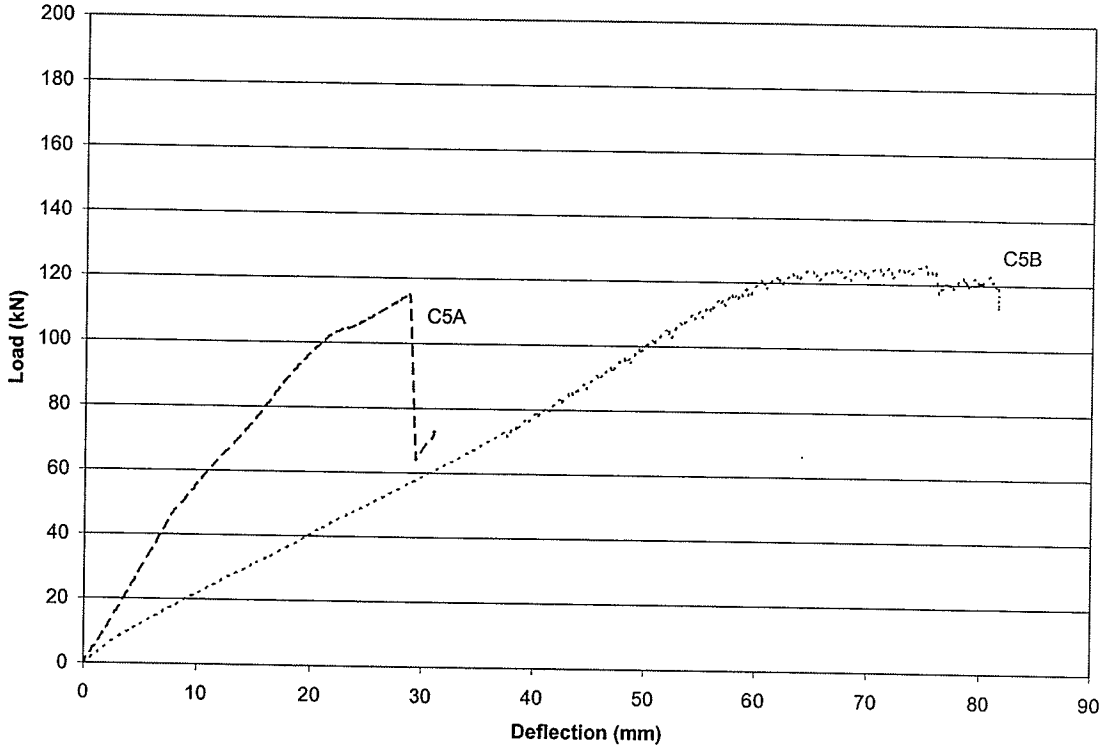

Figure A-5 Control Specimen C5 (Y2-33)

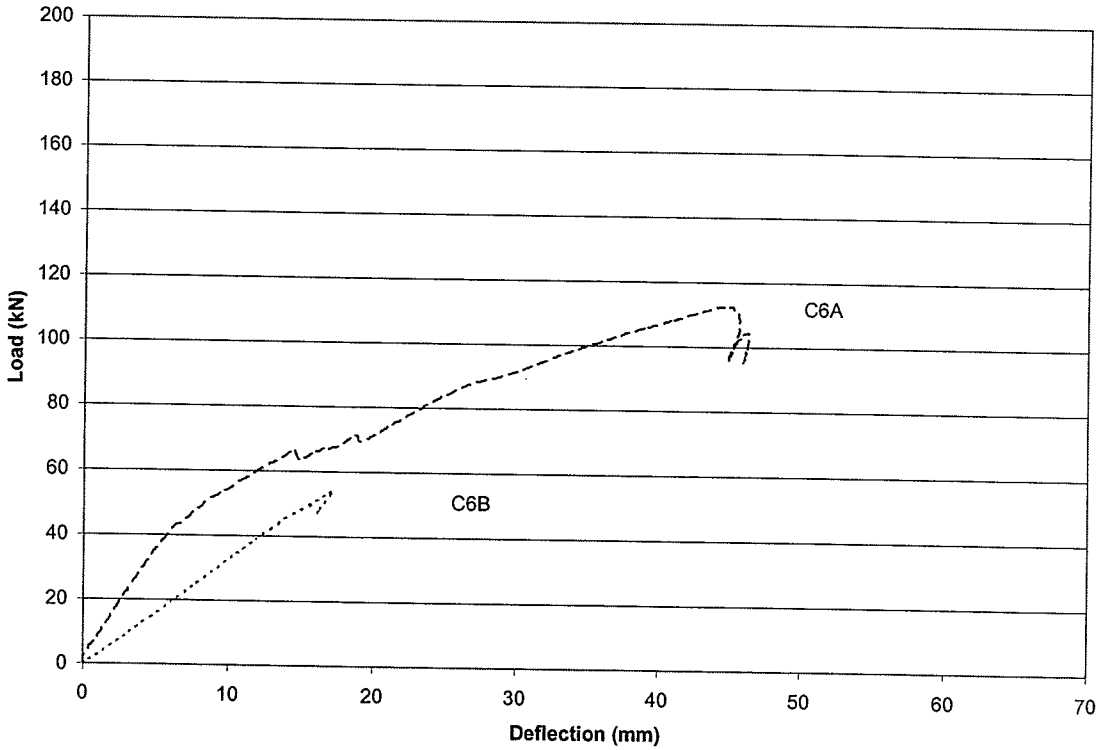

Figure A-6 Control Specimen C6 (Y2-9)

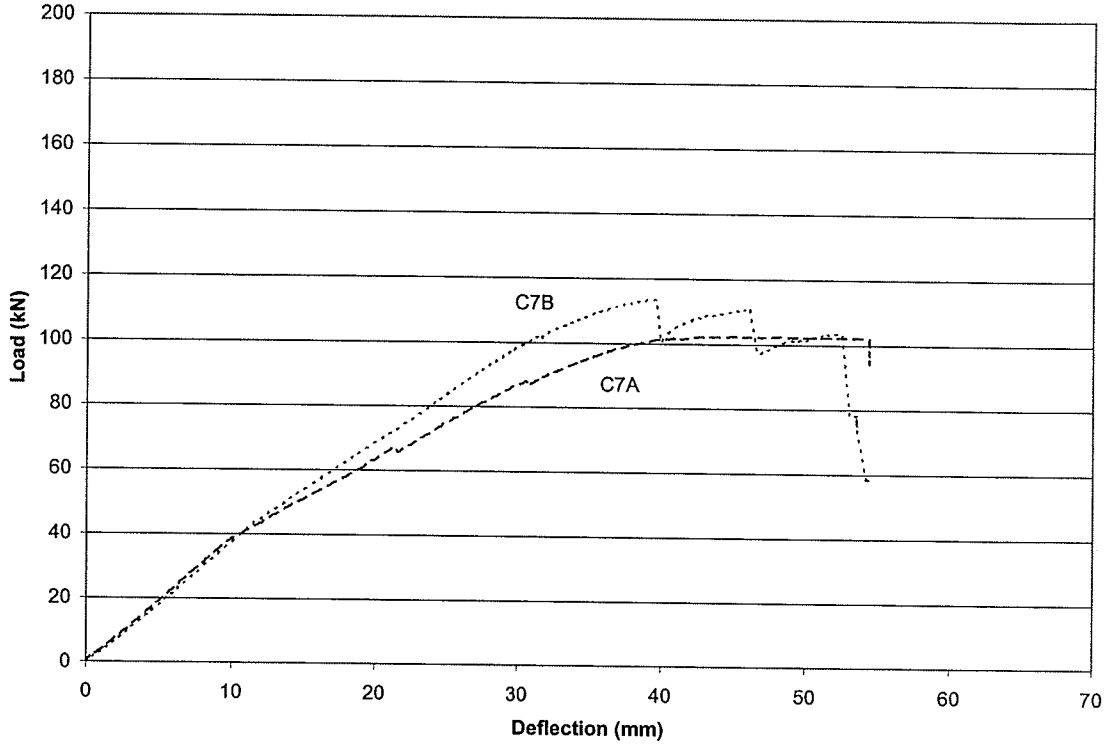

Figure A-7 Control Specimen C7 (Y2-4)

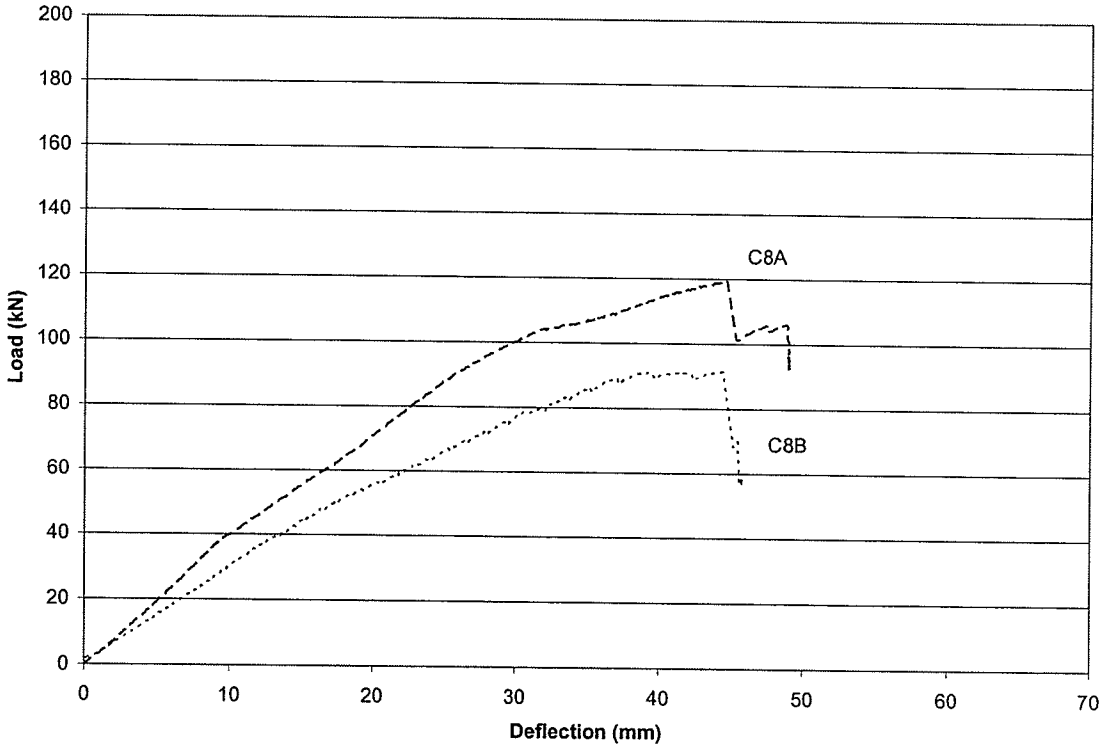

Figure A-8 Control Specimen C8 (Y2-5)

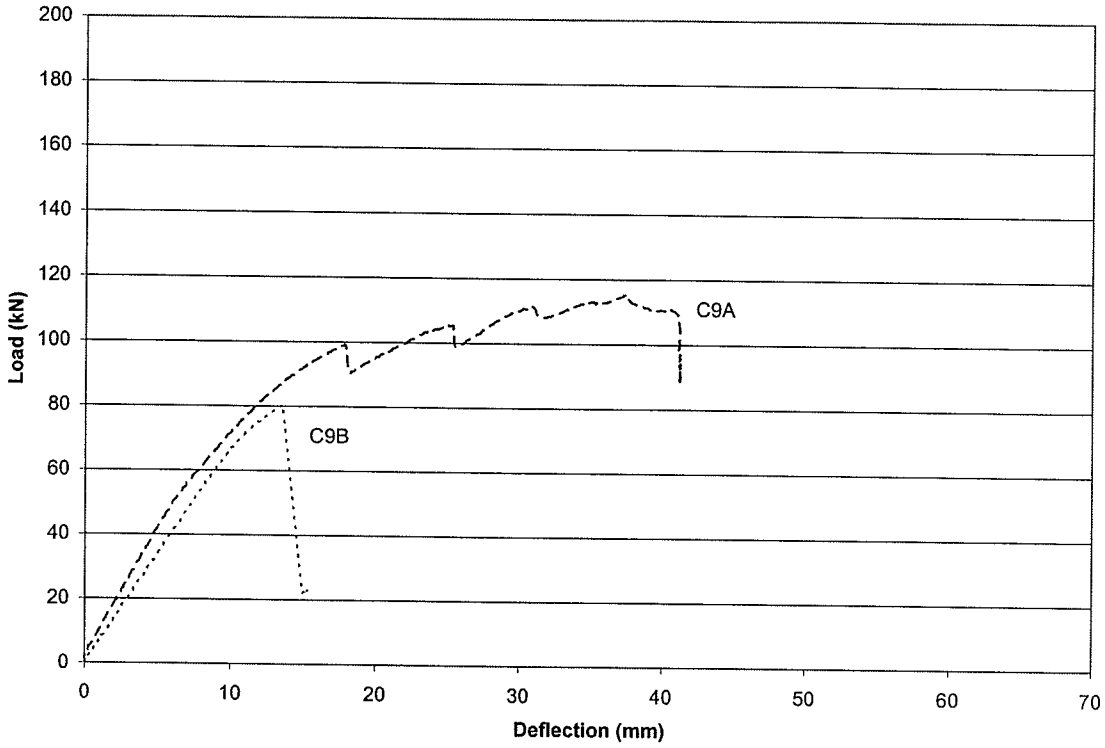

Figure A-9 Control Specimen C9 (Y2-29)

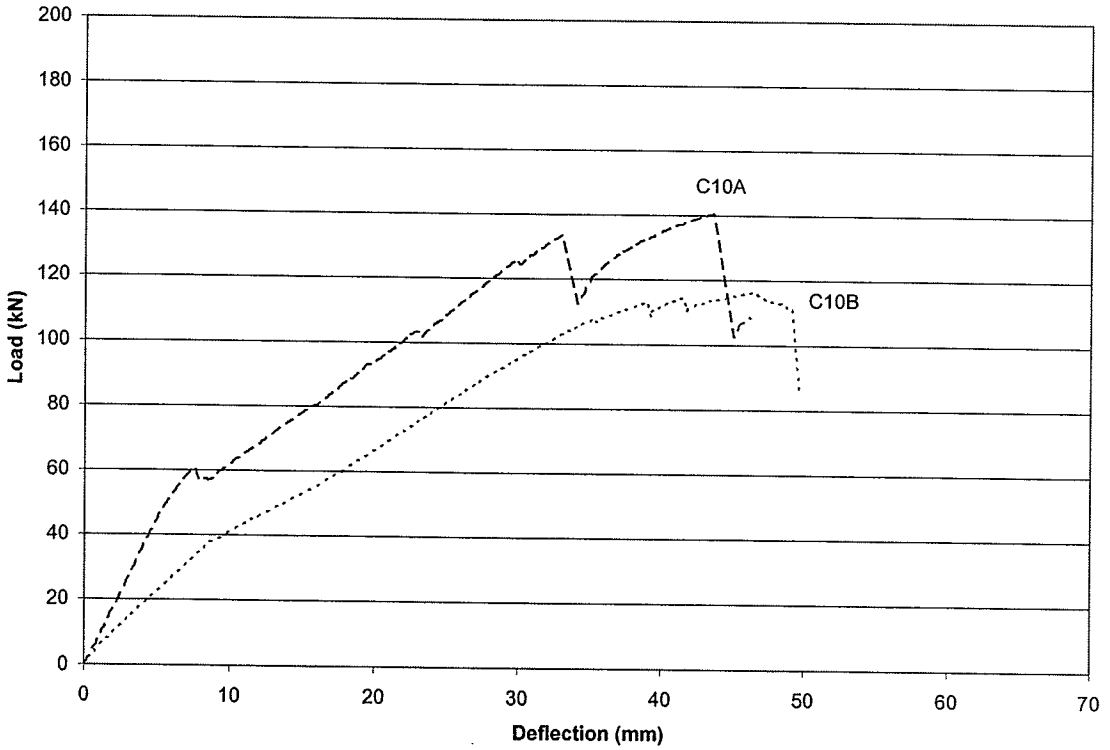

Figure A-10 Control Specimen C10 (B15)

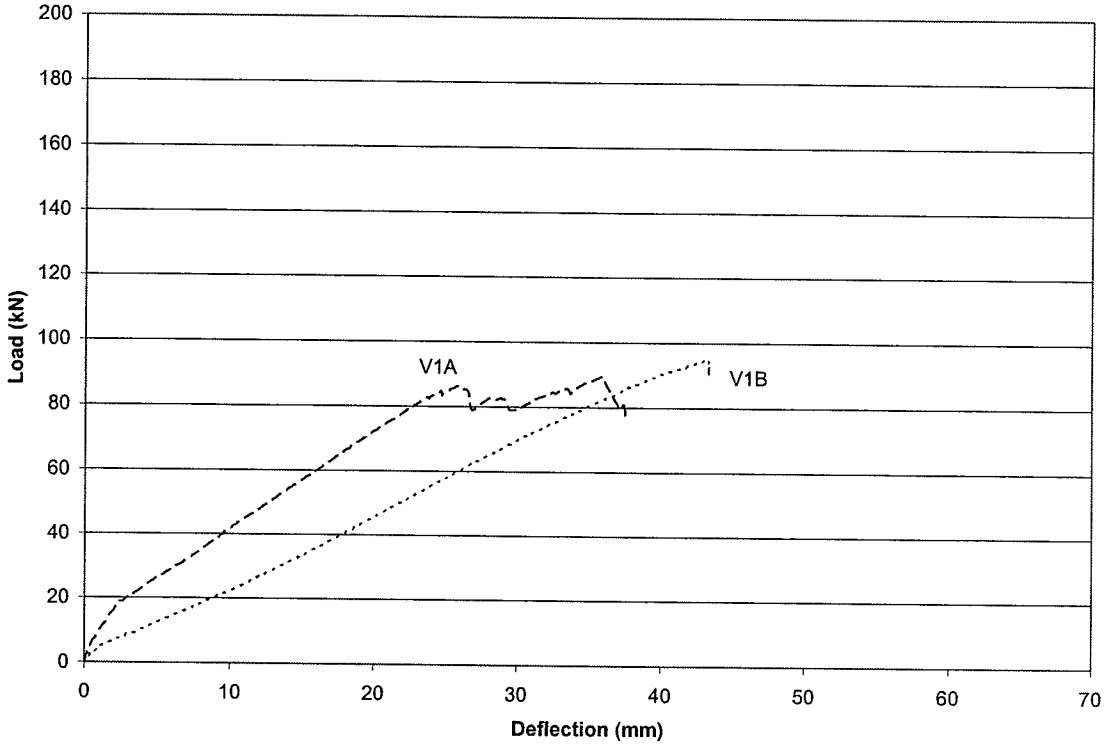

Figure A-11 Vertical Sheet Specimen V1 (Y2-22)

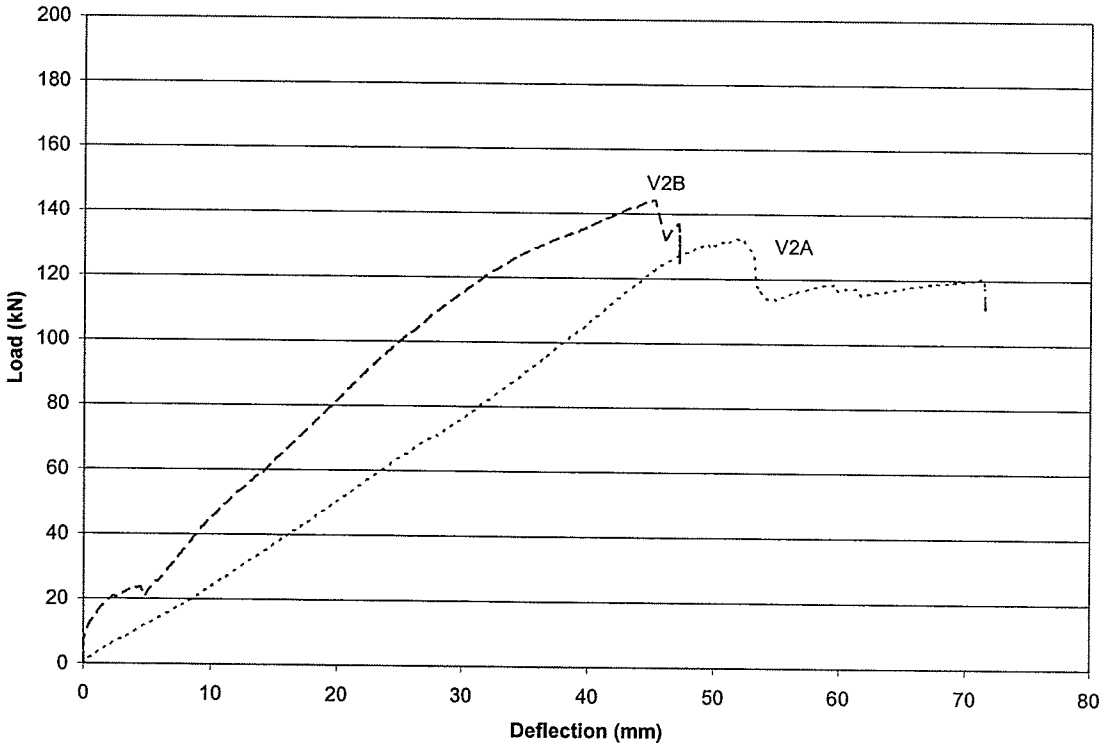

Figure A-12 Vertical Sheet Specimen V2 (Y2-13)

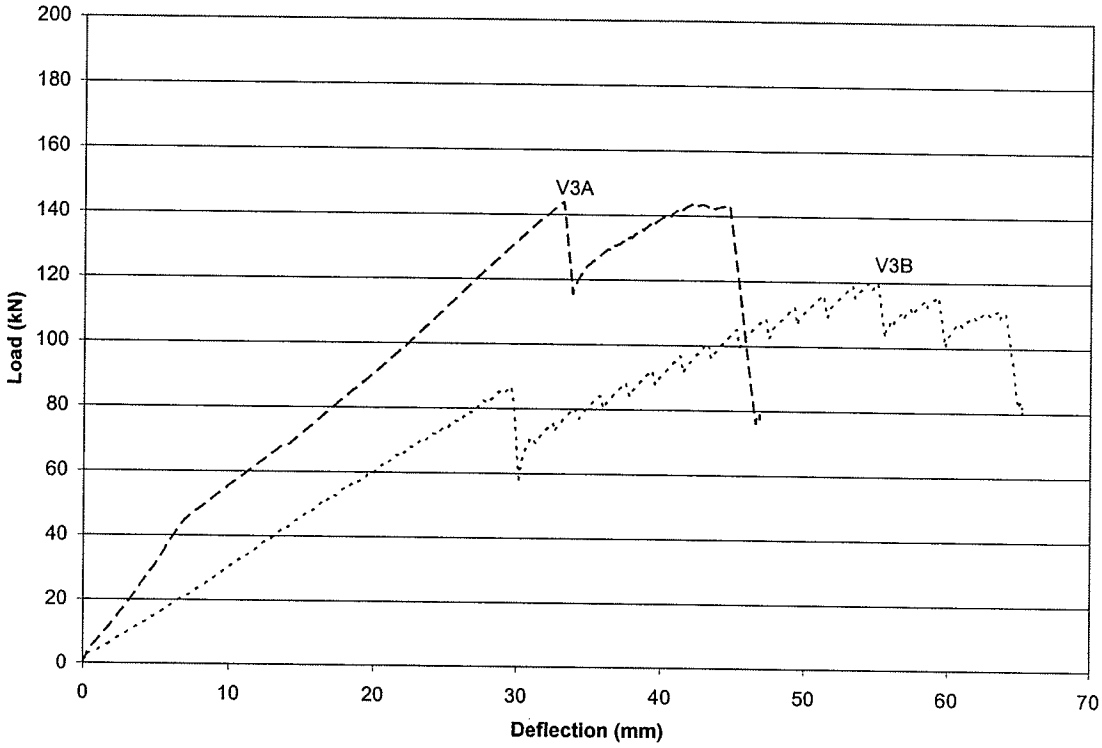

Figure A-13 Vertical Sheet Specimen V3 (Y2-10)

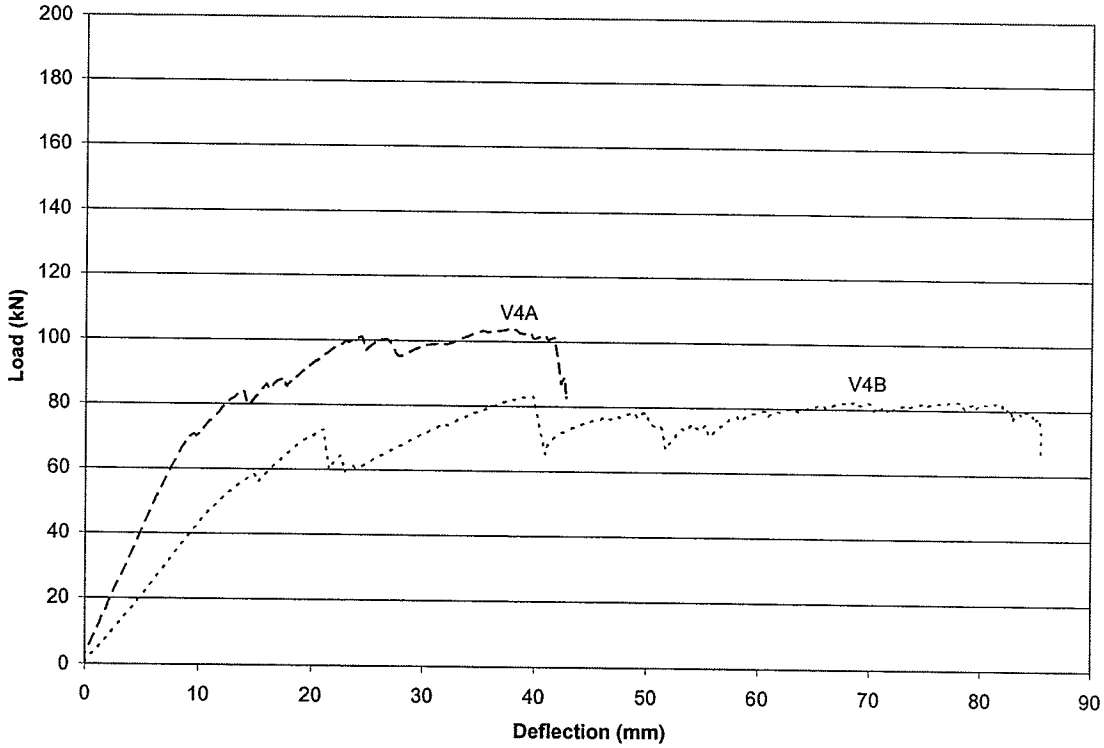

Figure A-14 Vertical Sheet Specimen V4 (Y2-32)

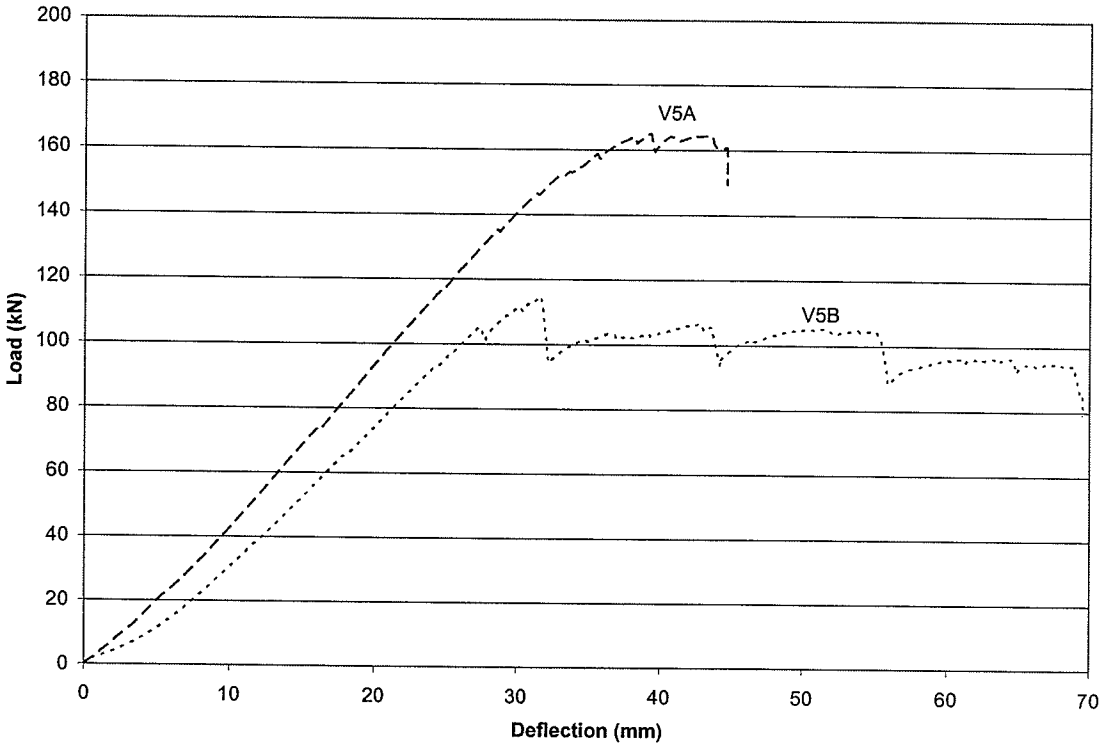

Figure A-15 Vertical Sheet Specimen V5 (Y2-8)

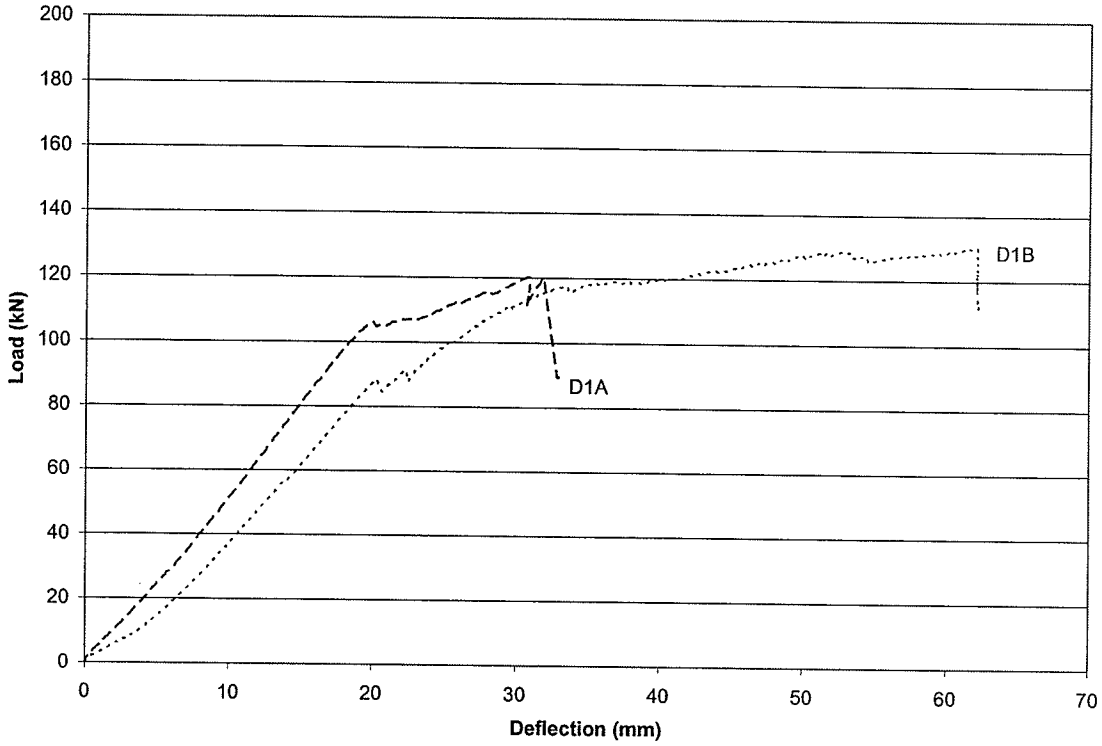

Figure A-16 Diagonal Sheet Specimen D1 (Y2-14), solid end tested first.

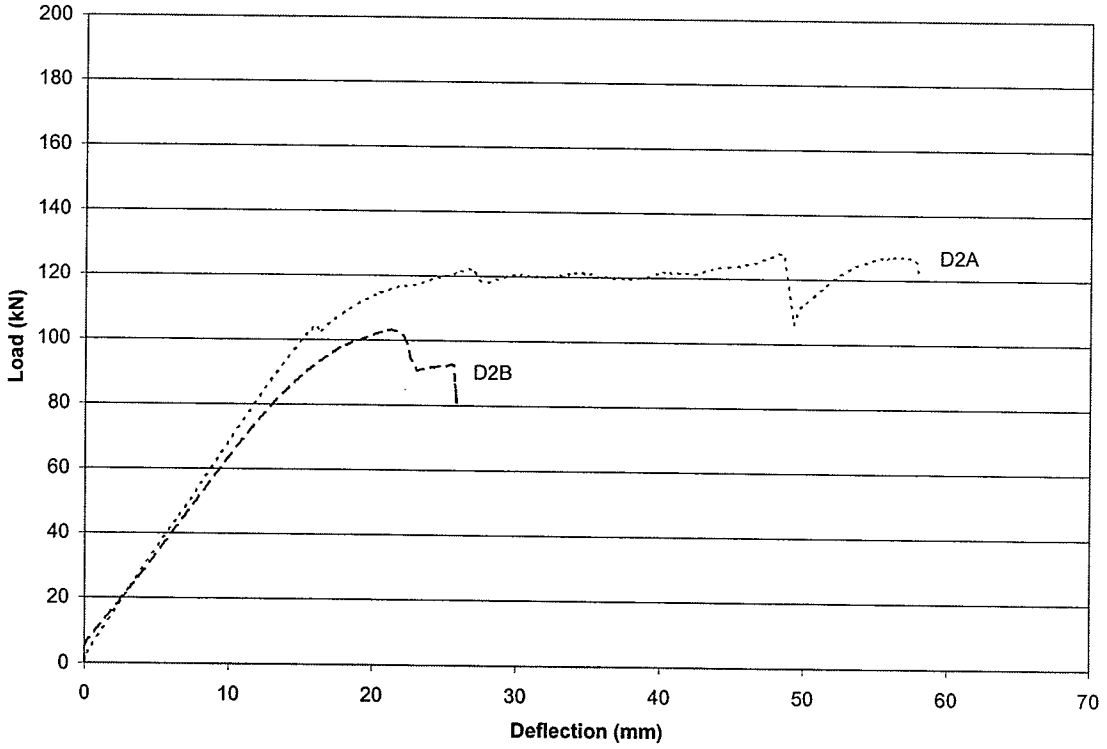

Figure A-17 Diagonal Sheet Specimen D2 (Y2-101)

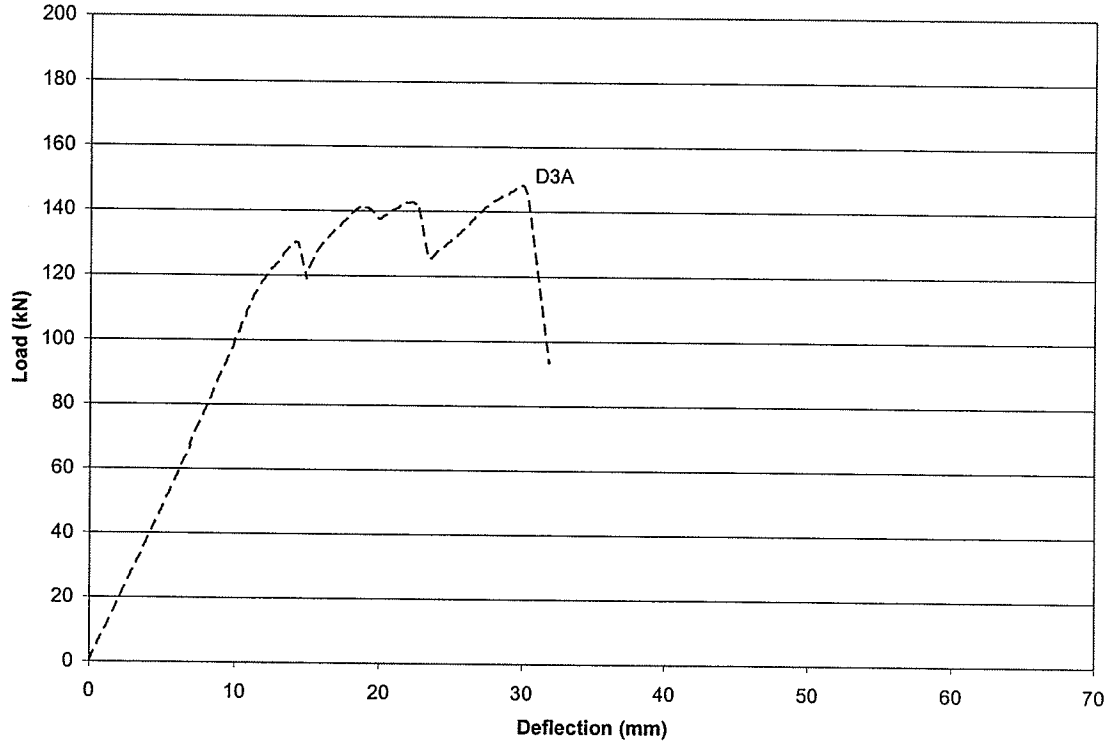

Figure A-18 Diagonal Sheet Specimen D3 (Y2-16), only solid end tested.

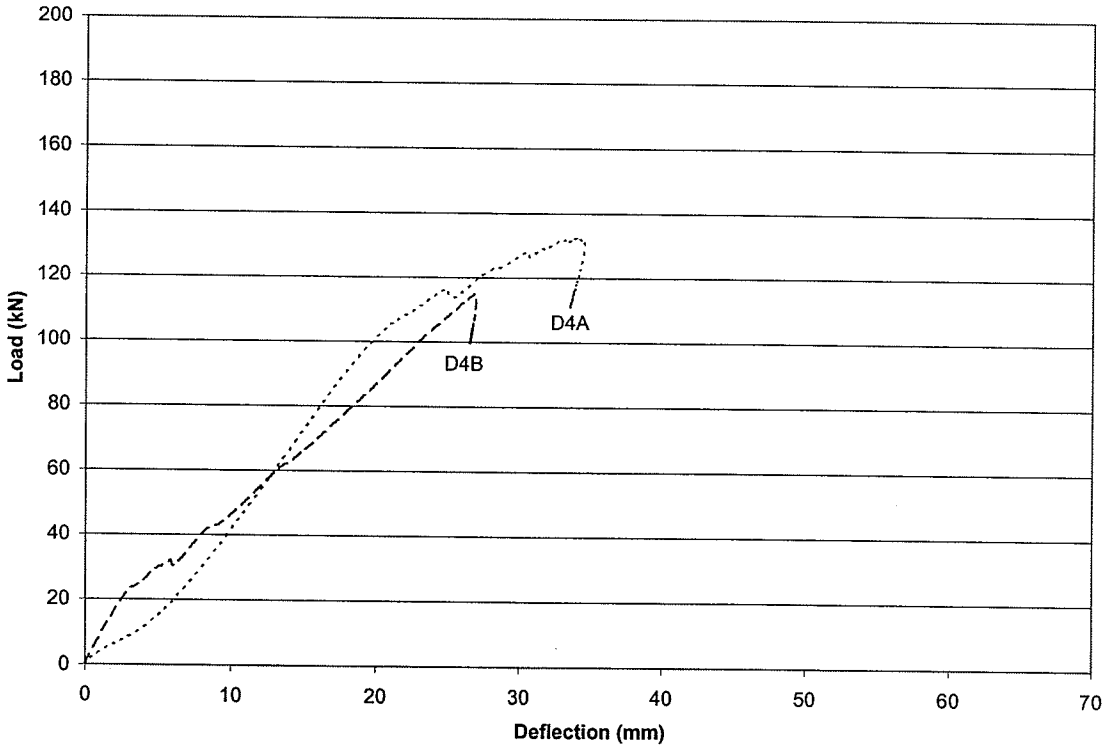

Figure A-19 Diagonal Sheet Specimen D4 (Y2-103)

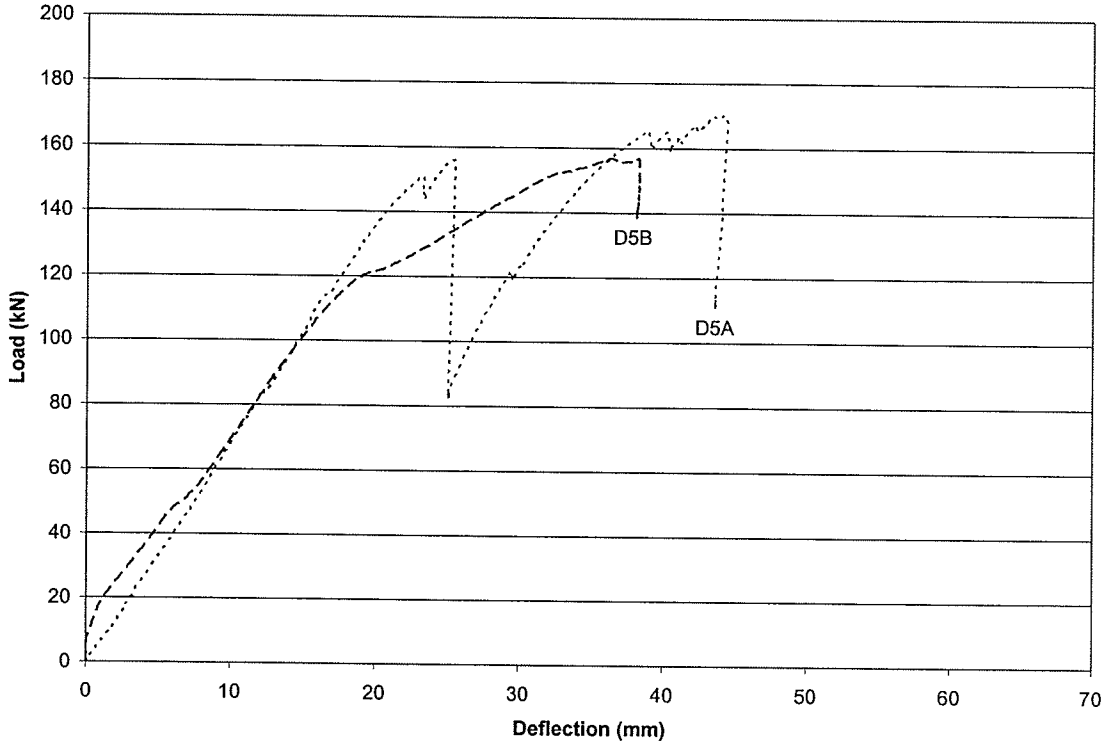

Figure A-20 Diagonal Sheet Specimen D5 (Y2-102)

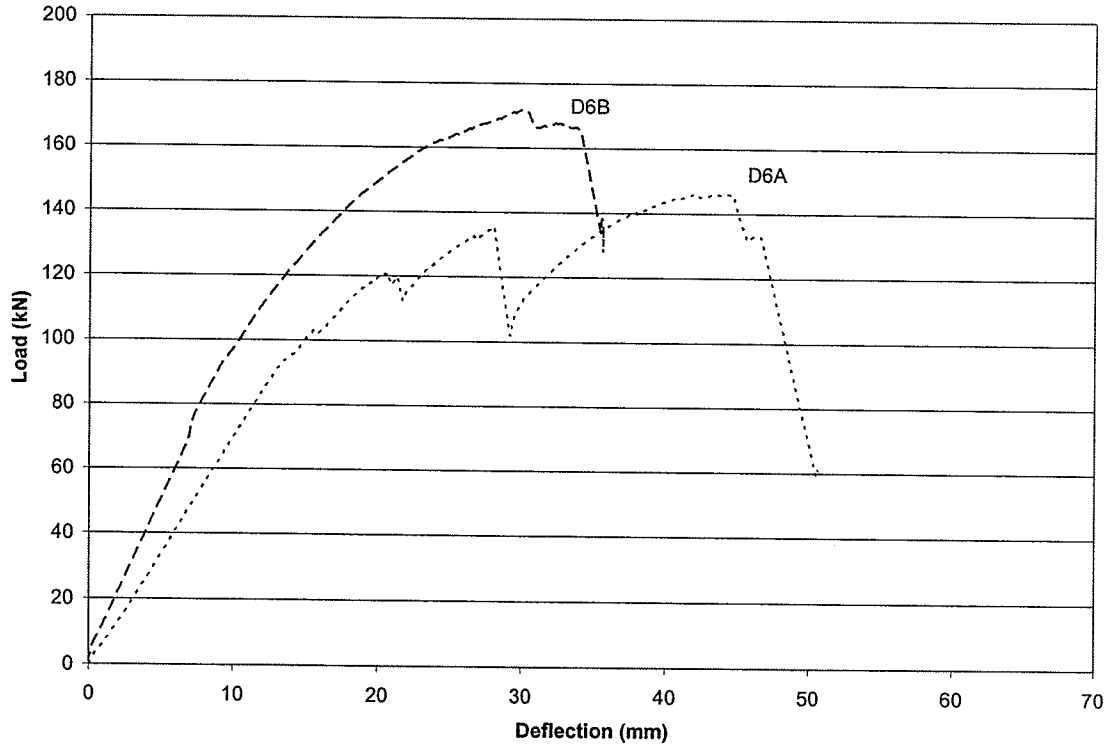

Figure A-21 Diagonal Sheet Specimen D6 (Y2-109)

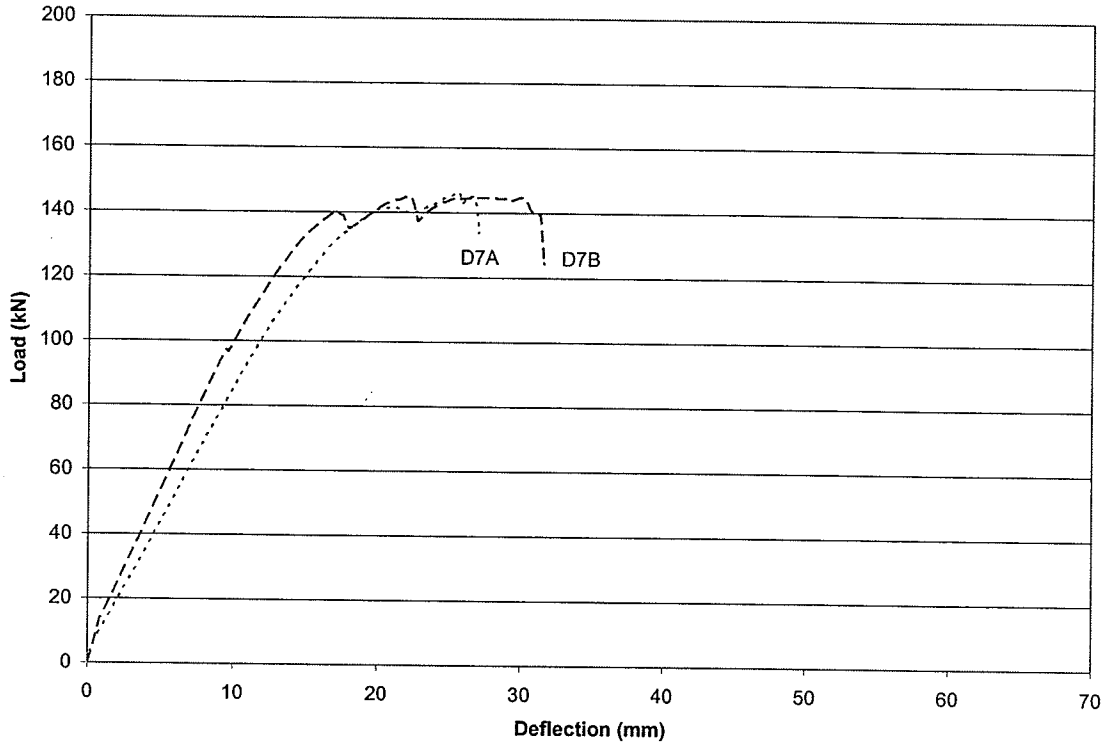

Figure A-22 Diagonal Sheet Specimen D7 (Y2-112)

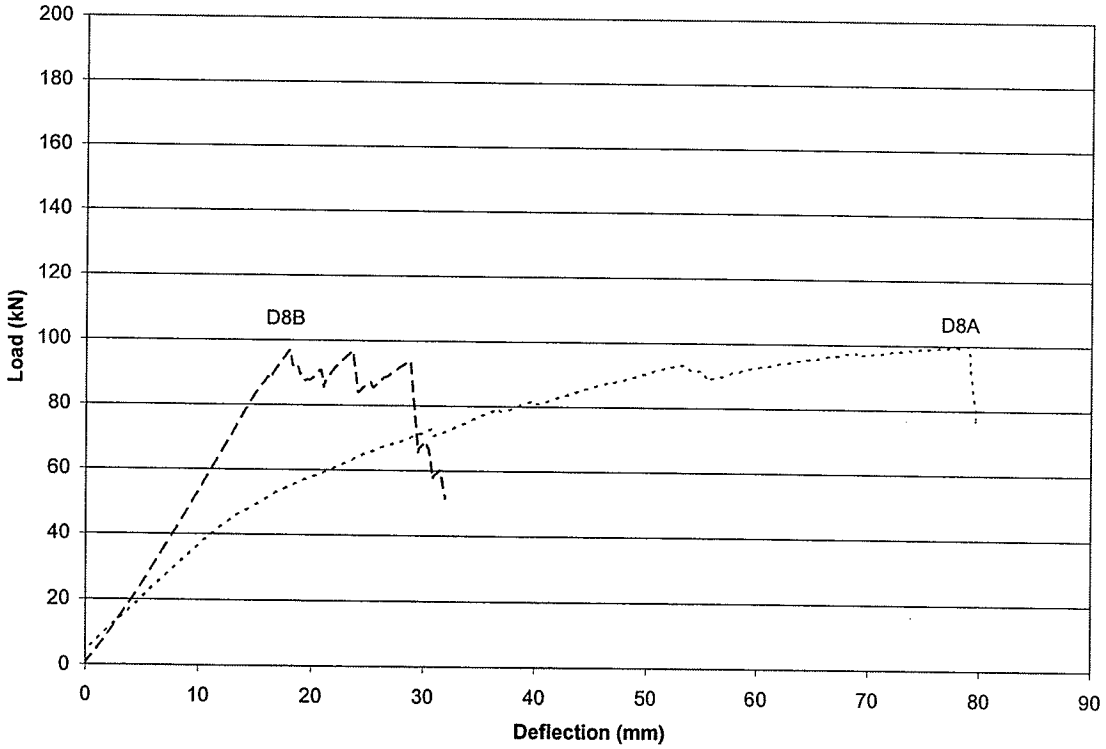

Figure A-23 Diagonal Sheet Specimens D8 (Y2-111)

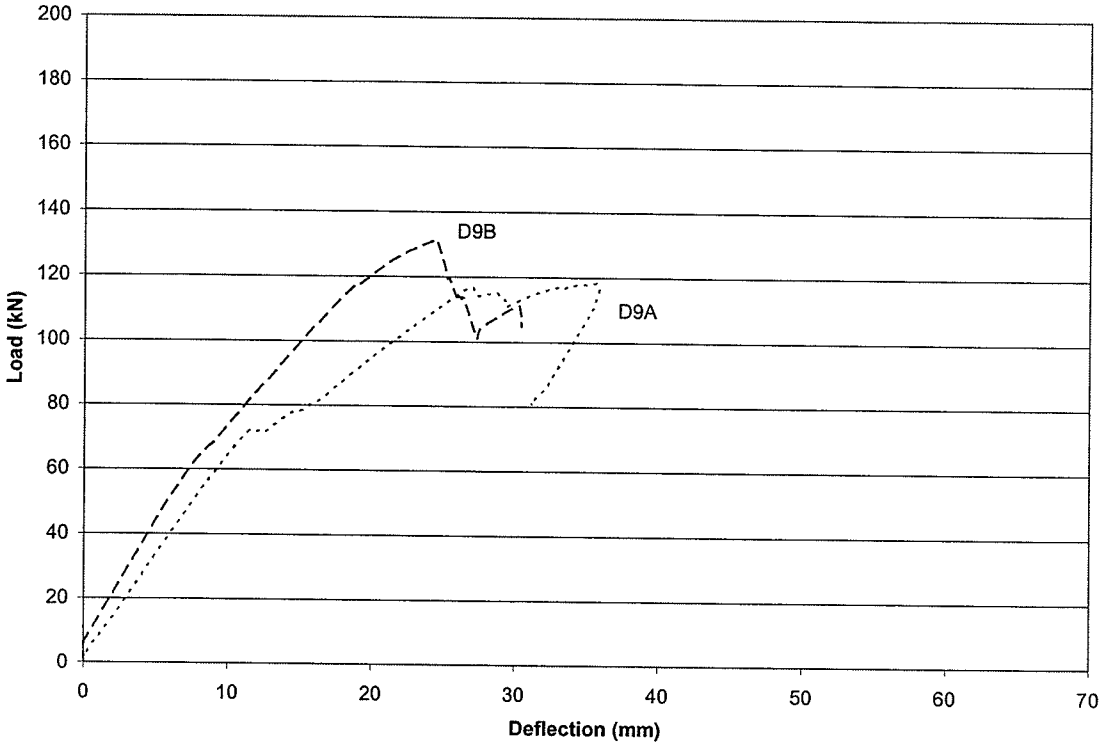

Figure A-24 Diagonal Sheet Specimen D9 (Y2-114)

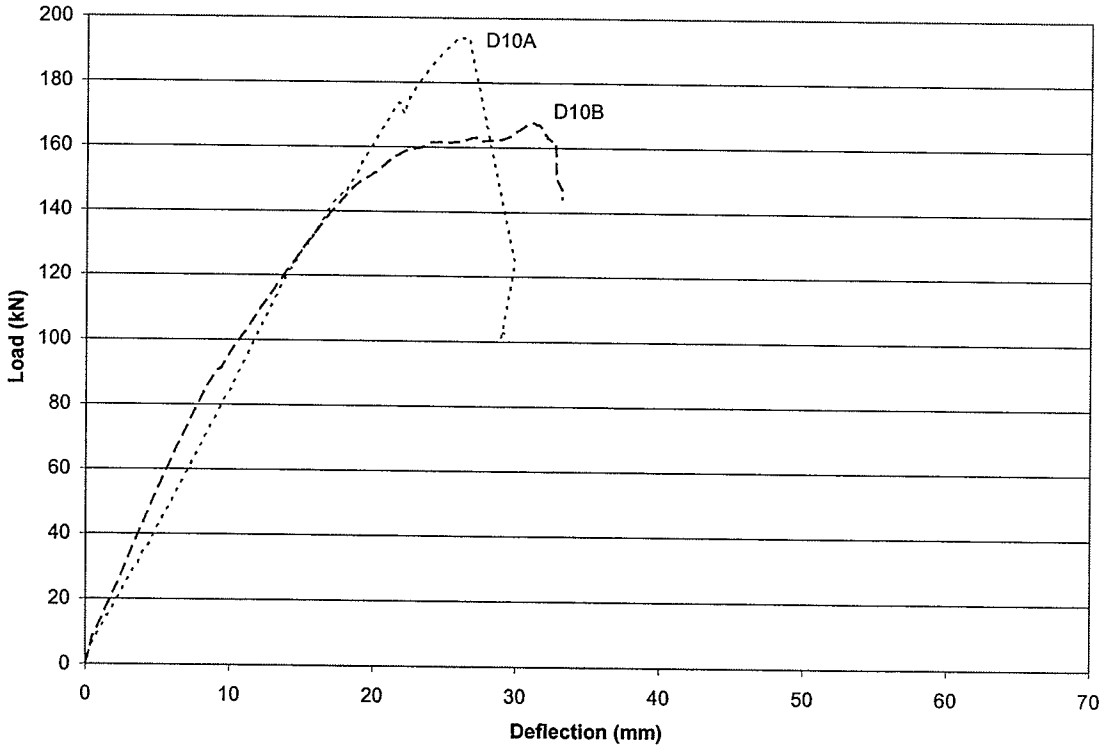

Figure A-25 Diagonal Sheet Specimen D10 (Y2-105)

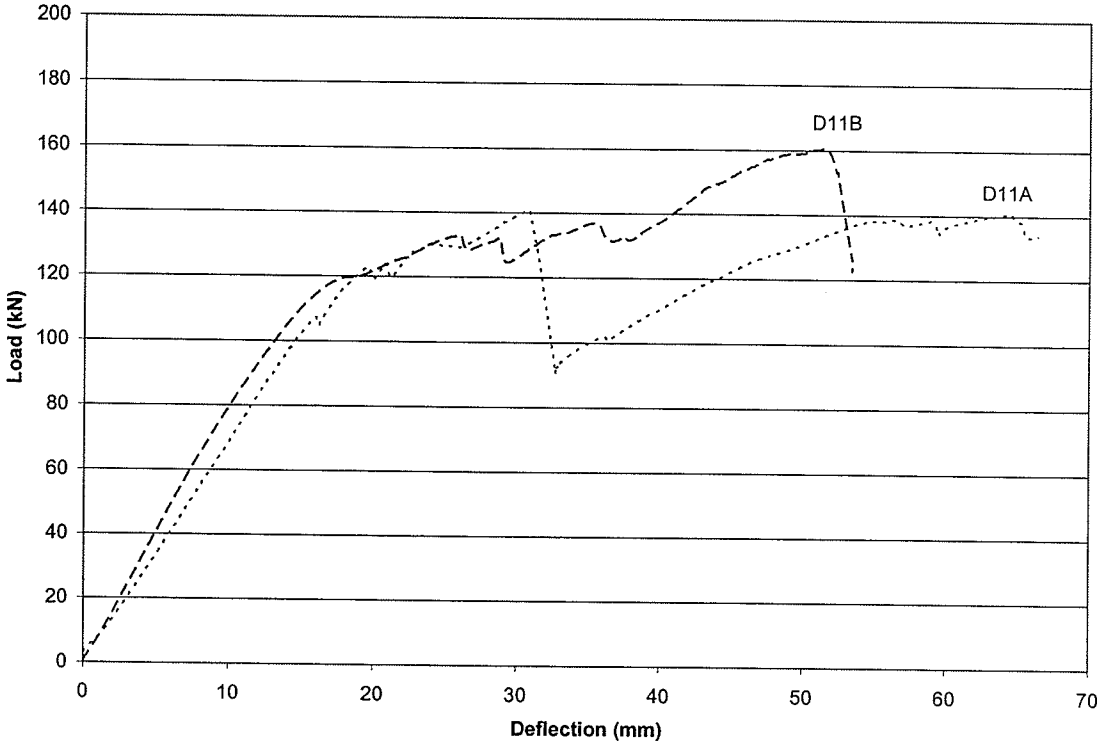

Figure A-26 Diagonal Sheet Specimen D11 (Y2-108)

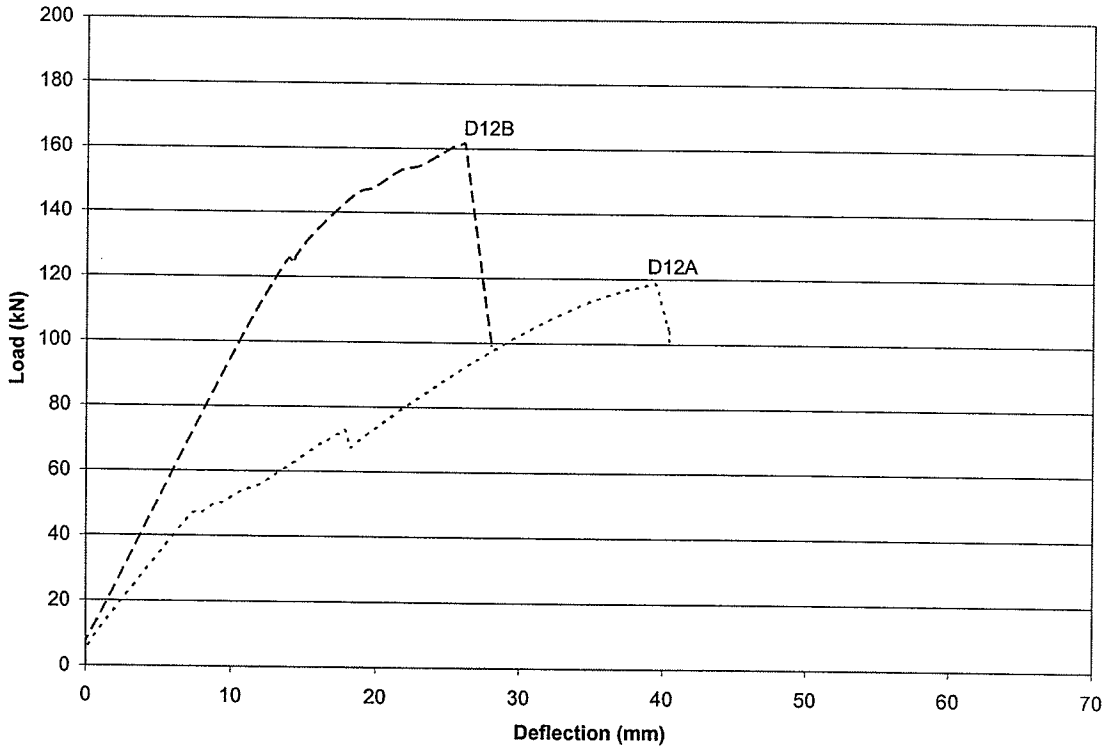

Figure A-27 Diagonal Sheet Specimen D12 (Y2-107)

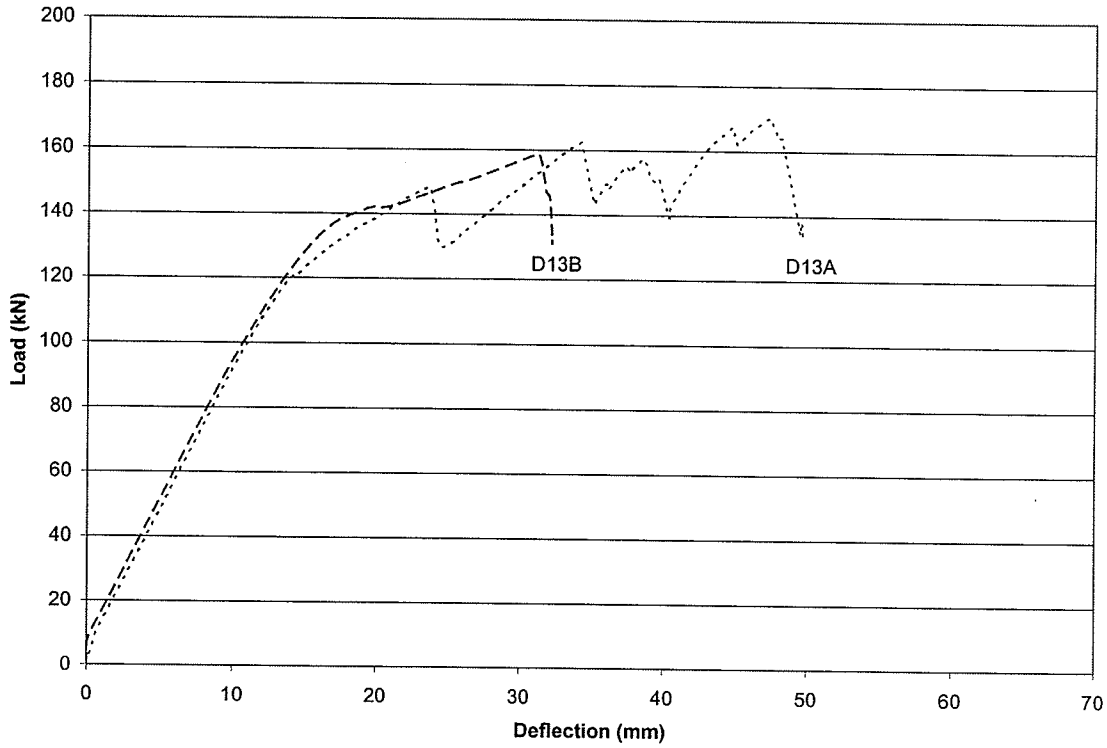

Figure A-28 Diagonal Sheet Specimen D13 (Y2-110)

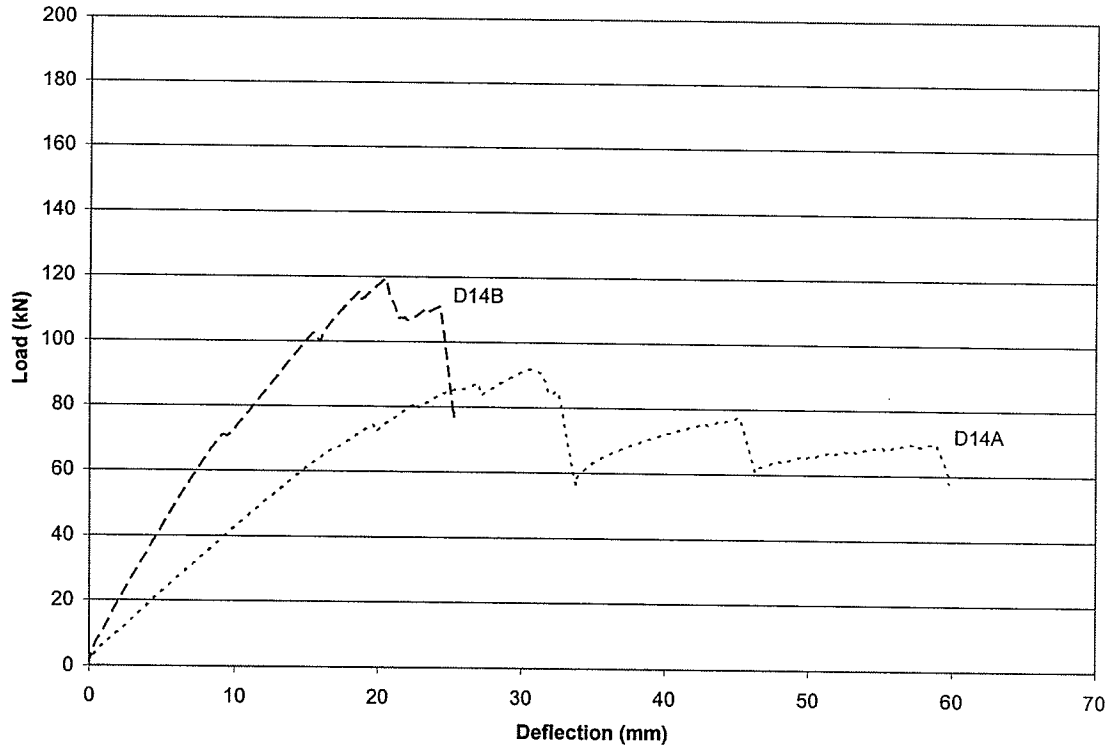

Figure A-29 Diagonal Sheet Specimen D14 (Y2-113)

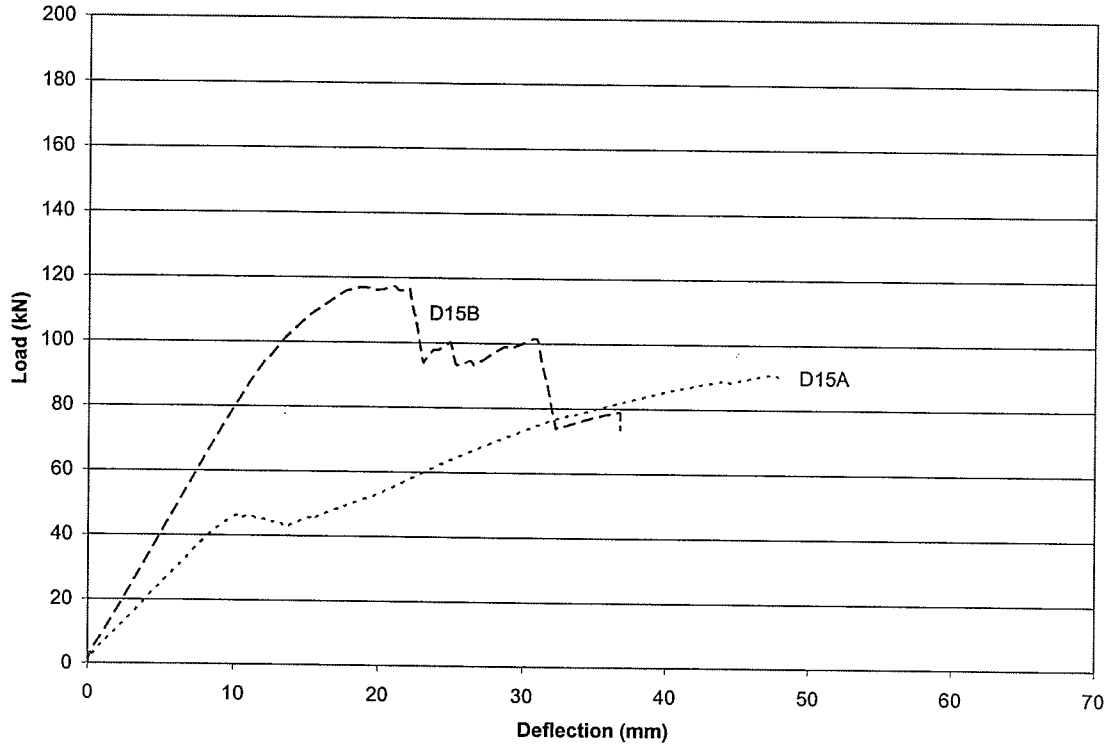

Figure A-30 Diagonal Sheet Specimen D15 (Y2-106)

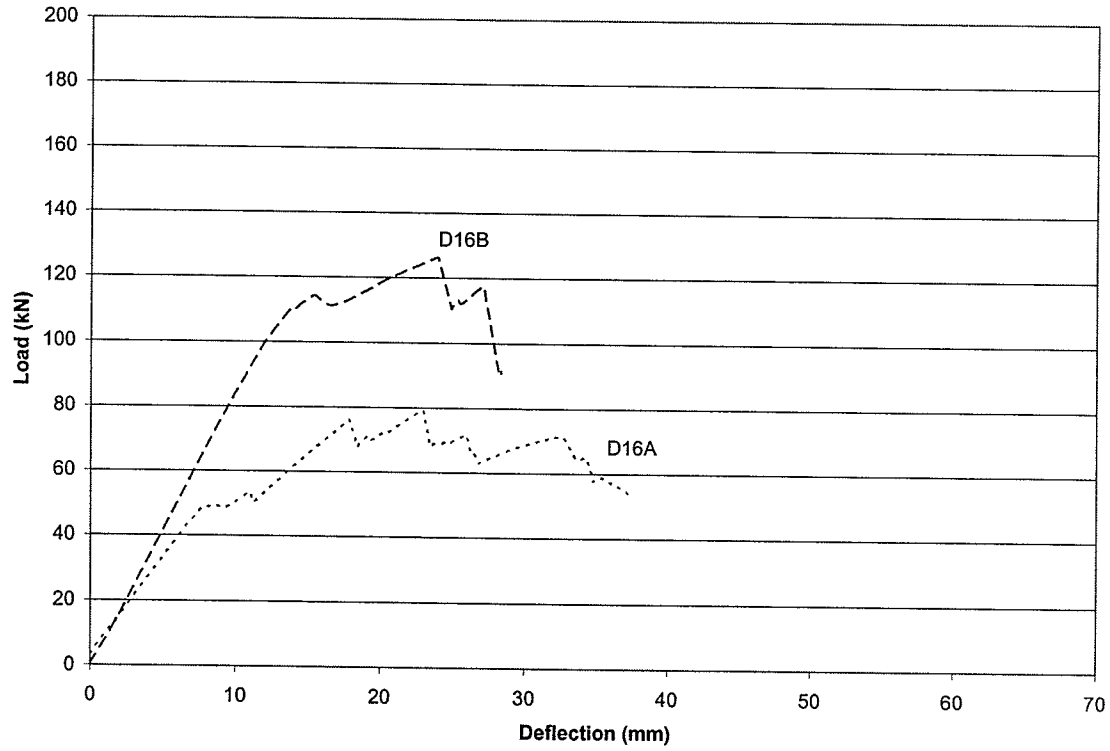

Figure A-31 Diagonal Sheet Specimen D16 (Y2-115)

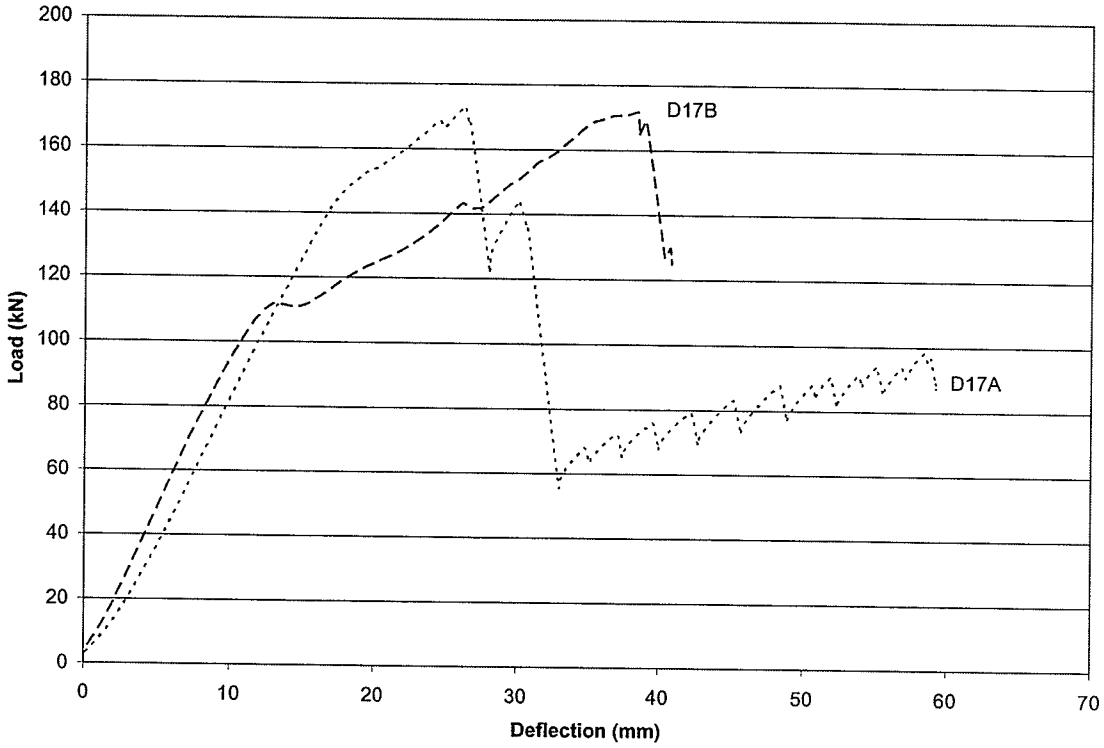

Figure A-32 Diagonal Sheet Specimen D17 (Y1-116)

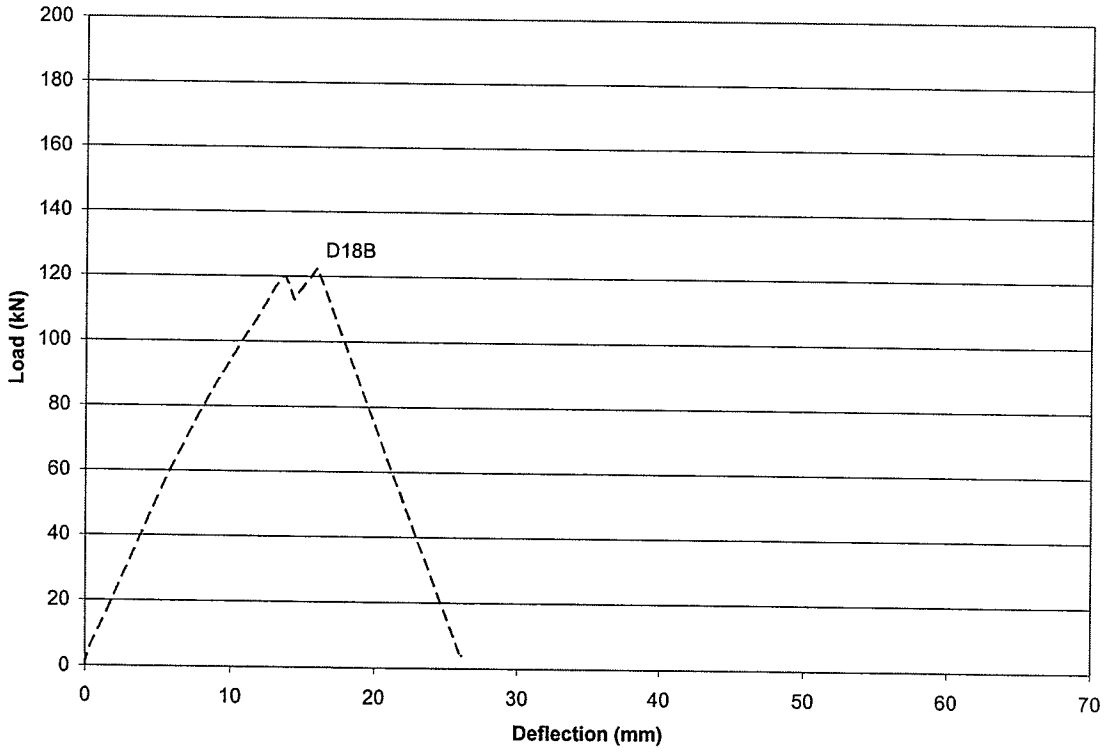

Figure A-33 Diagonal Sheet Specimen D18 (Y1-117)

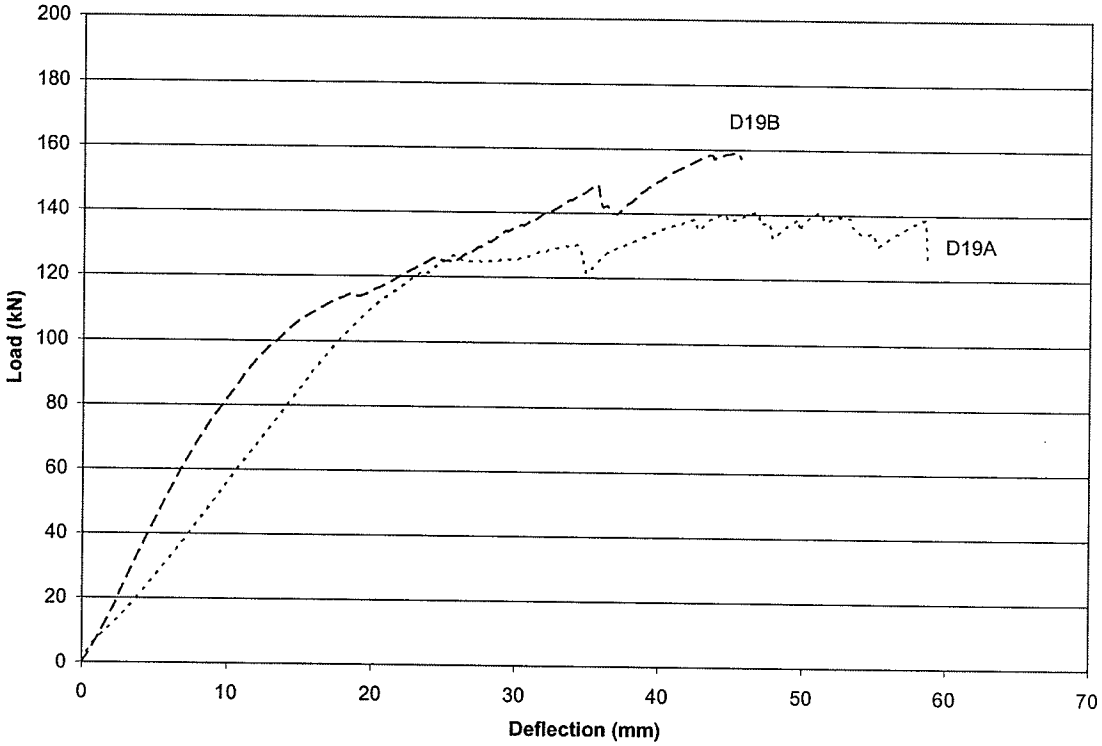

Figure A-34 Diagonal Sheet Specimen D19 (Y1-103)

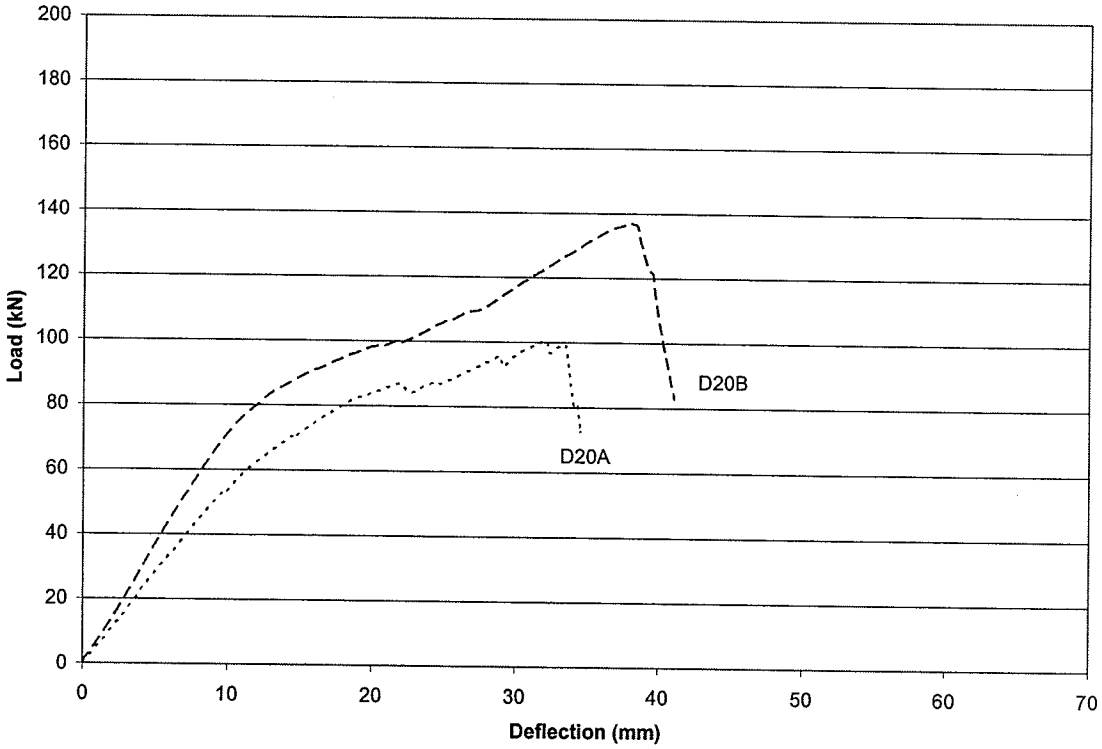

Figure A-35 Diagonal Sheet Specimen D20 (Y3-03)

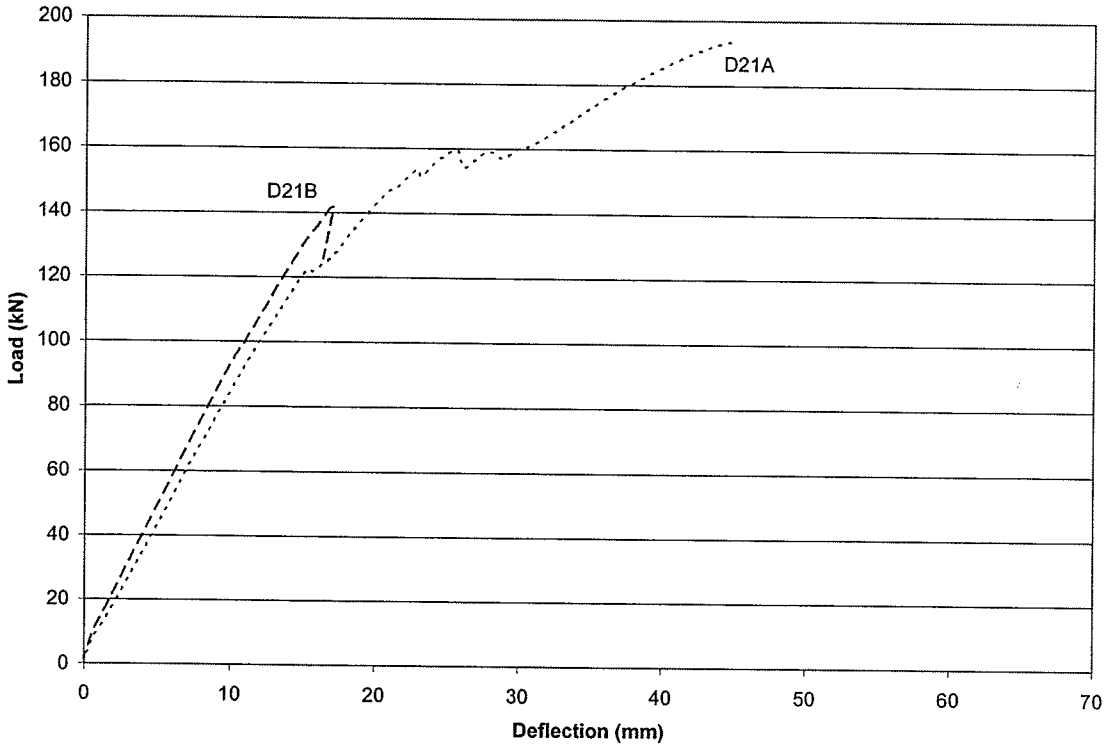

Figure A-36 Diagonal Sheet Specimen D21 (Y3-104)

APPENDIX B

STRAIN PROFILES FOR DIAGONAL SHEET SPECIMENS'

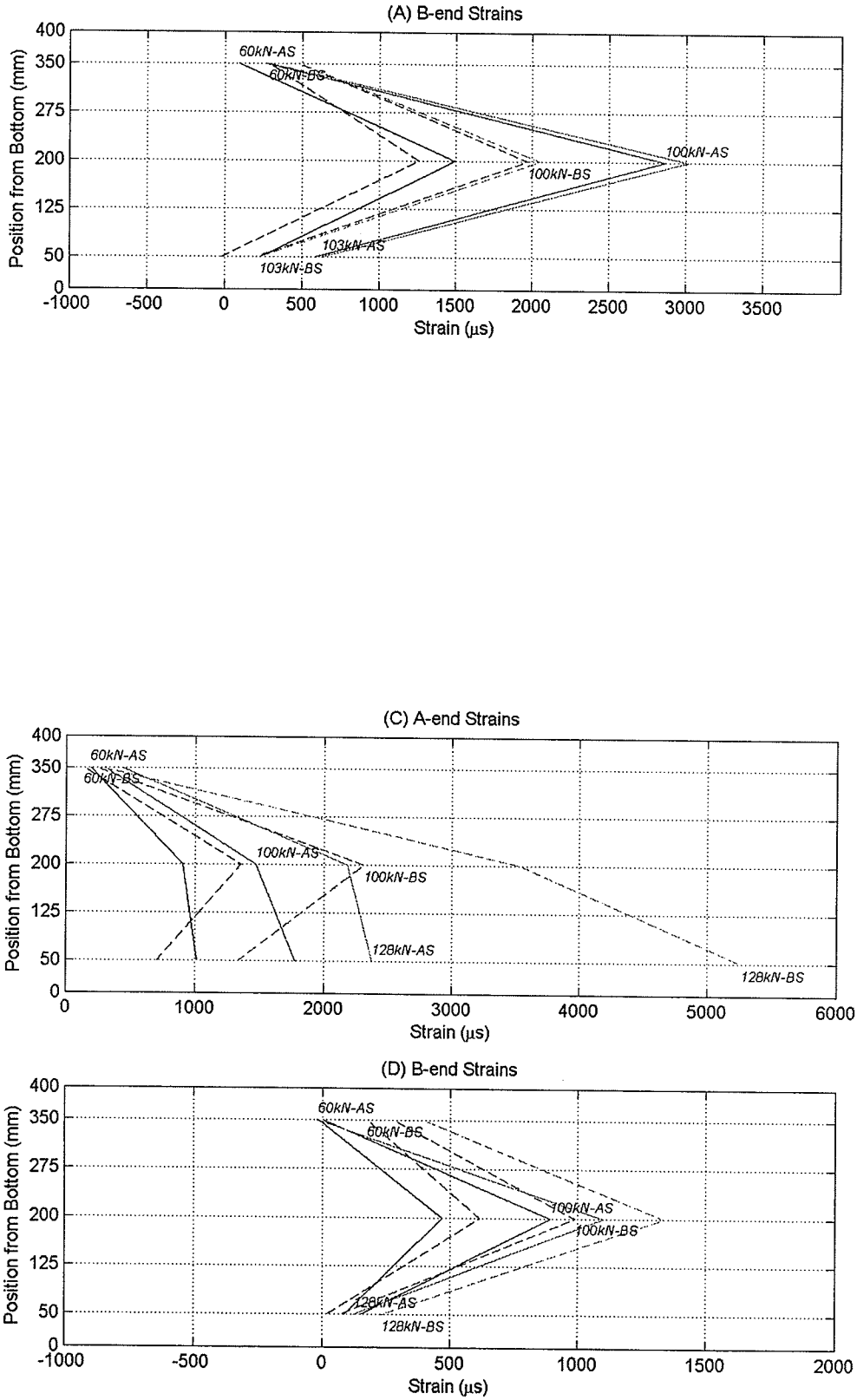

Figure B-1 Strain profile on sheets for D2 (Y2-101). Chart (A) is for split end (B-end) test and charts (C) & (D) is solid end (A-end) test.

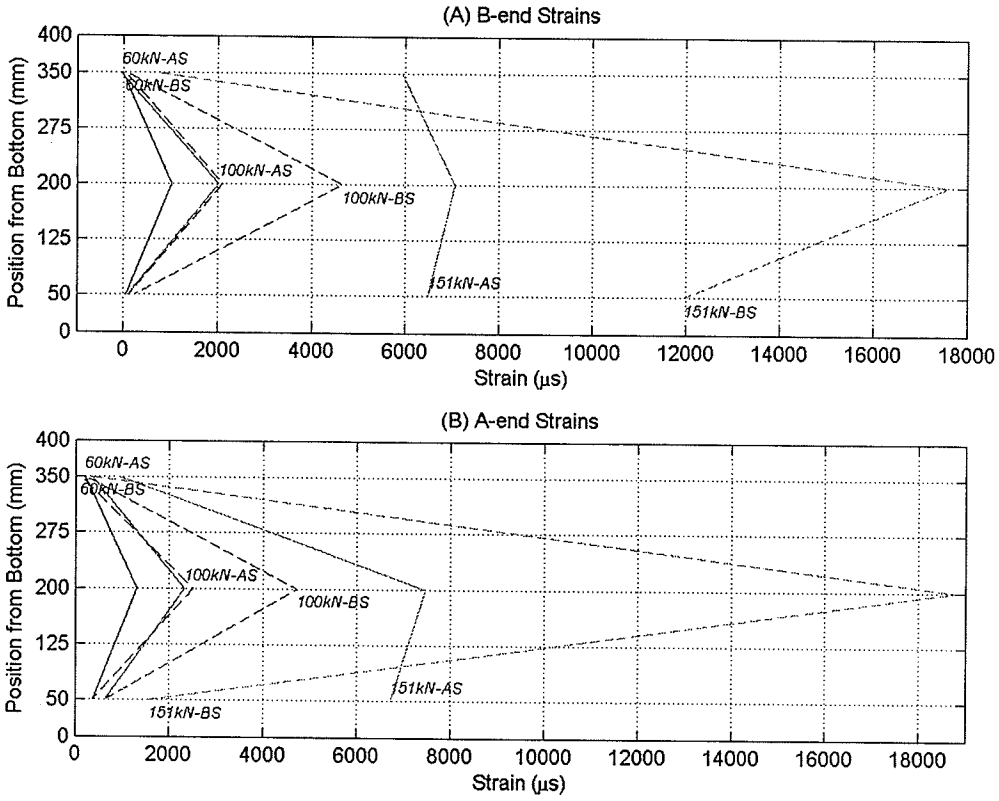

Figure B-2 Strain profiles for D3A (Y2-16B). Charts (A) & (B) is for the solid end test.

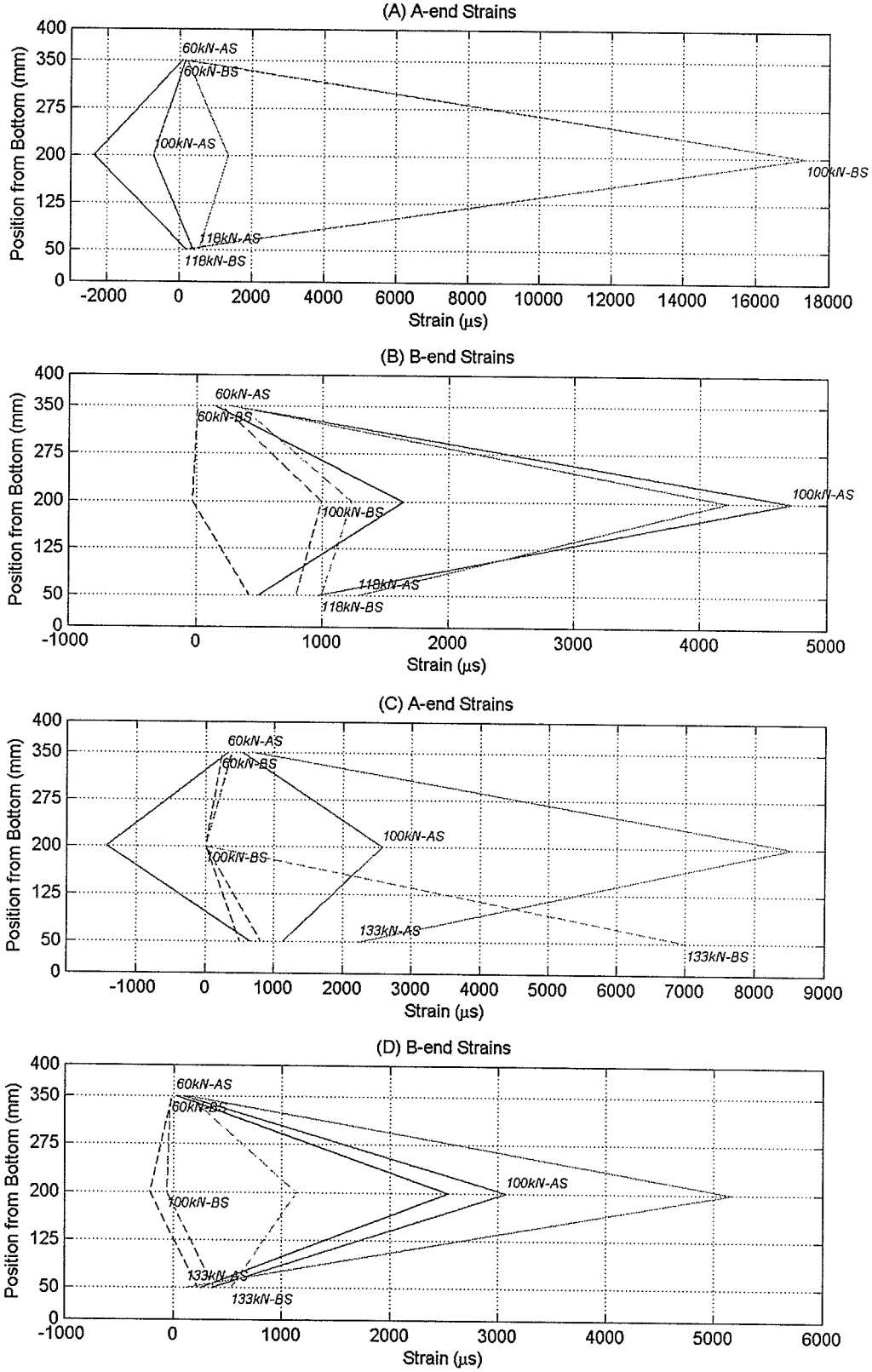

Figure B-3 Strain profile on sheets for D4 (Y2-103). Charts (A) & (B) is for split end (B-end) test and charts (C) & (D) is solid end (A-end) test.

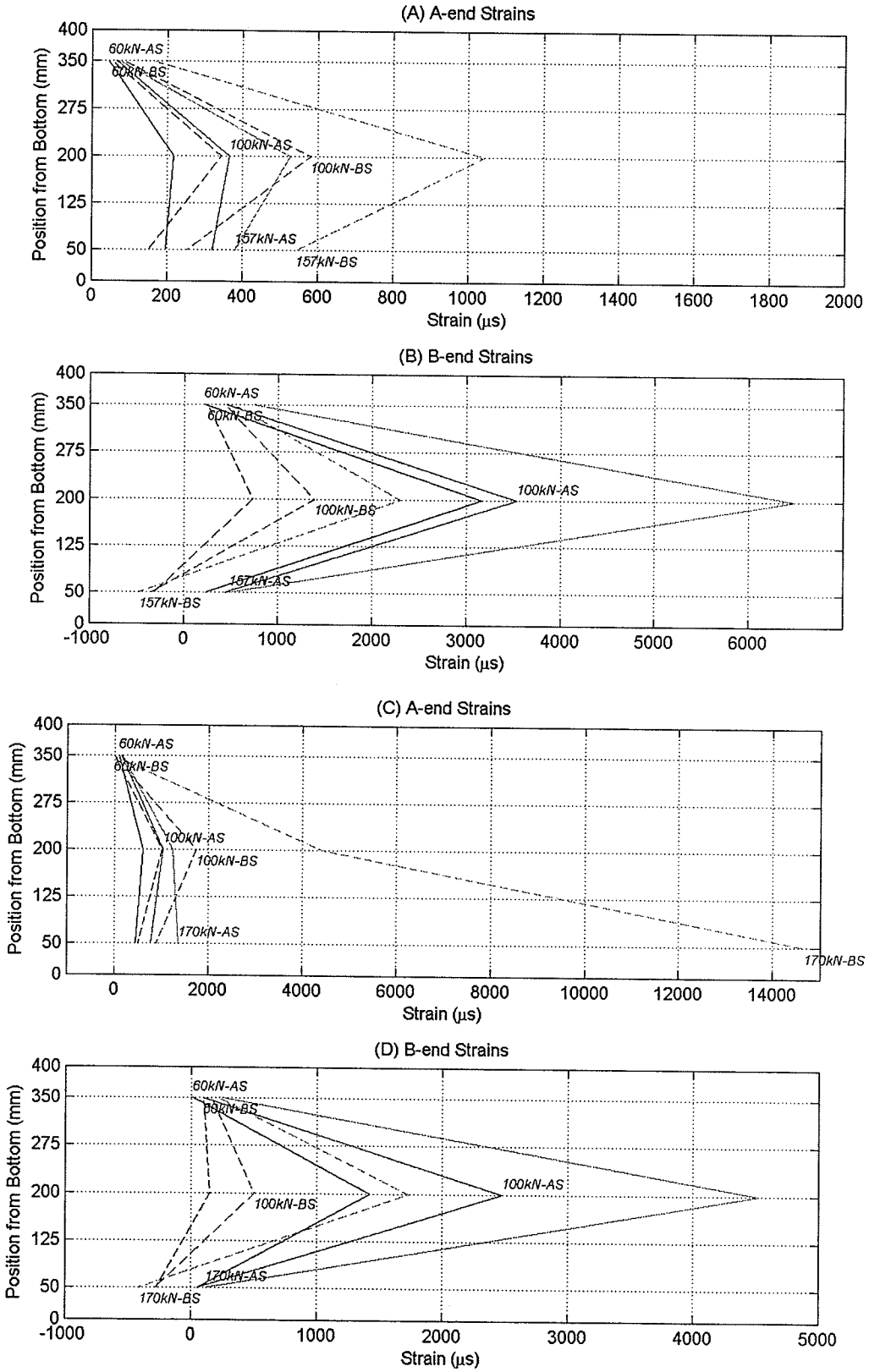

Figure B-4 Strain profile on sheets for D5 (Y2-102). Charts (A) & (B) is for split end (B-end) test and charts (C) & (D) is solid end (A-end) test.

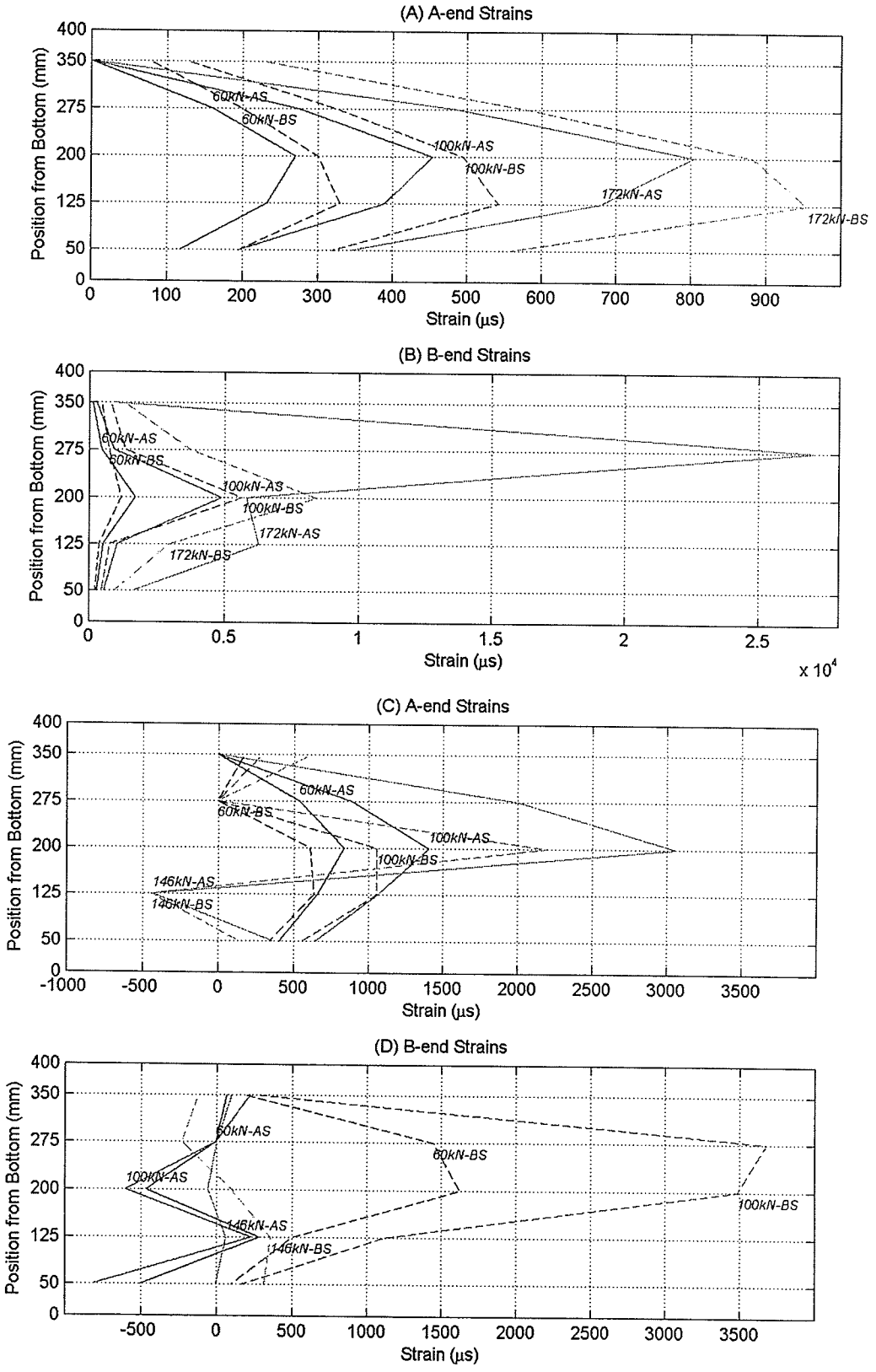

Figure B-5 Strain profile on sheets for D6 (Y2-109). Charts (A) & (B) is for split end (B-end) test and charts (C) & (D) is solid end (A-end) test.

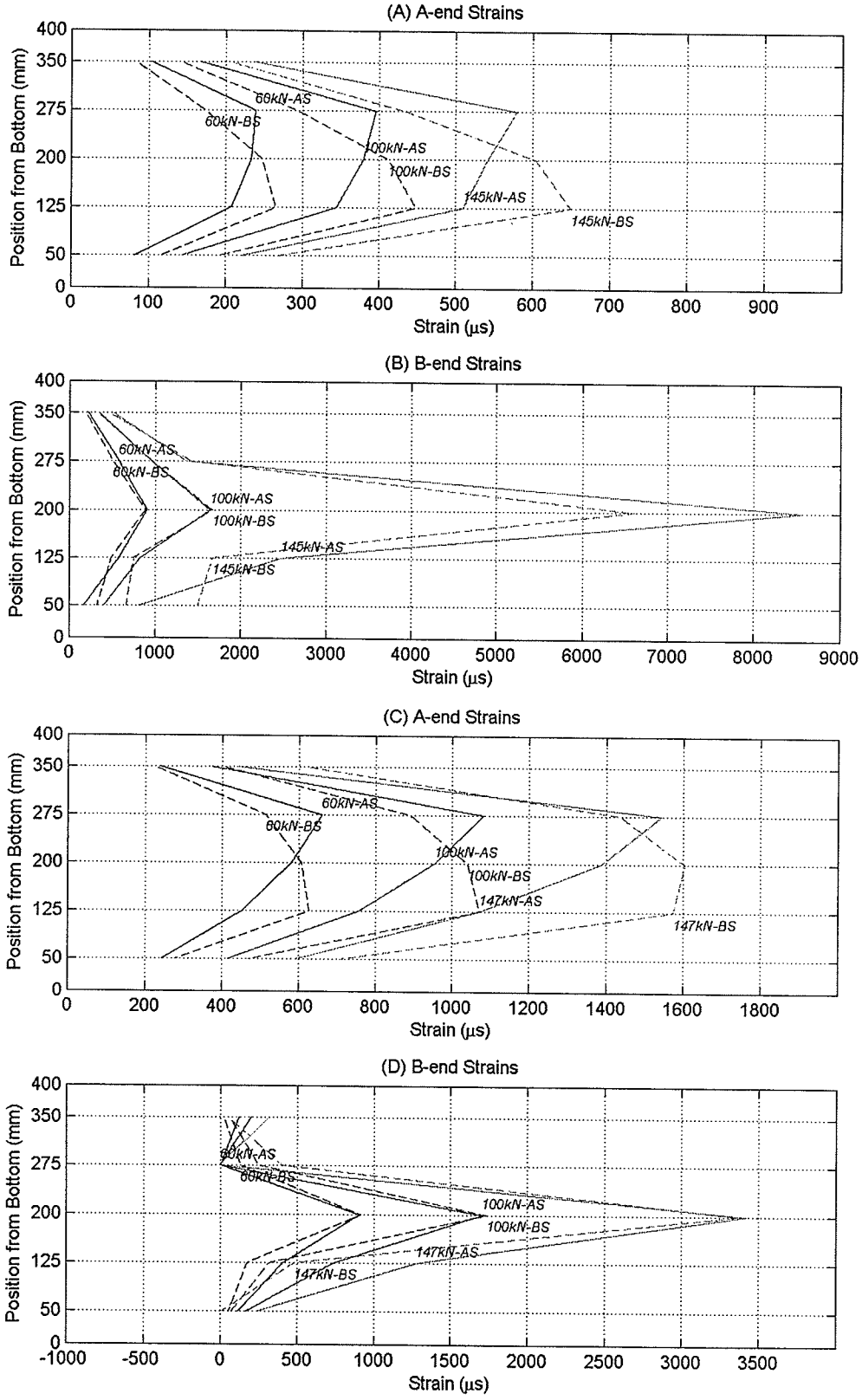

Figure B-6 Strain profile on sheets for D7 (Y2-112). Charts (A) & (B) is for split end (B-end) test and charts (C) & (D) is solid end (A-end) test.

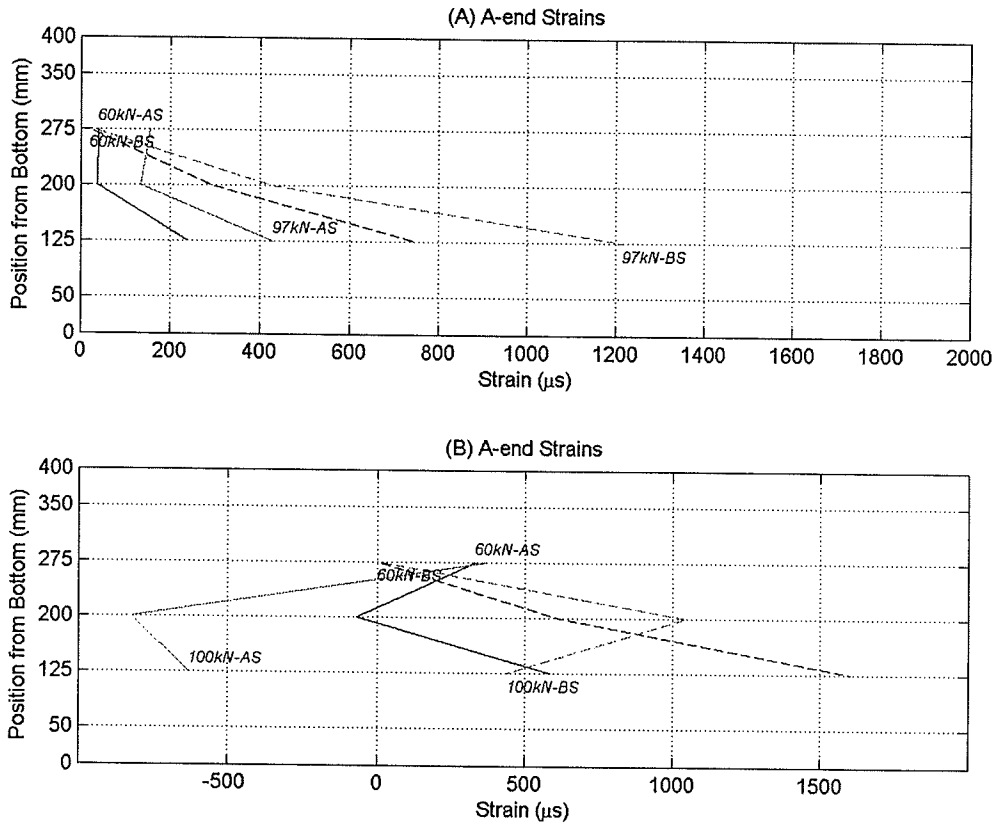

Figure B-7 Strain profile on sheets for D8 (Y2-111). Chart (A) is for split end (B-end) test and chart (B) is solid end (A-end) test.

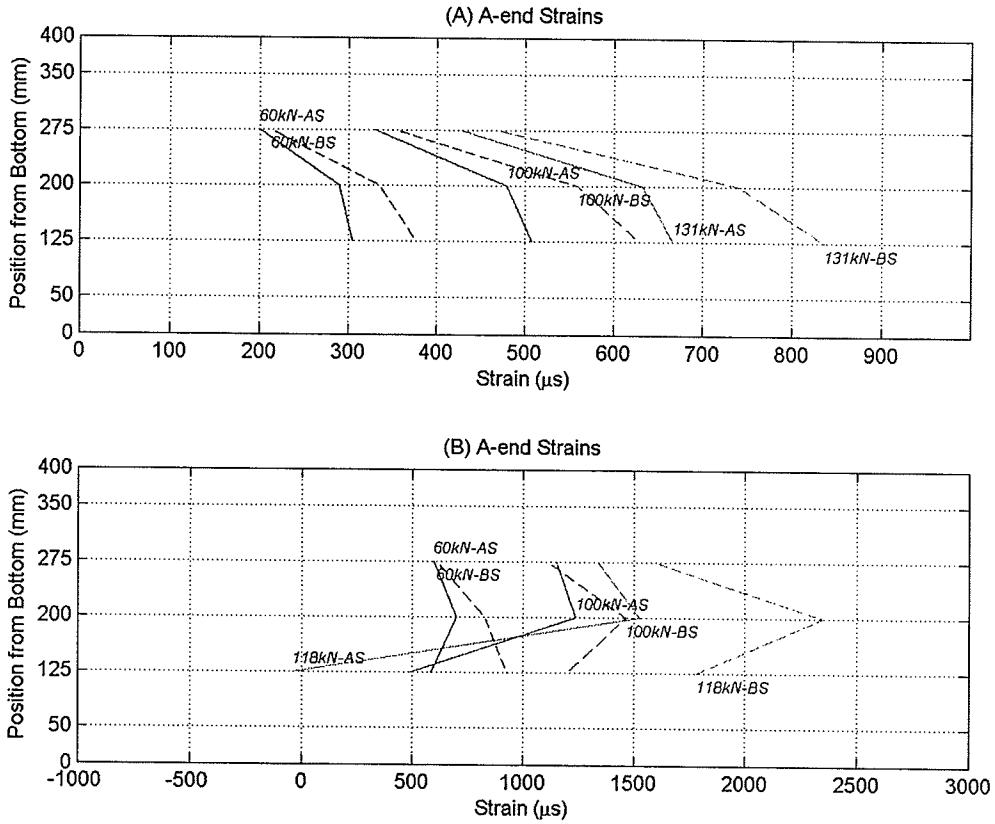

Figure B-8 Strain profile on sheets for D9 (Y2-114). Chart (A) is for split end (B-end) test and chart (B) is solid end (A-end) test.

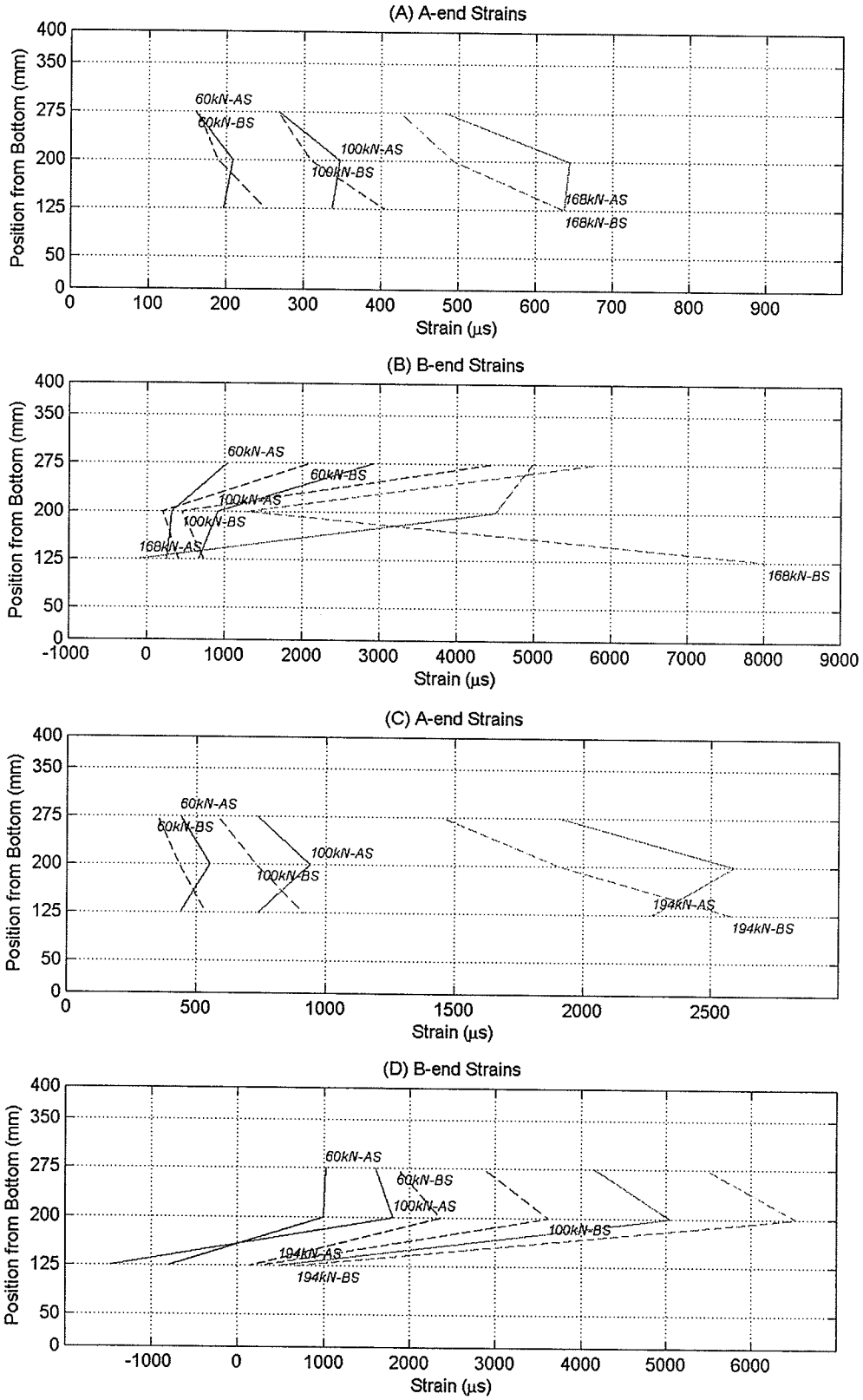

Figure B-9 Strain profile on sheets for D10 (Y2-105). Charts (A) & (B) is for split end (B-end) test and charts (C) & (D) is solid end (A-end) test.

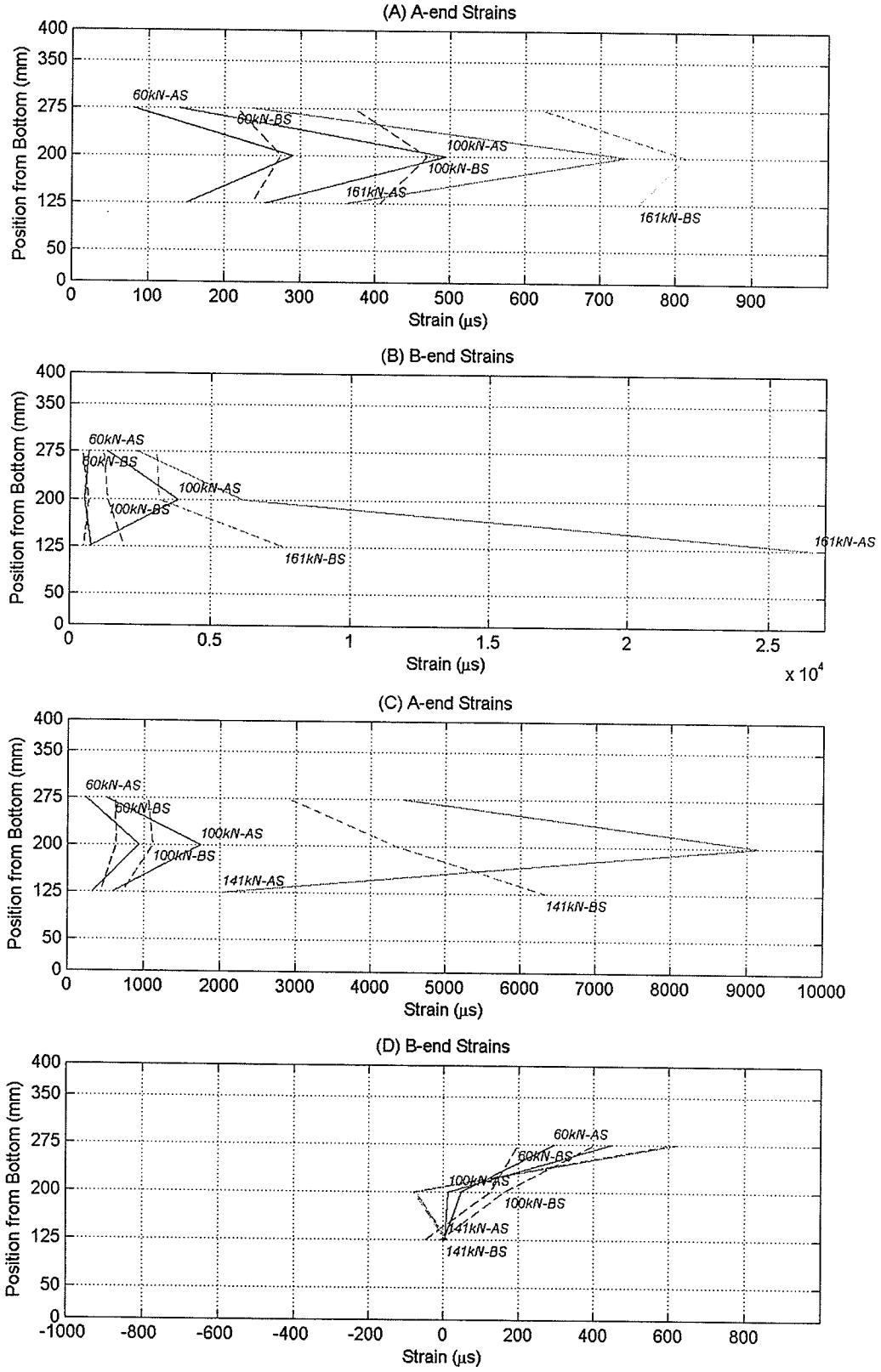

Figure B-10 Strain profile on sheets for D11 (Y2-108). Charts (A) & (B) is for split end (B-end) test and charts (C) & (D) is solid end (A-end) test.

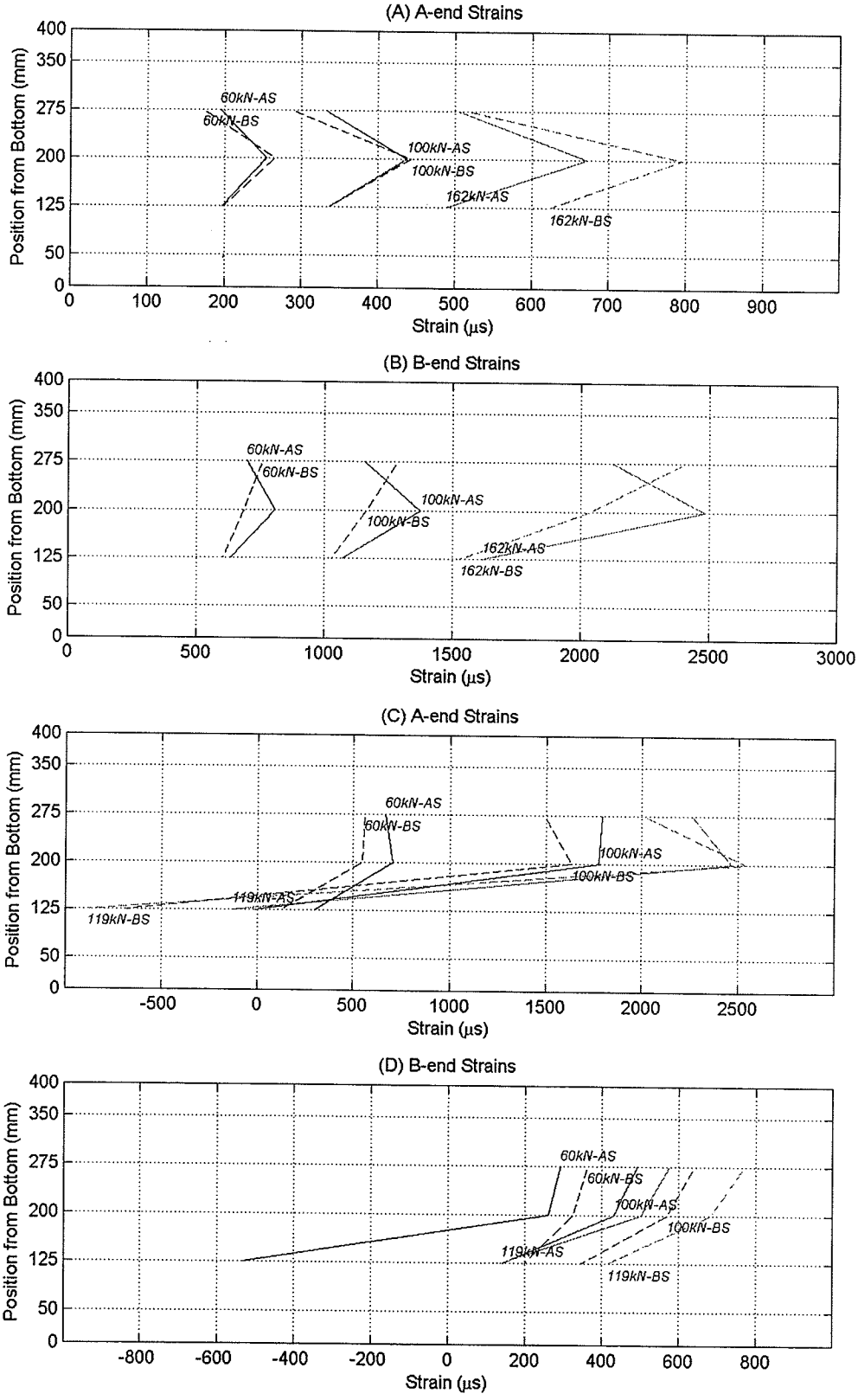

Figure B-11 Strain profile on sheets for D12 (Y2-107). Charts (A) & (B) is for split end (B-end) test and charts (C) & (D) is solid end (A-end) test.

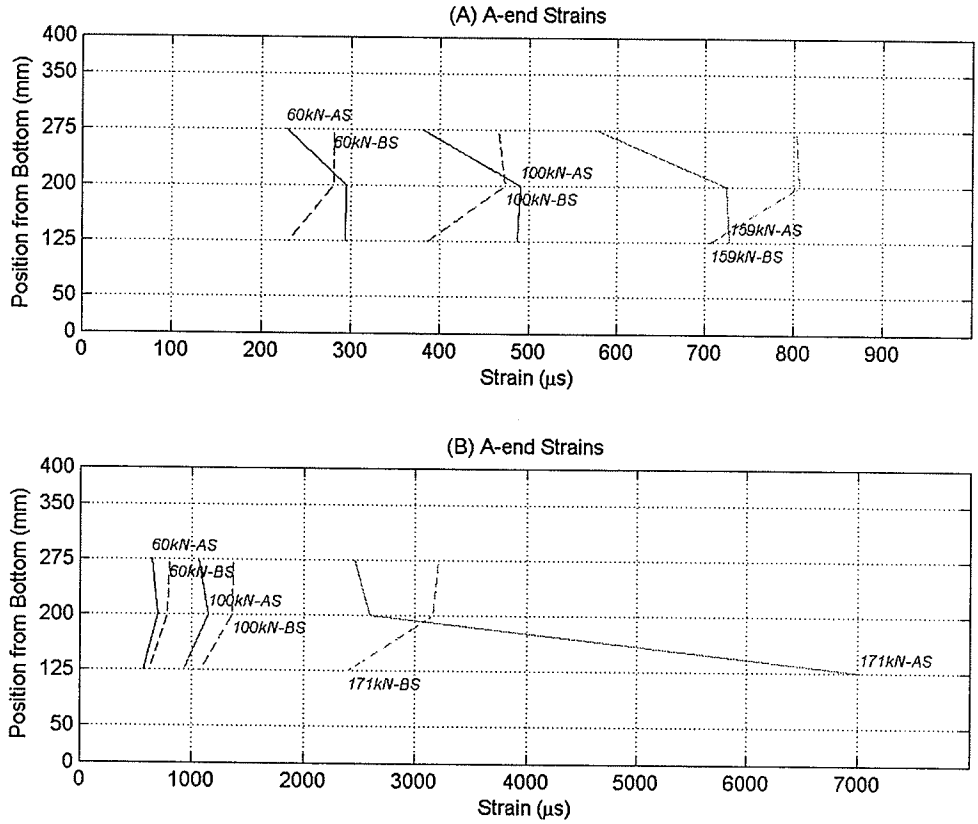

Figure B-12 Strain profile on sheets for D13 (Y2-110). Chart (A) is for split end (B-end) test and chart (B) is solid end (A-end) test.

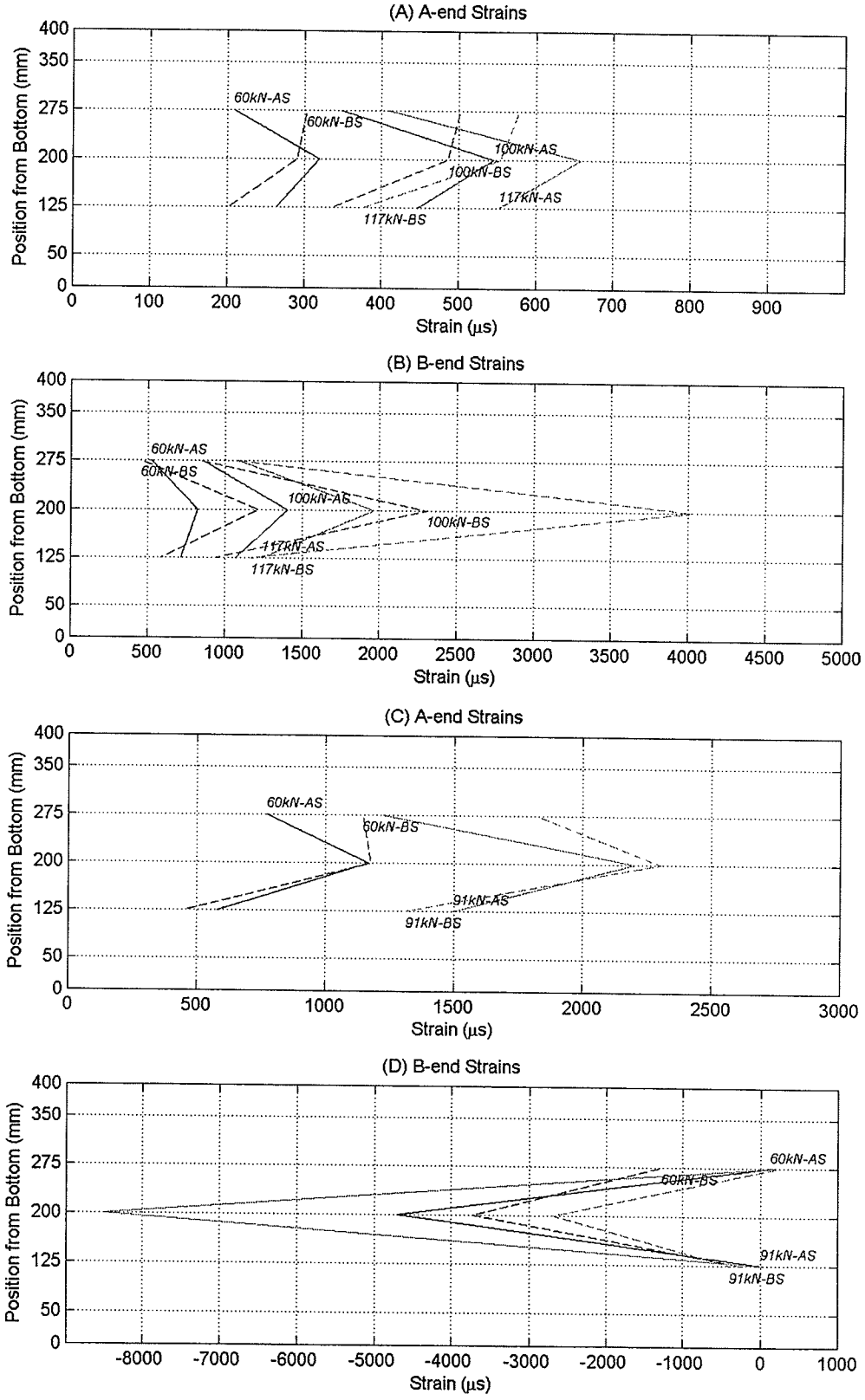

Figure B-13 Strain profile on sheets for D15 (Y2-106). Charts (A) & (B) is for split end (B-end) test and charts (C) & (D) is solid end (A-end) test.

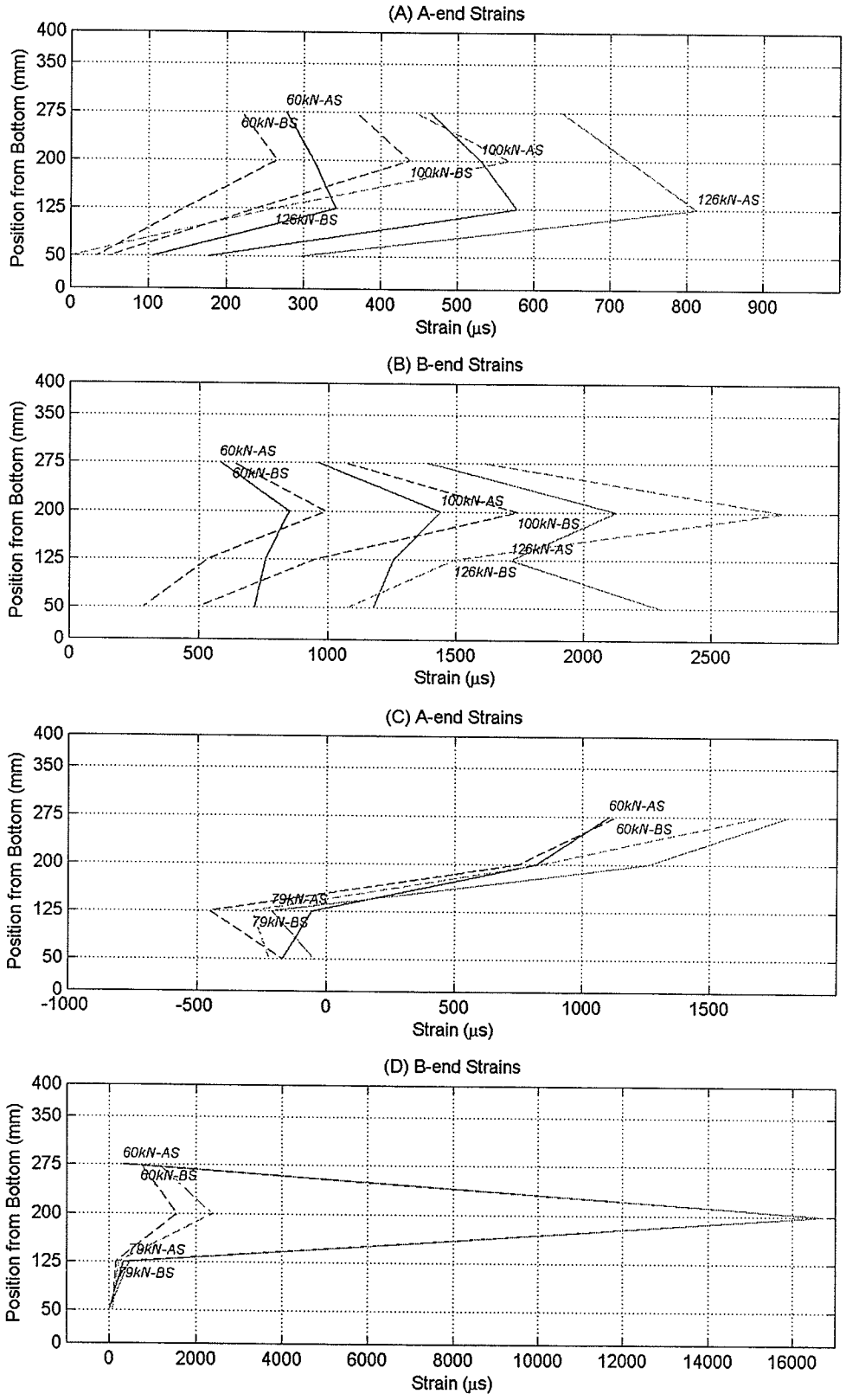

Figure B-14 Strain profile on sheets for D16 (Y2-115). Charts (A) & (B) is for split end (B-end) test and charts (C) & (D) is solid end (A-end) test.

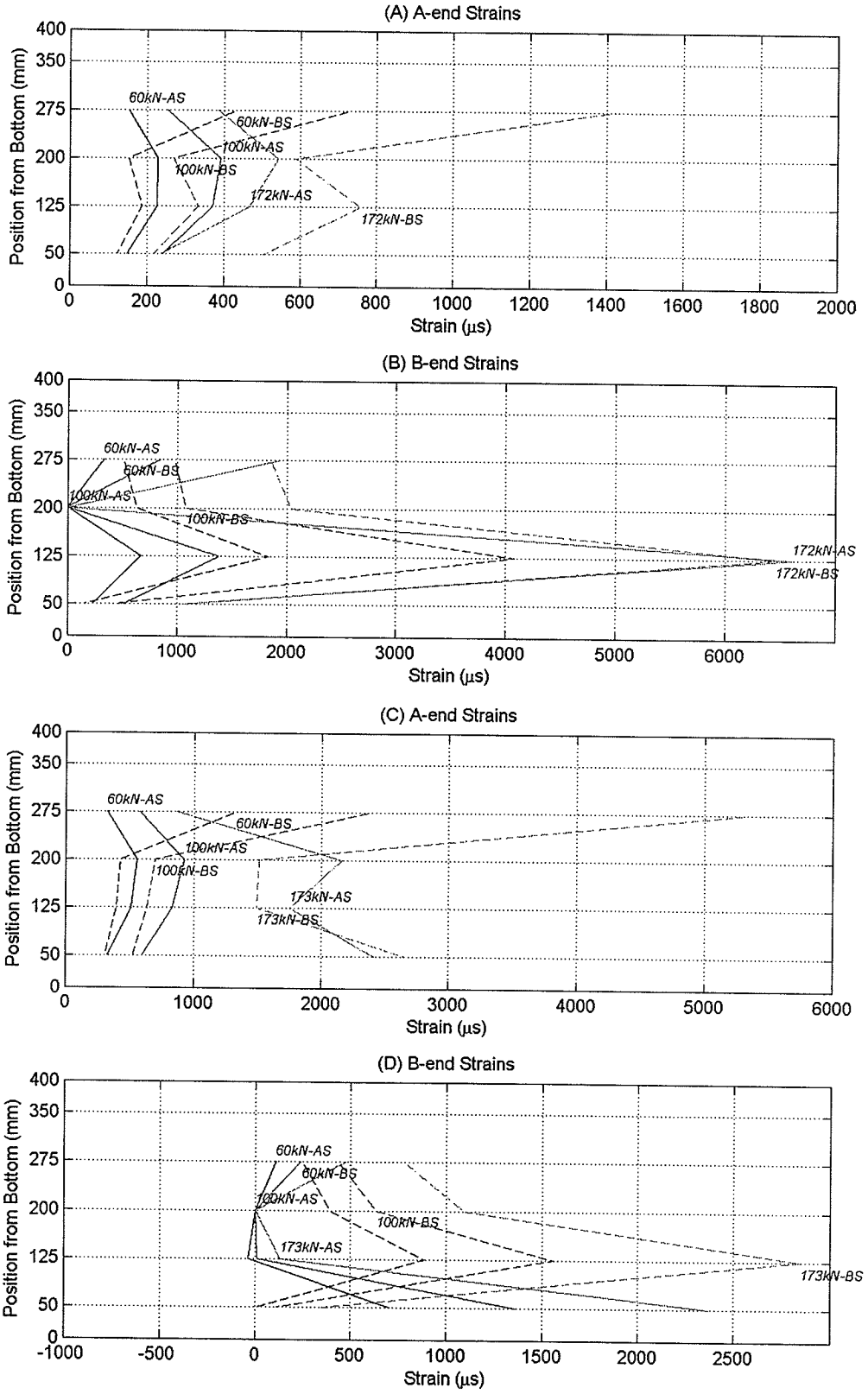

Figure B-15 Strain profile on sheets for D17 (Y1-116). Charts (A) & (B) is for split end (B-end) test and charts (C) & (D) is solid end (A-end) test.

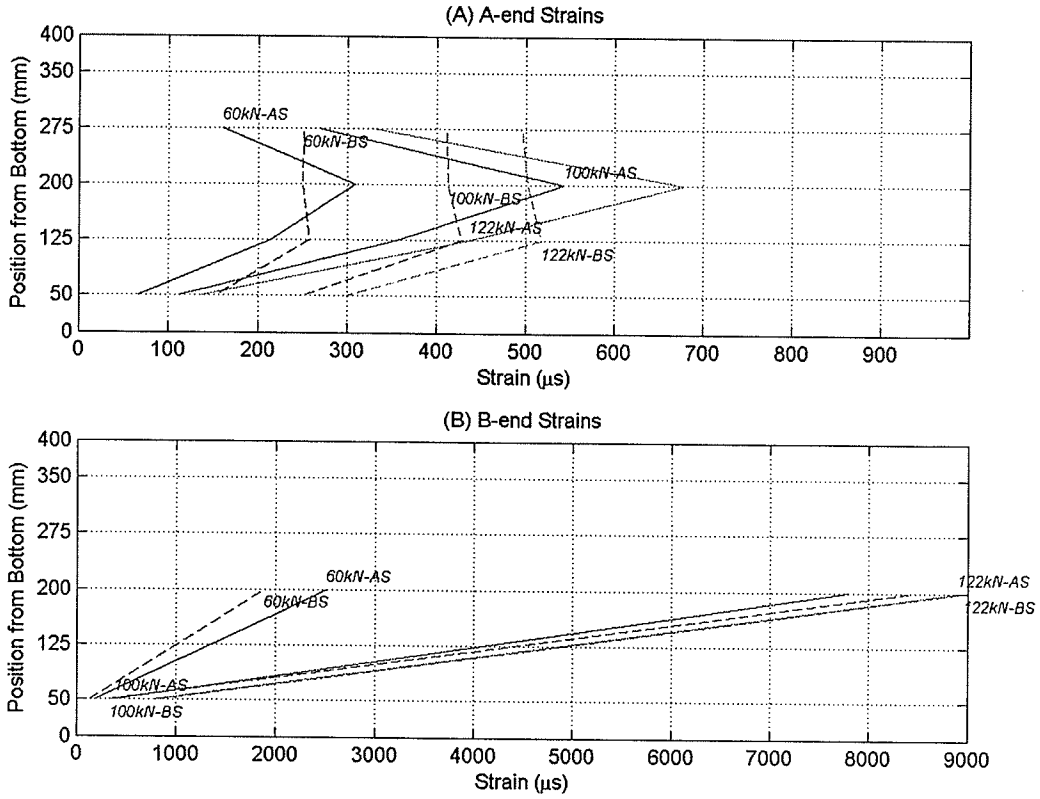

Figure B-16 Strain profiles for D18B (Y1-117B). Charts (A) & (B) is for the split end test.

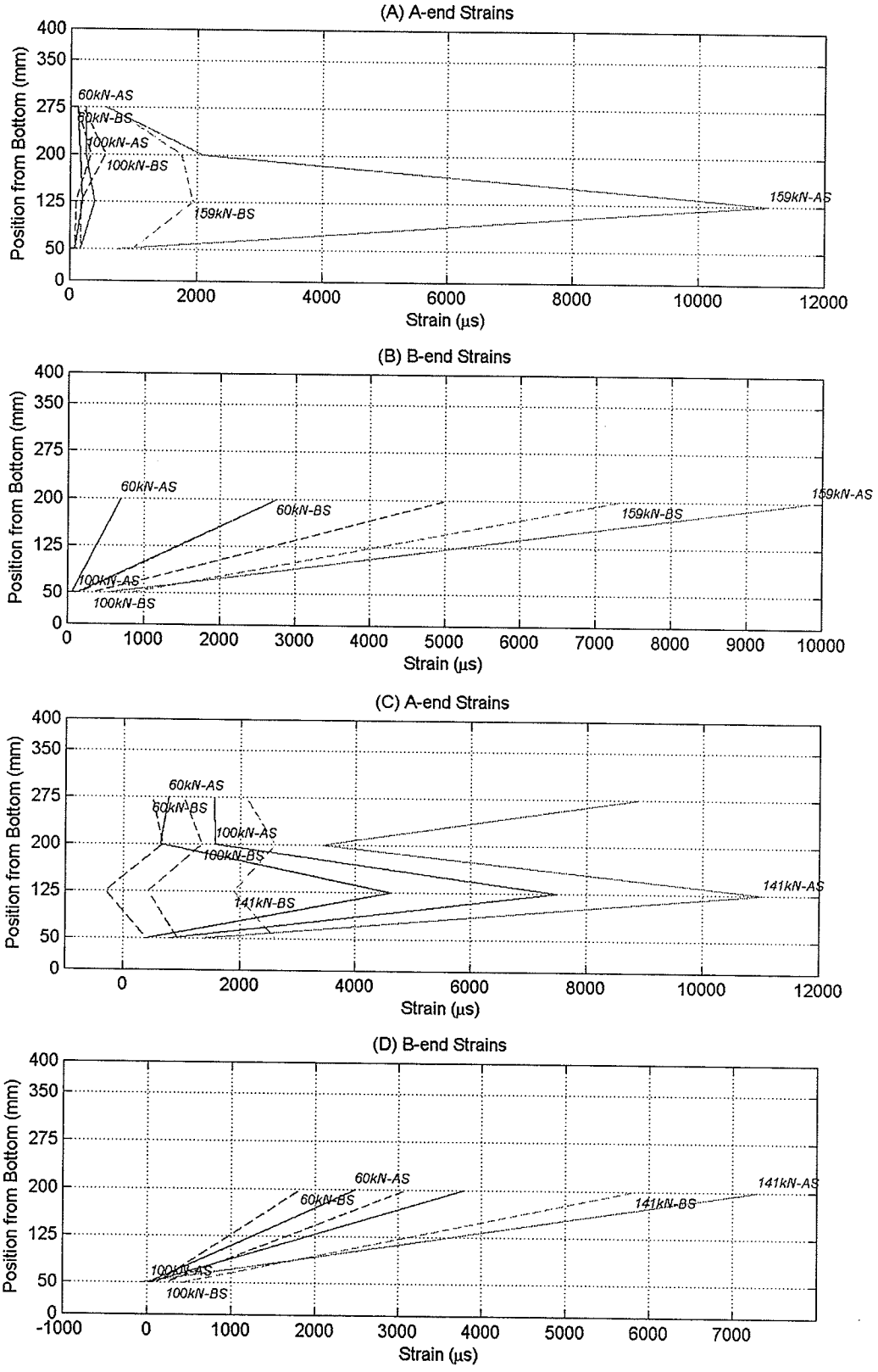

Figure B-17 Strain profile on sheets for D19 (Y1-03). Charts (A) & (B) is for split end (B-end) test and charts (C) & (D) is solid end (A-end) test.

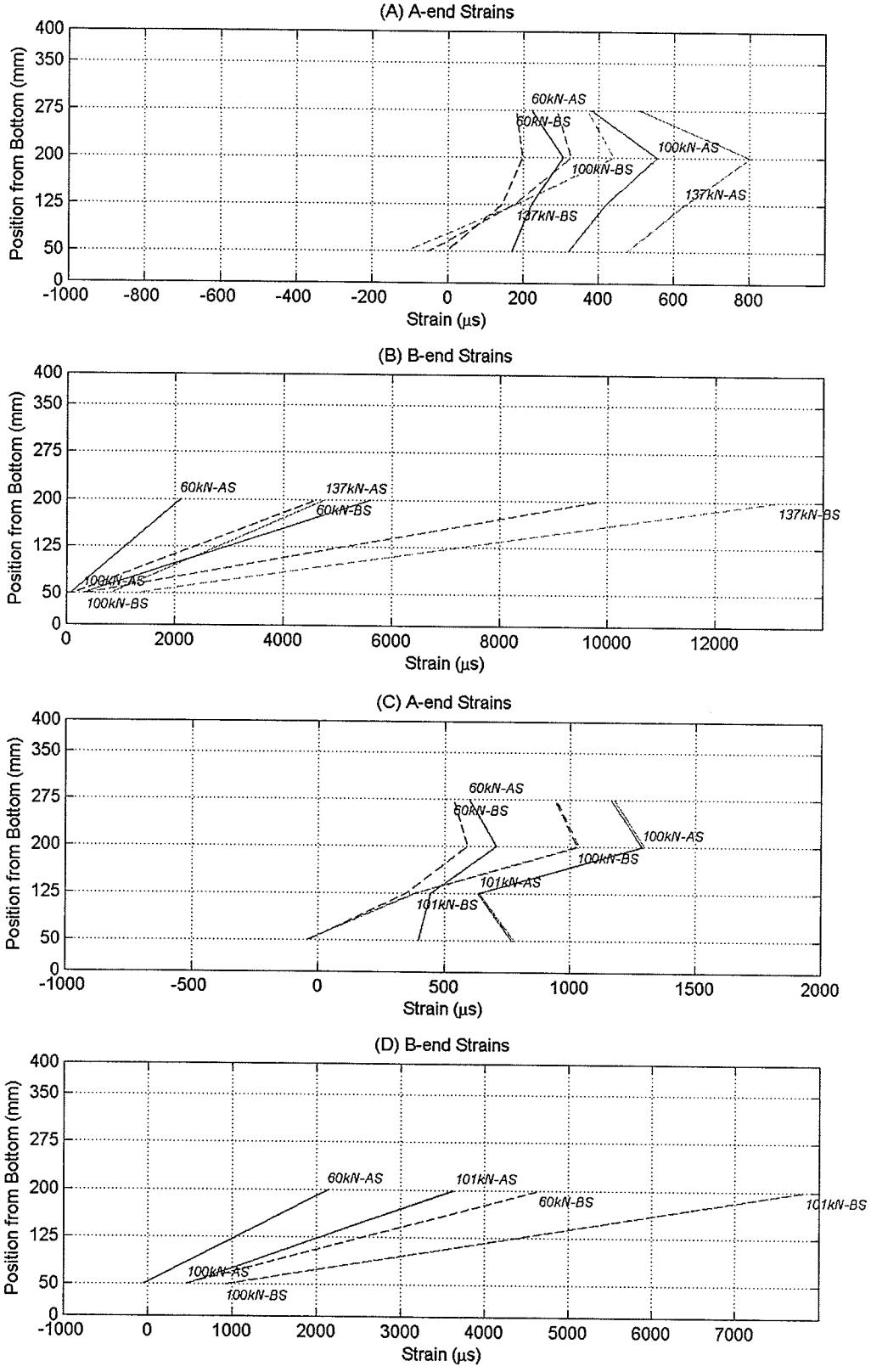

Figure B-18 Strain profile on sheets for D20 (Y3-03). Charts (A) & (B) is for split end (B-end) test and charts (C) & (D) is solid end (A-end) test.

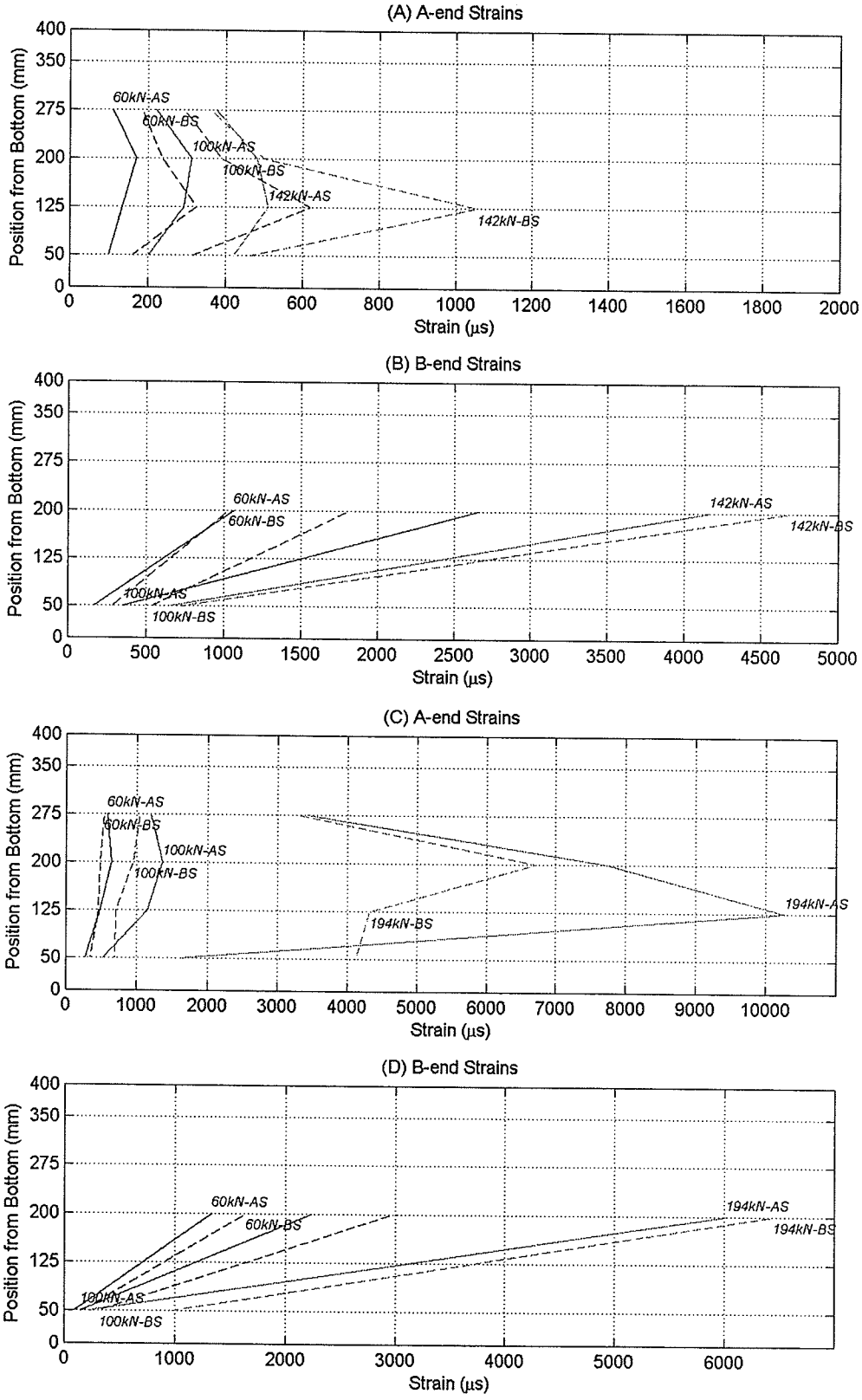

Figure B-19 Strain profile on sheets for D21 (Y3-104). Charts (A) & (B) is for split end (B-end) test and charts (C) & (D) is solid end (A-end) test.

APPENDIX C

SPLIT CLOSING DEVICE

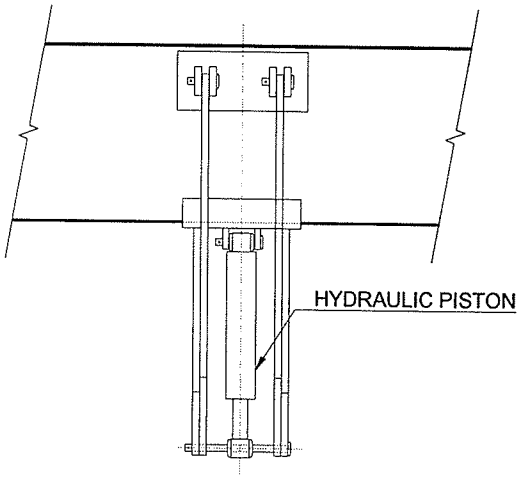

SIDE VIEW
NTS

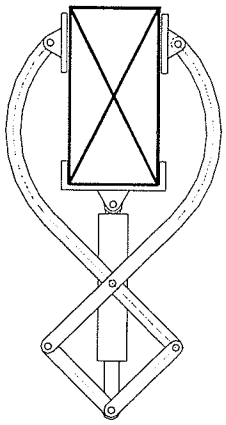

END VIEW
NTS

Note: This is just a concept by the author that was not built or experimented with.

APPENDIX D

DRAFT CODE PROVISIONS FOR ADDENDUM TO CAN/CSA-S6-00

$$L_e = \frac{23300}{(t_{FRP} E_{FRP})^{0.58}}$$

For prestressed concrete components, the General Method of Clause 8.9.3 shall be used to calculate the contribution of the FRP to the shear capacity.

For components with non-rectangular or non-T cross-sections, a rigorous analysis or test shall guide the design.

16.11.3.3 **Spacing and Strengthening Limits**

The spacing of FRP bands shall not be more than s_{FRP} given by the following equation.

$$s_{FRP} \leq w_{FRP} + \frac{d_{FRP}}{4}$$

The total factored shear resistance subsequent to FRP strengthening, V_r, shall not exceed 0.66 $b_w d(f'_c)^{0.5}$

16.12 **Rehabilitation of Timber Bridges**

16.12.1 **General**

The provisions of this clause apply to beams of timber and stringer grades strengthened with GFRP sheets or bars. The bars, if present, shall be either near-surface mounted or embedded in holes in timber. The empirical methods given in this clause may be used to determine the strength of timber beams strengthened with GFRP sheets or bars for either or both flexure and shear.

While the provisions are given specifically for GFRP bars and sheets, AFRP and CFRP bars and sheets can also be used in their place. If the strength for either flexure or shear is required to be more than given by these empirical methods, then experimental evidence shall be used to determine the amount of FRP reinforcement.

The procedures for handling, storage and protection of FRP sheets and bars shall be the same as prescribed for the same components in Clause 16.4.8 for rehabilitation of concrete structures.

The Plans shall provide details and specifications relevant to the following:

(a) Identification of the specific FRP strengthening system/s and protective coatings;
(f) Surface preparation;
(g) Shipping, storage and handling of the FRP strengthening systems;
(h) Installation of the FRP strengthening systems, including (i) the spacing and positioning of the components, (ii) locations of overlaps and multiple plies, (iii) installation procedures, and (iv) constraints for climatic conditions;
(i) Curing conditions of the strengthening system;
(f) Quality control of the strengthening system, similar to those given in Appendix A16.3 for concrete;
(j) Staff qualifications;
(k) Material inspection before, during, and after completion of the installation; and
(l) System maintenance requirements.

Prior to developing a rehabilitation strategy, an assessment of the existing structure or elements shall be conducted following the requirements of Section 14.

16.12.2 **Strengthening For Flexure**

16.12.2.1 **Flexural Strengthening with GFRP Sheets**

When the following minimum requirements are met for strengthening with GFRP sheets, the bending strength for beam and stringer grades used for the evaluation of these components shall be assumed to be $K_{bFRP} \times f_{bu}$, in which K_{bFRP} is obtained from Table 16.12.2.1 and f_{bu} from Table 9.11.2 (b).

(a) The minimum fibre volume fraction of GFRP system in the direction of the span of the beam is 30%.
(b) The GFRP sheet on the flexural tension face of the beam covers at least 90% of the width of the beam and has a minimum thickness of 0.1 mm.
(c) The adhesive used for bonding GFRP sheet to the timber beam is compatible with the preservative treatment used on the timber.
(d) In the longitudinal direction of the beam, the GFRP sheets extend as close to the beam supports as possible.
(e) The adhesive used for bonding the GFRP bars to the timber beam is compatible with the preservative treatment used on the timber and chosen such that it is compatible with expected volumetric changes of the timber.

Table 16.12.2.1 Values of K_{bFRP}

Grade of Original Beam	K_{bFRP}
SS	*
No. 1	1.2
No. 2	1.5

* This value shall be assumed to be 1.05 if the beam is not strengthened for shear; if the beam is also strengthened for shear then this value shall be 1.1.

16.12.2.2 **Flexural Strengthening with GFRP NSMR**

When the following minimum requirements are met for strengthening with GFRP NSMR, the bending strength for beam and stringer grades used for the evaluation of these components shall be assumed to be $K_{bFRP} \times f_{bu}$, in which K_{bFRP} is obtained from Table 16.12.2.1 and f_{bu} from Table 9.11.2 (b).

(a) The minimum fibre volume fraction for GFRP bars is 60%.
(b) There are at least two bars within the width of the beam.
(c) The total cross-sectional area for all bars on a beam is at least 0.002 times the cross-sectional area of the timber component.
(d) As shown in Fig. 16.12.2.2, each bar is embedded in a groove, preferably with a rounded end. The depth of each groove is between 1.6 to 2.0 times d_b, the bar diameter; the width of each groove is not less than d_b+5 mm; the edge distance of the outer groove is not less than 25 mm, nor less than $2d_b$; and the clear spacing between grooves is not less than 25 mm, nor less than $3d_b$.
(e) Before embedding the GFRP bars in them, the grooves in the beams are cleaned with pressurized air to remove any residue.
(f) The adhesive used for bonding the GFRP bars to the timber beam is compatible with the preservative treatment used on the timber and chosen such that it is compatible with the expected volumetric changes of the timber.
(g) In the longitudinal direction of the beam, the GFRP bar extends as close to the beam support as possible.
(h) Each GFRP bar is held in place as close to the tip of the groove as possible.

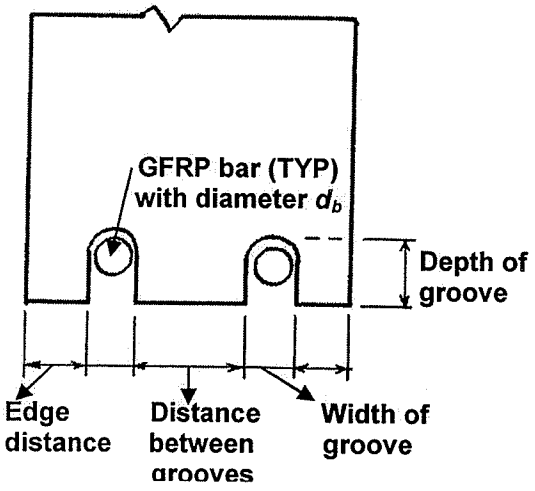

Figure 16.12.2.2 **Cross-section of a timber beam with GFRP NSMR**

16.12.3 **Strengthening For Shear**

16.12.3.1 **Shear Strengthening with GFRP Sheets**

When the following minimum requirements are met for shear strengthening with GFRP sheets, the shear strength for beam and stringer grades for the evaluation shall be assumed to be $K_{vFRP} \times f_{vu}$ in which K_{vFRP} is taken as 2.0 and f_{vu} is obtained from Table 9.11.2(b).

a) The minimum fibre volume fraction of GFRP sheets along their axes is 30% and the sheets have a minimum thickness of 0.1 mm.
b) Horizontal splits in beams, if present, are closed by a mechanical device before the application of the GFRP sheets.
c) The GFRP sheets have at least the same width as the width of the cross-section of the beam (Figure 16.12.3.1 a).
d) As shown in Figure 16.12.3.1 (a), the GFRP sheet is inclined to the beam axis at an angle of 45°±10° from the horizontal.
e) The top of the inclined GFRP sheet is as close to the centerline of the beam support as possible,
f) The adhesive used for bonding GFRP to the timber beam is compatible with the preservative treatment used on the timber and chosen such that it is compatible with the expected volumetric changes of the timber.
g) The top of the inclined GFRP sheet extends up to nearly the top of the beam.
h) The lower end of the inclined GFRP sheet extends to the bottom of the beam if there is no dap present (Figure 16.12.3.1 a). If there is a dap, the lower end is wrapped around the bottom and extends to at least half the width of the beam. In the latter case, the corner of the beam is rounded to a minimum radius of 12.5 mm, to provide full contact of the sheet with the beam (Figure 16.12.3.1 b).

℄

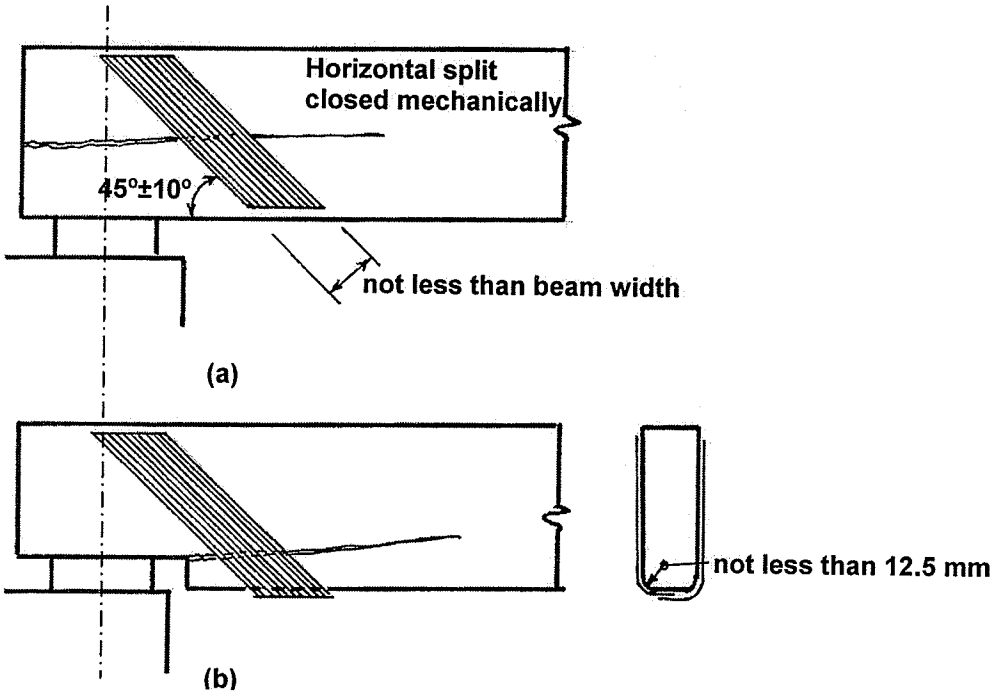

Figure 16.12.3.1 Elevation of timber beam with GFRP sheets for shear strengthening

16.12.3.2 Shear Strengthening with GFRP Embedded Bars

When the following minimum requirements are met for strengthening with GFRP bars, the shear strength for beam and stringer grades for the evaluation shall be assumed to be $K_{vFRP} \times f_{vu}$, in which K_{vFRP} is taken as 2.2 and f_{vu} is obtained from Table 9.11.2.

a) The minimum volume fraction of GFRP bars is 60%.
b) Horizontal splits in beams, if present, are closed by a mechanical device before the insertion of the GFRP bars.
c) As shown in Figure 16.12.3.2, there are at least three GFRP bars at each end of the beam.
d) The diameter of the GFRP bar, d_b, is at least 15 mm, and the minimum diameter of hole containing a bar is d_b+3 mm.
e) The spacing of bars along the length of the beam is 25 mm ± h, the depth of the beam.
f) The adhesive used for bonding the GFRP bars to the timber beam is compatible with the preservative treatment used on the timber and chosen such that it is compatible with the expected volumetric changes of the timber.
g) As shown in Figure 16.12.3.2, the GFRP bars are inclined to the beam axis at an angle of 45°±10° from the horizontal.
h) The tops of the inclined GFRP bars are within 10 to 25 mm from the top of the beam.
i) When there are daps present, the ingress of the drilled hole should be 100 mm ± 10 mm from the edge of the dap.

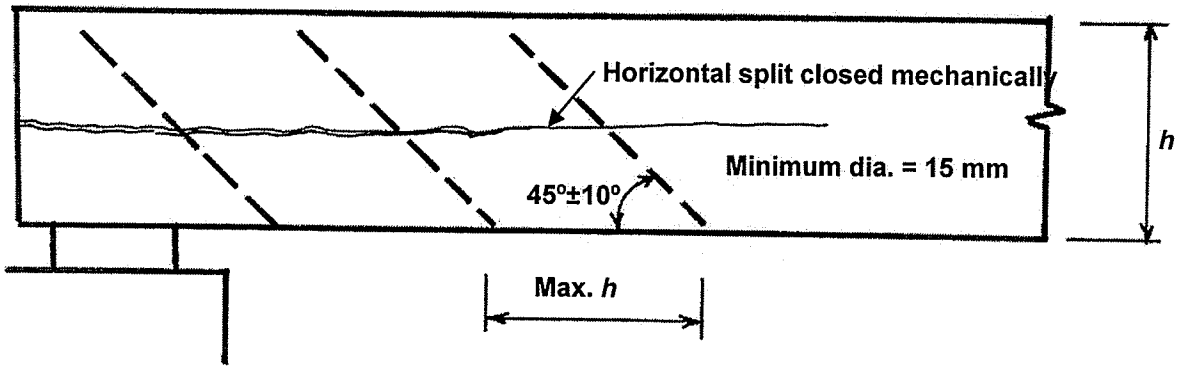

Figure 16.12.3.2 Elevation of timber beam with GFRP bars for shear strengthening